AD_____

GRANT NO:

DAMD17-94-J-4062

TITLE:
Molecular cloning and function of Fas/APO-1 associated protein in breast cancer.

PRINCIPAL INVESTIGATOR:

TAKAAKI SATO, Ph.D.
John Reed, Ph.D.

CONTRACTING ORGANIZATION:

La Jolla Cancer Research Foundation
10901 N. Torrey Pines Rd.,
La Jolla, CA 92037

REPORT DATE:

June 5, 1995

TYPE OF REPORT:

Annual report

PREPARED FOR: U.S. Army Medical Research and Materiel Command
Fort Detrick, MD 21702-5012

DISTRIBUTION STATEMENT: Approved for public release; distribution unlimited

REPORT DOCUMENTATION PAGE

Form Approved
OMB No. 0704-0188

1. AGENCY USE ONLY (Leave blank)	2. REPORT DATE	3. REPORT TYPE AND DATES COVERED
	June 5, 1995	annual report (5/9/94 - 5/8/95)

4. TITLE AND SUBTITLE

Molecular cloning and function of Fas/APO-1 associated protein in breast cancer.

5. FUNDING NUMBERS

DAMD17-94-J-4062

6. AUTHOR(S)

Takaaki Sato. Ph.D.
John Reed, Ph.D.

7. PERFORMING ORGANIZATION NAME(S) AND ADDRESS(ES)

La Jolla Cancer Research Foundation
10901 N. Torrey Pines Rd.,
La Jolla, CA 92037

8. PERFORMING ORGANIZATION REPORT NUMBER

9. SPONSORING/MONITORING AGENCY NAME(S) AND ADDRESS(ES)

U.S. Army Medical Research and Materiel Command
Fort Detrick, MD 21702-5012

10. SPONSORING/MONITORING AGENCY REPORT NUMBER

11. SUPPLEMENTARY NOTES

12a. DISTRIBUTION/AVAILABILITY STATEMENT

Approved for public release;
distribution unlimited

12b. DISTRIBUTION CODE

13. ABSTRACT *(Maximum 200 words)*

Fas/APO-1 is a cell surface receptor that controls a poorly understood signal transduction pathway leading to cell death via apoptosis. A protein tyrosine phosphatase, FAP-1 (Fas/APO-1 associated phosphatase), capable of interacting with the cytosolic domain of Fas, was isolated by yeast two hybrid system. The carboxy terminal 15 amino acids of Fas are necessary and sufficient for interaction with FAP-1. FAP-1 expression is highest in tissues and cell lines (including MCF7 breast cancer cell line) that are relatively resistant to Fas-mediated cytotoxicity. Gene transfer-mediated elevations in FAP-1 partially abolished Fas-induced apoptosis in a T-cell line. These findings are consistent with an inhibitory effect of FAP-1 on Fas-signal transduction.

Reference: Sato, T., Irie, S., Kitada, S., and Reed, J. C.: FAP-1: A Protein Tyrosine Phosphatase that associates with Fas. ***Science***, 268, 411-415. 1995.

14. SUBJECT TERMS	15. NUMBER OF PAGES
apoptosis, Fas/APO-1, breast cancer, programmed cell death, yeast two hybrid system, protein tyrosine phosphatase	51
	16. PRICE CODE

17. SECURITY CLASSIFICATION OF REPORT	18. SECURITY CLASSIFICATION OF THIS PAGE	19. SECURITY CLASSIFICATION OF ABSTRACT	20. LIMITATION OF ABSTRACT
unclassified	unclassified	unclassified	unlimited

GENERAL INSTRUCTIONS FOR COMPLETING SF 298

The Report Documentation Page (RDP) is used in announcing and cataloging reports. It is important that this information be consistent with the rest of the report, particularly the cover and title page. Instructions for filling in each block of the form follow. It is important to ***stay within the lines*** to meet ***optical scanning requirements***.

Block 1. Agency Use Only *(Leave blank)*.

Block 2. Report Date. Full publication date including day, month, and year, if available (e.g. 1 Jan 88). Must cite at least the year.

Block 3. Type of Report and Dates Covered. State whether report is interim, final, etc. If applicable, enter inclusive report dates (e.g. 10 Jun 87 - 30 Jun 88).

Block 4. Title and Subtitle. A title is taken from the part of the report that provides the most meaningful and complete information. When a report is prepared in more than one volume, repeat the primary title, add volume number, and include subtitle for the specific volume. On classified documents enter the title classification in parentheses.

Block 5. Funding Numbers. To include contract and grant numbers; may include program element number(s), project number(s), task number(s), and work unit number(s). Use the following labels:

C	- Contract	**PR**	- Project
G	- Grant	**TA**	- Task
PE	- Program Element	**WU**	- Work Unit Accession No.

Block 6. Author(s). Name(s) of person(s) responsible for writing the report, performing the research, or credited with the content of the report. If editor or compiler, this should follow the name(s).

Block 7. Performing Organization Name(s) and Address(es). Self-explanatory.

Block 8. Performing Organization Report Number. Enter the unique alphanumeric report number(s) assigned by the organization performing the report.

Block 9. Sponsoring/Monitoring Agency Name(s) and Address(es). Self-explanatory.

Block 10. Sponsoring/Monitoring Agency Report Number. *(If known)*

Block 11. Supplementary Notes. Enter information not included elsewhere such as: Prepared in cooperation with...; Trans. of...; To be published in.... When a report is revised, include a statement whether the new report supersedes or supplements the older report.

Block 12a. Distribution/Availability Statement. Denotes public availability or limitations. Cite any availability to the public. Enter additional limitations or special markings in all capitals (e.g. NOFORN, REL, ITAR).

- **DOD** - See DoDD 5230.24, "Distribution Statements on Technical Documents."
- **DOE** - See authorities.
- **NASA** - See Handbook NHB 2200.2.
- **NTIS** - Leave blank.

Block 12b. Distribution Code.

- **DOD** - Leave blank.
- **DOE** - Enter DOE distribution categories from the Standard Distribution for Unclassified Scientific and Technical Reports.
- **NASA** - Leave blank.
- **NTIS** - Leave blank.

Block 13. Abstract. Include a brief *(Maximum 200 words)* factual summary of the most significant information contained in the report.

Block 14. Subject Terms. Keywords or phrases identifying major subjects in the report.

Block 15. Number of Pages. Enter the total number of pages.

Block 16. Price Code. Enter appropriate price code *(NTIS only)*.

Blocks 17. - 19. Security Classifications. Self-explanatory. Enter U.S. Security Classification in accordance with U.S. Security Regulations (i.e., UNCLASSIFIED). If form contains classified information, stamp classification on the top and bottom of the page.

Block 20. Limitation of Abstract. This block must be completed to assign a limitation to the abstract. Enter either UL (unlimited) or SAR (same as report). An entry in this block is necessary if the abstract is to be limited. If blank, the abstract is assumed to be unlimited.

★U.S.GPO:1991-0-299-935

FOREWORD

Opinions, interpretations, conclusions and recommendations are those of the author and are not necessarily endorsed by the US Army.

T.S. Where copyrighted material is quoted, permission has been obtained to use such material.

T.S. Where material from documents designated for limited distribution is quoted, permission has been obtained to use the material.

____ Citations of commercial organizations and trade names in this report do not constitute an official Department of Army endorsement or approval of the products or services of these organizations.

T.S. In conducting research using animals, the investigator(s) adhered to the "Guide for the Care and Use of Laboratory Animals," prepared by the Committee on Care and Use of Laboratory Animals of the Institute of Laboratory Resources, National Research Council (NIH Publication No. 86-23, Revised 1985).

____ For the protection of human subjects, the investigator(s) adhered to policies of applicable Federal Law 45 CFR 46.

T.S. In conducting research utilizing recombinant DNA technology, the investigator(s) adhered to current guidelines promulgated by the National Institutes of Health.

T.S. In the conduct of research utilizing recombinant DNA, the investigator(s) adhered to the NIH Guidelines for Research Involving Recombinant DNA Molecules.

T.S. In the conduct of research involving hazardous organisms, the investigator(s) adhered to the CDC-NIH Guide for Biosafety in Microbiological and Biomedical Laboratories.

Salcedo Salto 6/5/95

PI - Signature Date

ANNUAL REPORT (GRANT NO. DAMD17-94-J-4062)

TABLE OF CONTENTS

Sato, T., Hanada, M., Bodrug, S., Irie, S., Iwama, N., Boise, L., Tompson, C., Golemis, E., Fong, L., Wang, H.-G., and Reed, J. C.: Investigation of Bcl-2 protein family interaction using yeast two-hybrid system. ***Proc. Natl. Acad. Sci. U. S. A.*** 91, 9238-9242, 1994.

Takayama, S., **Sato, T.**, Krajewski, S., Kochel, K., Irie, S., Millan, J., and Reed, J. C.: Cloning and functional analysis of BAG-1: A novel Bcl-2 binding protein with anti-cell death activity. ***Cell***, 80, 279-284, 1995.

Sato, T., Irie, S., and Reed, J. C.: A novel member of the TRAF family of putative signal transducing proteins binds to the cytosolic domain of CD40. ***FEBS letter***, 358, 113-118, 1995.

Sato, T., Irie, S., Kitada, S., and Reed, J. C.: FAP-1: a protein tyrosine phosphatase that associates with Fas. ***Science***, 268, 411-415, 1995.

Fukuda, M. N., **Sato, T.**, Nakayama, J., Klier, G., Mikami, M., Aoki, D., and Nozawa, S.: Trophonin and tastin, a novel cell adhesion molecule complex with potential involvement in embryo implantation. ***Genes & Dev.*** 9, 1199-1210,1995.

I. INTRODUCTION

1. BACKGROUND AND SIGNIFICANCE

The Fas/APO-1 antigen is a member of the Tumor Necrosis Factor Receptor (TNFR) family. Antibodies directed against this cell surface receptor trigger apoptosis in a wide variety of cells. The ligand for this receptor has yet to be molecularly described, but is known to be present on cytotoxic T-cells. Fas/APO-1 thus may serve as a conduit through which the immune system can fight off cancer.

The signal transduction mechanisms that are involved in Fas/APO-1-induced apoptosis remain poorly understood. Examination of the predicted amino-acid sequence of this receptor has failed to suggest an obvious mechanism. The cytosolic domain of Fas/APO-1 however shares homology with some other members of the TNFR family within a 45 amino-acid segment. Deletion of this region has been shown to abrogate the function of Fas/APO-1. These findings lead to the hypothesis that some critical signal transducing molecules associate with the cytosolic tail of Fas/APO-1.

The goal of this proposal is to clone cDNAs encoding proteins that bind to the cytosolic domain of Fas/APO-1. The binding sites for these proteins will be mapped within the cytosolic domain of Fas/APO-1 and their function tested through gene transfer experiments. Taken together, these investigations are predicted to result in an improved understanding of the mechanisms through which Fas/APO-1 regulates apoptosis, and may lead eventually to improved therapies for patients with cancer, including cancer of the breast.

1. *Fas/APO-1 antigen and apoptosis*

Apoptosis or programmed cell death (PCD) plays a critical role in a variety of systems during both embryonic development and postembryonic life (1-3). Examples of this phenomenon include death of the cells in the tadpole tail following stimulation with thyroid hormone (4-5), clonal deletion of autoreactive T cells in the thymus (6), and neuronal cell death during formation of the brain (7). The morphological characteristics of apoptotic cells include condensed chromatin and fragmented nuclei, loss of plasma membrane microvilli and the appearance of plasma membrane blebs. Biochemical events include the degradation of chromosomal DNA into oligomers of oligonucleosome-sized fragment (about 180 bp) which occurs in many but not all cells undergoing apoptosis. Overall, however, the biochemical and molecular mechanisms that regulate apoptosis remain poorly understood.

Recently, monoclonal antibodies were established against the human surface antigen Fas/APO-1 (CD95) by two independent groups (8-9). These anti-Fas antibodies induce apoptosis in cells expressing Fas antigen. Interestingly, the expression level of Fas antigen is significantly upregulated by treatment of cells with interferon-g (IFN-γ) (10) and cytotoxicity induced by anti Fas antibodies is enhanced by cycloheximide (CHX) or actinomycin D (Act D), similar to previous reports about tumor necrosis factor (TNF) receptors (11). cDNAs encoding the human Fas antigen have been isolated by expression cloning using anti-Fas antibodies (10-12). The polypeptide deduced from the cDNA sequence consists of 319 amino acids (45.0 kDa) and has a single transmembrane domain. The extracellular domain is highly rich in cysteine residues, and similar to that of the p55 and p75 tumor necrosis factor receptors (TNFR) (13, 14), the human B cell antigen CD40 (15), T cell antigen OX40 (16), and other members of the TNFR family including CD27 (17), CD30 (18), and the p75 NGF receptor (19). Though the cytosolic domains of the various members of this receptor family are not well conserved, Fas and p55 TNFR contain a 45 amino acid domain within their cytoplasmic domains that is homologous (10). This region is also weakly homologous to a segment in the cytosolic domains of CD40 and OX40, receptors which interestingly rescue cells from apoptotic death rather than inducing it (15-16). The Fas mRNA is expressed in thymus, liver, heart, lung and ovary but not in brain and spleen. Moreover, Fas antigen is also detected in some types of solid tumors including breast, prostate, colon, and pancreatic cancer. The human Fas gene has been mapped to 10q24, a region not infrequently deleted in prostate cancers and some other solid tumors (20-21).

The structure of Fas has suggested that it might be a receptor for unknown cytokine of the TNF family. Recently, the rat Fas ligand has been cloned by expression cloning using a cytotoxic T-cell hybridoma, d10S-2 (22). Its mouse homolog was also cloned by crosshybridization (23). The structure of Fas ligand shows no signal sequence, but does contain a transmembrane domain, indicating that it is a type II membrane protein. The Fas ligand shares strong homology with TNFα and TNFβ (27.8% and 28.7% identity, respectively). However, despite this significant similarity, the cloned rat Fas ligand could neither bind to the human TNFRI nor active the mouse TNFRI in WR19L cells (22). The recombinant Fas ligand expressed in Cos cells induced apoptosis in Fas-expressing target cells, indicating that Fas ligand is a death factor and that is its receptor.

2. *Loss of Fas function in lpr mice*

The mouse homolog of the Fas antigen has been cloned and compared to human Fas at both the nucleotide and amino acid levels (24). The mouse Fas antigen is 306 amino acids in length (MW. 35.0 kDa) and like the human antigen, contains a single

transmembrane domain which divides the molecule into extracellular and cytoplasmic domains. The nucleotide and amino acid sequences of mouse Fas antigen are 58.5% and 49.3% identical to the human Fas antigen, respectively. In particular, the amino acids from 217 to 272 of cytoplasmic domain in mouse Fas antigen are highly homologous with the corresponding region in the human antigen. As mentioned above, this region is well conserved among TNFR, NGFR, CD40, and OX40.

Mice homozygous for *lpr* (lymphoproliferation) or *gld* (generalized lymphoproliferative disease) develop lymphadenopathy and suffer from autoimmune disease. The chromosomal localization of mouse Fas gene was also determined by interspecific backcross analysis and mapped to chromosome 19 (25, 26). The gene responsible for the lymphoproliferation mutation (*lpr*) had been mapped to the chromosomal region close to the position of mouse Fas gene on chromosome 19. The *lpr* mutation is transmitted as an autosomal recessive phenotype. These mutant mice develop multiple auto-antibodies, accumulation of large numbers of non- malignant double-negative ($CD4^-CD8^-$) T lymphocytes in lymph nodes and the spleen, and an SLE-like autoimmune disease (27). From these experimental observations, candidate gene approaches were performed to confirm whether mouse Fas antigen is mutated in *lpr* mouse. The results revealed that expression of Fas mRNA was absent in the *lpr* mouse because of a gene rearrangement (28). The Fas gene of the lpr^{cg} (*lpr* complementing *gld*) mutant mouse which exhibits the same phenotype as the *lpr* mutant, was discovered to have a single point mutation [Ile^{225}(wild type) to Asn^{225}] within the well conserved cytoplasmic domain in the Fas antigen (28). Anti-Fas antibodies cannot induce apoptosis in cells expressing Fas antigen from lpr^{cg} mice. Presumably, the defect of this mutant Fas antigen reflects a problem with signal transduction, and suggests that some regulatory protein may fail to bind to this mutated cytoplasmic domain.

Recently, the mouse Fas ligand was mapped close to the antithrombin III (*AT-III*) gene on chromosome 1 where the *gld* mutation is linked. Furthermore, Fas ligand in *gld* mice carries a point mutation in the C-terminal region [Phe^{273} (wild type) to Leu^{273}], which is highly conserved among members of the TNF family, and could not induce apoptosis in Fas-expressing cells (23). These and other results indicate that *lpr* and *gld* are mutations in Fas receptor and Fas ligand, respectively, and suggest important physiological roles of the Fas system in the regulation of the overall number of T-cells in vivo, as well as in the eradication of autoreactive lymphocytes.

3. *Mutational analysis of Human Fas antigen and TNF receptor*

To examine the regions critical for signal transduction of Fas antigen as an apoptotic inducer, deletion mutants of cytoplasmic domains were constructed (29). Interestingly, the mutant lacking the C-terminal 15 amino acids dramatically increased the anti-Fas antibody induced killing activity, however a further deletion resulted in loss of its activity (29). These results imply the existence of a regulatory factor that inhibits Fas function as well as a signal transducing domain in the cytoplasmic region of the Fas antigen necessary for activation of apoptosis pathways.

The cytoplasmic domain of Fas is highly homologous to TNF receptor type I. Extensive studies by alanine-scanning mutagenesis of TNFRI suggested that many of the amino acids conserved within the Fas antigen are very important for generating cytotoxic signals. In addition, some regions within the cytosolic tail of TNFR-1 may play an important role in receptor clustering after ligand binding, and thus contribute importantly to receptor activation (30).

4. *Possible role of Fas in cancer and autoimmune disease.*

Dysregulation of Fas expression or function could also play a role in neoplasia. For example, abnormally low levels of Fas expression have been reported on some tumors, based on comparisons to their normal tissue counterparts (31), suggesting that loss of Fas expression could be involved in malignancy perhaps as a mechanisms of avoidance of some immune surveillance mechanisms. Alternatively, some tumors have been reported to over-express Fas (31) and anti-Fas antibodies have been shown to induce cell proliferation rather than apoptosis in some tumor cell lines (32). Thus the response of tumor cells to Fas activation appears to vary, presumably because of as yet unknown differences in intracellular signal transduction apparatus that may exist in transformed cells. In this regard, a study of anti-Fas antibody effects on freshly isolated Chronic Lymphocytic Leukemia (CLL) specimens reported that dysregulation of *bcl-2* gene expression was associated with anti-Fas antibody-induced proliferation rather than cell death (33), suggesting at least one potential mechanism for paradoxical induction of proliferation by anti-Fas antibodies in some cases of cancer.

In addition, insufficient levels of Fas activity may play a significant role in some autoimmune diseases. Recently, Cheng, et al. (34) described an alternatively spliced form of Fas that lacks a transmembrane domain and is therefore secreted from cells. Levels of this secreted form of Fas were shown

to be elevated in patients with Systemic Lupus Erythematosis (SLE) and mice injected with soluble Fas displayed autoimmune features. Soluble Fas was also demonstrated in vitro to block apoptosis induced by anti-Fas antibodies, suggesting that secreted Fas could potentially neutralize Fas-ligand and thus lead to insufficient levels of Fas activation on lymphocytes.

5. *Mechanisms of Fas-mediated signal transduction*

At present, relatively little is known about the molecular mechanisms by which Fas transduces signals into cells. Examination of the predicted amino acid sequence of the cytosolic domain of this receptor reveals no motifs that might suggest a biochemical activity. Deletion of the intracellular domain of Fas that shares 51% homology over a stretch of 45 amino acids with a region located in the cytosolic domain of the p55-TNFRI (10) has been reported to abrogate the ability of Fas to trigger cell death (29). Interestingly, the "death domains" of Fas and TNFRI also share homology with a cytosolic domain in CD40. Unlike Fas and TNFRI, however, crosslinking of CD40 via anti-CD40 antibodies delivers signals for suppression of apoptotic cell death and induction of *bcl-2* gene expression in germinal center B-cells (35). Thus, this domain may not strictly be involved in the activation of signal transduction pathways leading to cell death. It should be noted however that CD40 and at least some other members of TNFR family that have traditionally been thought of as regulating pathways for suppression of cell death, specifically the p75-nerve growth factor receptor, can also induce or accelerate cell death in the absence of ligand (36, 37).

Recently, we and other groups have isolated a CD40-associated protein (CAP-1) by yeast two hybrid screening (38, 39). Furthermore, the region within the cytosolic domain of CD40 that shares homology with the death domains of TNFRI and Fas is both necessary and sufficient for binding to the CAP-1 protein. The CAP-1 protein contains a C-terminal domain that shares strong amino acid sequence homology with a unique domain found in two putative signal transducing proteins that bind to the cytosolic tail of p75-TNFRII, TRAF1 and TRAF2 (40). The N-terminal portion of CAP-1 contains a RING finger motif and three zinc finger-like domains similar to those found in several regulatory proteins that interact with DNA or RNA. It is possible that CAP-1 and TRAF-2 may participate directly in signal transduction from membrane to nucleus by analogy to the STAT proteins. The CAP-1 protein however does not bind to the cytosolic domains of both Fas and TNFRI. Nevertheless, these results raise to the possibility that other TRAF-family proteins may interact with the cytosolic domains of Fas and TNFRI, thus physically and functionally linking Fas and TNFRI to proteins involved in a signal transduction cascade that results in cell death.

In addition, both anti-Fas antibodies and TNF sometimes induce cell death only when protein synthesis has first been inhibited with cycloheximide, at least in some types of cultured cells (41). This finding has implied the existence of short-lived proteins that oppose the cytotoxic actions of Fas and TNF. In fact, deletional analysis of Fas has demonstrated that removal of the C-terminal amino acids abrogates the dependence on cycloheximide for anti-Fas antibody-mediated cytotoxicity in at least the one cell line examined thus far (29). Possibly, therefore, an inhibitory protein that antagonizes Fas function requires these C-terminal 15 amino acids for interaction with Fas. Alternatively, by analogy to some other receptors such as the EGF receptor kinase whose C-terminus negatively regulates the catalytic domain of the receptor when phosphorylated on tyrosines, it could be that the C-terminus of Fas loops back to interact with other parts of the receptor. In this regard, it has been pointed out previously that Fas has potential sites for serine phosphorylation in its C-terminus but no tyrosine residues are found in this region (29).

Finally, sphingomyelin (SM) hydrolysis, ceramide generation, or both have been implicated in a signal transduction pathway through Fas, as well as TNFα, IFN-γ, and IL-1β (42-45). These different cytokine receptors have been shown to trigger SM turnover upon ligand binding. Furthermore, ceramide has been shown to induce apoptosis in several types of cells (46). Thus, it is possible that the SM pathway might be involved in Fas-induced apoptosis signaling.

2. Hypothesis and Purpose

Fas/APO-1 is a cell surface protein that mediates apoptosis. Specific regions within the cytoplasmic domain of Fas/APO-1 are required for this function The mechanisms of Fas/APO-1 signal transduction are still unclear, but by analogy to other cytokine receptors we hypothesize that critical signal transducing moleules bind to the cytoplasmic domain of Fas/APO-1. Consistent with this hypothesis, we have detected several Fas/APO-1 binding proteins in breast cancer cell lines as well as ovarian, colon, prostate, and lung cancer cell lines. It is possible that the cytoplasmic domain of Fas/APO-1 antigen may associated with several molecules such as G proteins, phospholipases or protein kinases necessary for signal transduction. In order to confirm this hypothesis, we will isolate cDNAs encoding Fas/APO-1 binding proteins and study the role of these encoded proteins in Fas/APO-1-mediated apoptosis in breast cancer cell lines *in vitro*.

3. Methods of Approach

The yeast two-hybrid system, originally developed by Fields and Song (47), provides a powerful tool for studying protein-protein interactions. To confirm this hypothesis, we will isolate cDNAs encoding Fas/APO-1-binding proteins using the yeast two-hybrid system and screening of l-phage expression libraries with recombinant GST-Fas/APO-1 fusion proteins. The specific region within the cytoplasmic domain of Fas/APO-1 required for binding of these proteins will be determined. Furthermore, the function of Fas/APO-1-binding proteins will be explored through gene transfer experiments using various cell lines, including breast cancer cells. Taken together, these investigations of Fas/APO-1 binding proteins will improve understanding of the signal transduction pathways through which Fas/APO-1 controls apoptosis and could ultimately provide insights that would lead to more effective therapies for human tumors, including cancer of the breast.

II. RESULTS AND DISCUSSIONS:

1. Use of yeast two-hybrid system to clone cDNAs encoding Fas-binding proteins.

To identify cDNAs encoding proteins that can potentially modulate the activity of Fas, we employed a yeast two-hybrid system for cDNA library screening. We used the cytosolic domain of human Fas cDNA corresponding to amino-acids 191 to 335 (representing the cytosolic domain of the protein from the transmembrane domain to the C-terminus of the protein) as a target protein. This portion of Fas cDNA was PCR-engineered into the yeast expression plasmid pBTM116 in-frame with sequences encoding the LexA DNA-binding domain (48). This plasmid was then introduced into L40 cells [*a his3 trp1 leu2 ade2 LYS2: (lexAop)4-HIS3 URA3:: (lexAop)8-lacZ*] which contain histidine synthetase (*HIS3*) and b-galactosidase (*lacZ*) reporter genes under the control of lexA operators (48). The resulting transformants were selected for ability to grow on media lacking tryptophan, since the pBTM116 plasmid contains a TRP1 gene that complements the defect in the host strain. Expression of the LexA-Fas (191-335) protein was then verified by immunoblotting using an antiserum specific for LexA. A cDNA library prepared from mouse embryo mRNA and cloned into the yeast expression plasmid pVP16 was then introduced into these LexA/Fas-expressing cells by a high efficiency LiOAc transformation method (49-51). Transformants were selected by growth on plates lacking leucine, based on the presence of a *LEU2* gene in the library plasmid pVP16.

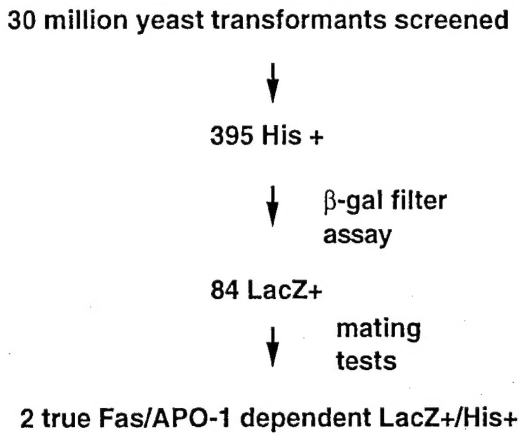

Fig. 1. The summary of the yeast-two hybrid screening.

Those colonies expressing cDNAs encoding candidate Fas-binding proteins were then identified initially by their ability on grow on histidine-deficient media, utilizing the lexA-operator/*HIS3* reporter gene construct in these yeast cells. The summary of the results of the cDNA library screening is shown in **Fig. 1**. From a screen of ~30 million cDNAs, an initial set of 395 His^+ colonies were identified. These 395 clones were then tested by a b-galactosidase colorimetric filter assay (52), utilizing the *lacZ* reporter gene under the control of 8 lexA operators, thus narrowing the pool of candidate clones to 84. These 84 candidates were then "cured" of their LexA/Fas-encoding plasmids by growth in tryptophan containing media, and mated with a panel of Mat*a*-type yeast, strain NA87-11A [*a leu2 his3 trp1 pho3 pho5*] into which we had introduced various control plasmids that produce LexA fusion proteins, including LexA/Fas, LexA/Ras, LexA/CD40, LexA/Bcl-2, and LexA/lamin. These cells were selected for growth in tryptophan and leucine-deficient media to generate cells that contained the pVP16-cDNA clones together with one of the LexA-fusion proteins. Among the 84 candidate clones, only 2 reacted specifically with the LexA/Fas protein, as determined in both His^+ phenotype and b-galactosidase filter assays (**Table 1** and **Fig. 2**).

Table 1. Specific interaction of FAP-1 with Fas cytosolic domain.

pBMT116 (LexA)	pVP16	Growth on His- plate	Color
Fas(191-335)		+	Blue
Ras(V12)		-	White
Ras(L35R37)		-	White
CD40 (216-277)	# 31 & #43	-	White
CD40 (225-269)		-	White
Bcl-2 (83-218)		-	White
Lamin		-	White
Ras(V12)	c-Raf	+	Blue
Lamin		-	White

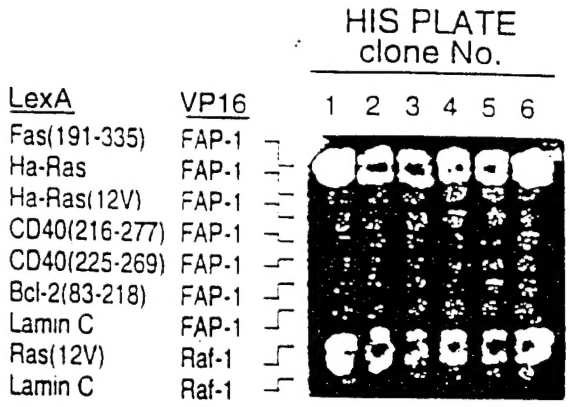

Fig. 2. Demonstration of specific interaction of FAP-1 with Fas on His$^+$ phenotypes by yeast-two hybrid system.

These mouse cDNAs represented overlapping independent clones, having insert sizes of 381 bp (#31) and 351 bp (#43) and sharing > 95% homology with a human cDNA sequence encoding a protein tyrosine phosphatase (PTPase) termed PTP-BAS (53). Because of its ability to bind to Fas, we have renamed this protein, Fas-associated phosphatase-1 (FAP-1) (54).

2. Structural Characteristics of FAP-1.

PTP-BAS was originally cloned from human basophils by a reverse transcriptase-polymerase chain reaction (RT-PCR) method that utilized degenerate primers targeted against conserved sequences found in PTPases. Three isoforms arising due to alternative splicing have been identified by cDNA cloning, the longest of which is predicted to encode a 2,485 amino-acid protein (53). PTP-BAS lacks a transmembrane domain, but contains a membrane-binding domain similar to that found in the cytoskeleton-associated proteins, ezrin (55), radixin (56), moesin (57) and protein 4.1 (58), as well as in the PTPases PTPH1 (59), PTP-MEG (60) and PTPD1 (61). In addition to a catalytic domain located near its carboxy terminus, PTP-BAS contains six GLGF repeats (**Fig. 3**).

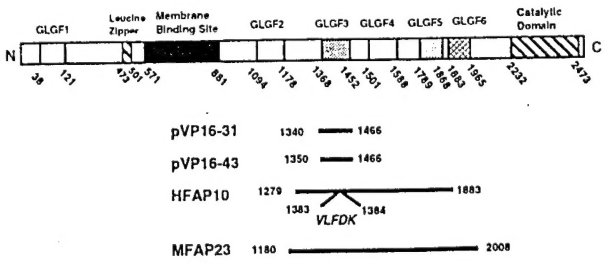

Fig. 3. Schematic representation of FAP-1 structure.

The structure of the 2,485 amino-acid human FAP-1 protein (also known as PTP-BAS; type-1) (53) (top), showing the locations of the catalytic, membrane binding, and GLGF repeat domains (53). The cDNAs identified by two-hybrid screening of a mouse embryo cDNA library, pVP16-31 and pVP16-43 with encoded amino-acids relative to the human FAP-1 protein, as also shown. A human FAP-1 partial cDNA (HFAP-10) (encoding amino-acids 1279-1883 of PTP-BAS; type-1) from brain was cloned and found to contain a five amino-acid insert in the GLGF-3 domain compared to the published sequence (53). A mouse cDNA clone (MFAP-23) was also isolated from lgt11 mouse kidney cDNA libraries (GenBank accession #s: L34581; L34582; L34583).

These structures are thought to mediate intra-and inter-molecular interactions among protein domains and may play a role in targeting proteins to the submembranous cytoskeleton or in regulating enzyme activity (53). GLGF repeats have been found previously in guanylate kinases, as well as the rat post-synaptic density protein (PSD-95), which is a homolog of the Drosphilia tumor suppressor protein, lethal-(1)-disc-large-1 [*dls*] (62, 63). Furthermore, the FAP-1 protein contains a leucine zipper motif ($LX_6LX_6LX_6MX_6L$), suggesting that the FAP-1 leucine zipper may mediate homo- and hetero-dimerization to modulate the PTPase activity or Fas-mediated signal transduction. **Fig. 3** summarizes the structural features of FAP-1 (PTPase-BAS).

Fig. 3 also shows the two cDNA clones that were identified through the two-hybrid screen, VP16-31 and VP16-43. Note that both of these cDNAs coincide with the third GLGF repeat in FAP-1. This suggests that the GLGF repeats are involved in the interaction of FAP-1 with the Fas antigen. Also depicted in the Figure are a human (HFAP-10) and a mouse (MFAP-23) cDNA clone that were obtained by hybridization screening of cDNA libraries using ^{32}P-labeled pVP16-31 as a probe.

3. Mapping of the regions in Fas required for interactions with FAP-1.

As an initial attempt to confirm the interaction of FAP-1 with the Fas antigen and to map the regions within the cytosolic domain of Fas required for binding to FAP-1, we generated a series of GST-Fas fusion proteins in *E. coli* using the plasmid pGEX2T (Pharmacia, Inc.) as summarized in **Fig. 4**. The GST-fusion proteins contained the following segments of the Fas cytosolic domain: (**A**) amino-acids 191-335 corresponding to the entire cytosolic domain; (**B**) 191-290, representing the region from the transmembrane domain to the end of the "death domain" in Fas; (**C**) 246-335, coinciding with the regions from the beginning of the "death domain" to the C-terminus of the protein; (**D**) 246-290, death domain alone; (**E**) 191-320, the

cytoplasmic domain without C-terminal 15 amino-acids; and (**F**) 321-335, representing the C-terminal 15 amino-acids of Fas, which have been reported to constitute **a negative regulatory domain**. The production of these GST-Fas fusion proteins was induced in *E. coli* under the control of a *tac* promoter using 1 mM IPTG and purified by affinity chromatography from bacterial lysates using glutathione-Sepharose 4B. SDS-PAGE analysis and Coomassie blue staining confirmed the production of all five of the GST-FAS fusion proteins (**Fig. 4, A-F**) and verified that they were of the expected molecular weights (not shown).

To explore the interaction of FAP-1 with these GST-Fas fusion proteins, the longer of the two clones identified by the two-hybrid approach described above was used as a hybridization probe

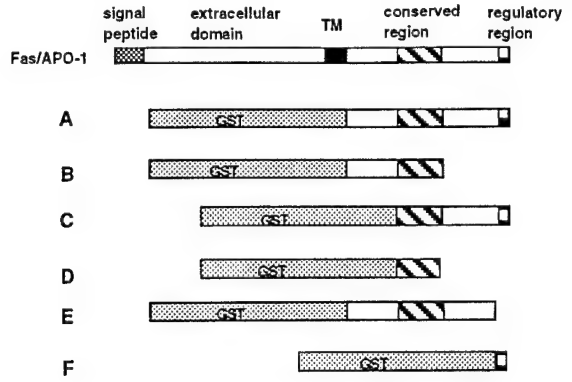

Fig. 4. Schematic representation of a series of GST-Fas fusion proteins.

to screen a human fetal brain cDNA library prepared in lambda-ZAP (Stratagen, Inc.). A ~1.8 kbp clone (HFAP-10) was obtained that corresponds to amino-acids 1279 to 1889 of the human PTPase-BAS. This cDNA was subcloned into the Bluescript vector pSK-II (Stratagene, Inc.) and in vitro translated from an internal methionine codon in the presence of ^{35}S-L-methionine using a coupled in vitro transcription/translation system (Promega, Inc.; TNT lysate) and T7 RNA polymerase. The resulting ^{35}S-labeled protein was incubated with various GST-Fas fusion proteins that had been immobilized on beads in a buffer containing 150mM NaCl, 50mM Tris [pH 8.0], 5mM DTT, 2mM EDTA, 0.1% NP-40, 1mM PMSF, 1mg/ml leupeptin for 16 hrs at 4°C. After washing vigorously 10-times in the same buffer, associated proteins were recovered with the glutathione-Sepharose beads by centrifugation, eluted into boiling Laemmli buffer, and analyzed by SDS-PAGE and fluorography.

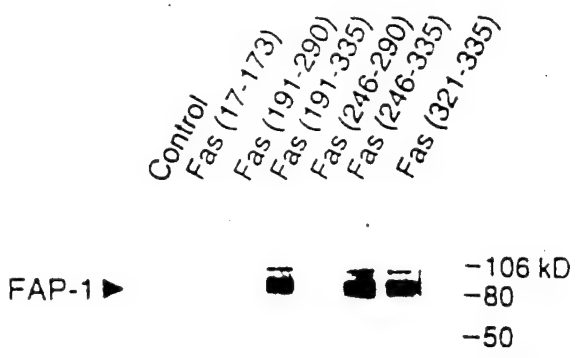

Fig. 5a. In vitro binding assay of FAP-1 with various GST-Fas proteins.

As shown in **Fig. 5a**, the polypeptide derived from the human version of FAP-1 bound specificially to GST-Fas fusion proteins containing the entire cytosolic domain (191-335), the region of Fas from the death domain to the C-terminus (246-335) and the C-terminal 15 amino-acids (321-335) (constructs **A**, **C**, and **F** in **Fig. 4**). In contrast, the FAP-1 polypeptide did not bind to GST-fusion proteins containing the death domain alone or the region of Fas beginning from the transmembrane domain to the end of the death domain (constructs **B** and **D** in **Fig. 4**). The FAP-1 polypeptide also did not bind to non-fusion GST protein (**Fig. 5a**). These results therefore suggest that the C-terminal 15 amino-acids of Fas are sufficient for interaction of FAP-1. However, because the binding studies have not been performed with the full-length PTPase, we cannot exclude the possibility that other regions within Fas can be sufficient for binding of FAP-1.

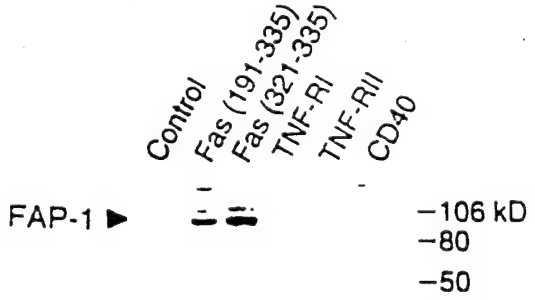

Fig. 5b. In vitro binding assay of FAP-1 with GST-TNFRs family.

The p55 receptor for TNF (TNF-R1) has been reported to induce cell death but the mechanism appears to be distinct, at least in part, from that involved in Fas-mediated killing (41). We therefore examined the ability of ^{35}S-labeled, in vitro translated FAP-1 polypeptide to bind to GST-fusion proteins containing the cytosolic domains of either p55-TNF-R1 or p75-TNF-R2. As shown in **Fig. 5b**, while the FAP-1 polypeptide bound to GST-fusion proteins containing either the full-length Fas

cytosolic domain or only the C-terminal 15 amino-acids of Fas, it did not bind to GST-fusion protein containing the cytosolic domains of Fas without the C-terminal 15 amino-acids (construct **E** in **Fig. 4**) as well as the p55 or p75 TNF receptors. This finding suggests that FAP-1 is not involved in TNF signal transduction events. In addition to p55-TNF-R1, the death domain of Fas shares at least some homology with a region in the cytosolic domain of CD40. However, as shown in **Fig. 5b**, the FAP-1 polypeptide also did not bind to a GST fusion protein containing the entire cytosolic domain of CD40, further confirming the specificity of the interaction of FAP-1 with Fas.

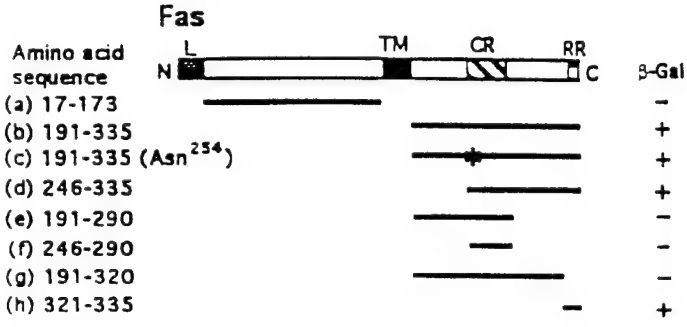

Fig. 5c. Schematic representation of mapping site on Fas involved in binding to GLGF3 domain of FAP-1.

We also confirmed the in vitro mapping data derived from use of *E. coli* produced GST-Fas fusion proteins by use of the yeast two-hybrid system. For these experiments, LexA-Fas fusion proteins were expressed in yeast using a slightly different two-hybrid system that was provided to us by Drs. Erica Golemis and Roger Brent (64, 65). We chose this two-hybrid system, in part, because it gave us an opportunity to confirm the specificity of the interaction of FAP-1 derived polypeptides with Fas in a different strain of yeast (EGY48) and with a slightly different lexA operator-*lacZ* reporter gene plasmid. As shown in **Fig. 5c**, thus far we have analyzed the interaction of the longer of the original two cDNAs identified during the cDNA library screen (VP16-31) with LexA-Fas fusion proteins analogous to constructs **A-F** presented in **Fig. 4**. Based on both His^+ phenotype and b-galactosidase filter assays, the FAP-1 polypeptide reacted specifically with all LexA/Fas fusion proteins that contained the C-terminus of Fas (321-335) but not with those that lacked this region (191-320) (**Fig. 5d**). The FAP-1 polypeptide also did not react with the extracellular domain of Fas in these assays (**Fig. 5c**). Using this two-hybrid system, identical results were obtained as with in vitro binding assay approach. Namely, the last 15 amino acids of Fas were found to be both

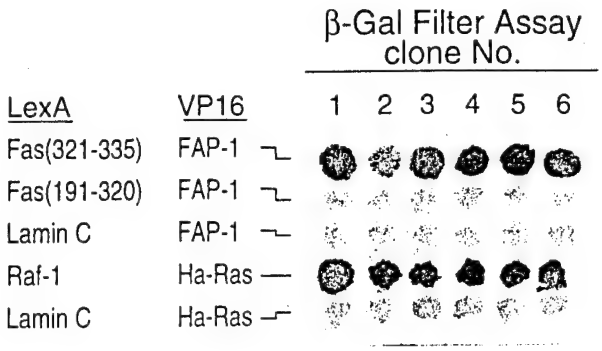

Fig. 5d. Demonstration of specific interaction of FAP-1 with C-terminal 15 amino acids of Fas by β-galactosidase filter assay.

necessary and sufficient for binding to the FAP-1 fragment.

4. <u>Gene Transfer Experiments to Assess Function of FAP-1</u>.

The finding that FAP-1 interacts with the C-terminal negative regulatory domain of Fas suggests that this PTPase may somehow inhibits Fas-generated signals that lead to apoptosis. As an initial attempt to explore this possibility, we correlated the presence or absence of FAP-1 expression with relative sensitivity to apoptosis induced by anti-Fas antibody in a variety of cell lines that express Fas. Four of four tumor cell lines (SNG-M, Jurkat, HepG2, Raji) that lacked FAP-1 mRNA, as determined by Northern blotting, were sensitive to anti-Fas antibody induced cell death to variable extents (**Fig. 6**). In contrast, all three tumor lines tested which expressed FAP-1 (RS11846, 380, COS-Fas) were completely resistant to anti-Fas. This resistance could not be explained by differences in the relative levels of Fas antigen expressed on the surface of the cells, as determined by immunofluorescence flow-cytometric analysis.

Next, a cDNA encoding the full-length FAP-1 protein was expressed in a Fas-sensitive clone from the T-cell leukemia line Jurkat. Analysis of several independent transfected clones revealed a significant correlation between the levels of FAP-1 expression and relative resistance to Fas-mediated cytotoxicity. **Fig. 7a**, for example, shows the results for some representative clones that expressed the FAP-1 plasmid at various levels, as determined by a quantitative RT-PCR analysis. These cells were treated with anti-Fas antibody for four hrs and DNA fragmentation indicative of apoptosis was detected by TUNEL assay (66), demonstrating marked resistance to Fas-mediated apoptosis in clones with higher levels of FAP-1 expression (**Fig. 7a**). Transfected Jurkat clones with high levels of FAP-1 expression also remained viable for longer periods of time than

control cells when cultured with anti-Fas antibody and withstood higher concentrations of antibody (**Fig. 7b**). In contrast to Jurkat cells which expressed full-length FAP-1, transfectants expressing a truncated version of FAP-1 lacking the catalytic domain were not protected from Fas-induced DNA degradation (**Fig. 7c**). Relative levels of Fas expression were equivalent for all subclones shown, based on immunofluorescence flow-cytometry assays.

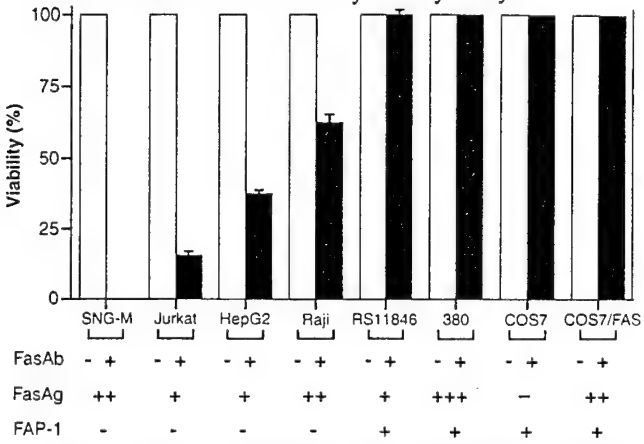

Fig. 6. FAP-1 expression with resistance to Fas-induced apoptosis in tumor cell lines.

Cells at 2 X 10^5 per ml were cultured for 24 hrs with (+) or without (-) 1 mg/ml anti-Fas antibody CH11 (Medical & Biological Labs, Inc.) and cell viability was assessed by trypan blue dye exclusion. Data are expressed as a percentage relative to untreated cells (mean +/-standard deviation; n=3). Relative FAP-1 and Fas mRNA levels were assessed by Northern blotting.

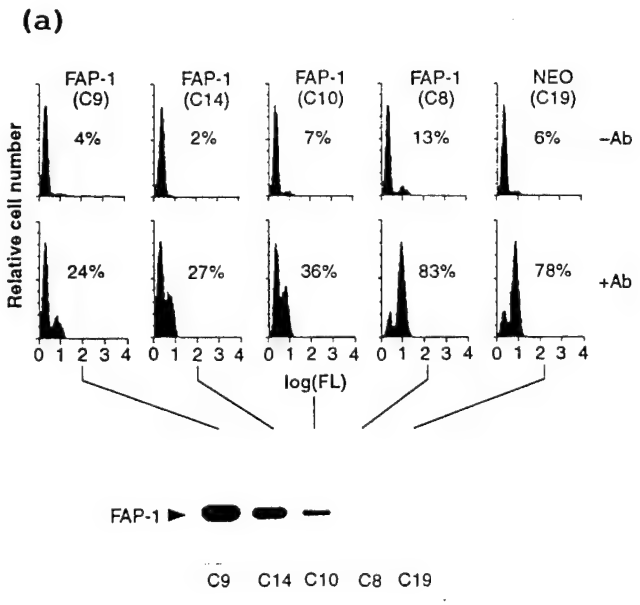

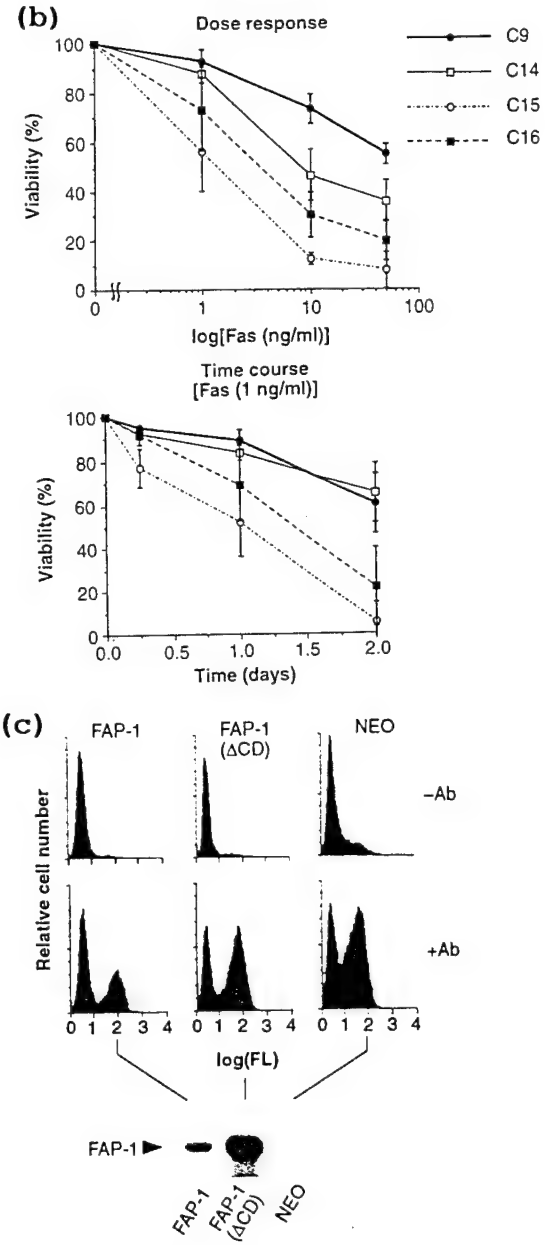

Fig. 7. Correlation of FAP-1 expression with resistance to anti-Fas antibody induced cell death. (**a**) Jurkat cells were stably transfected with a FAP-1 expression plasmid or the parental plasmid lacking FAP-1 as a control . The relative levels of FAP-1 expression in G418-resistant subclones were then determined by a RT-PCR assay (bottom). Data shown are derived from a single exposure of the same blot (lanes reordered for clarity of presentation). Transfected clones were incubated with (+Ab) or without (-Ab) 50 ng/ml of anti-Fas antibody CH-11 and TUNEL assay was performed 4 hrs later (66). Representative histograms are shown (**top**). Clones C8, C9, C10, and C14 received the FAP-1 plasmid pRc/CMV-FAP-1, whereas clone C19 was transfected with the parental pRc/CMV plasmid. Data are representative of multiple clones. A control IgM antibody (MOPC-104E; Cappel, Inc.) failed to induce DNA fragmentation and apoptosis in Jurkat cells (not shown). (**b**), FAP-1 transfectant clones C9

and C14 were compared with Neo-control clones C15 and C16 with regards to survival (determined by trypan blue dye exclusion [mean +/- std dev.; n=3]) when cultured for ~1 day with various concentrations of CH-11 antibody (**top**; C=no antibody) or for various times with 1 ng/ml CH-11 antibody (**bottom**). Cell viabilty was >95% for cells treated with a IgM control antibody (not shown). (**c**), TUNEL assays and RT-PCR analyses were performed as described for Fig. 7a using untransfected Jurkat cells and bulk-transfectants that expressed either full-length FAP-1 or a truncated FAP lacking the catalytic domain (ΔCD).

III. CONCLUSIONS AND FUTURE WORKS

We were able to isolate Fas-associated proteins using a yeast two-hybrid approach and identified a protein tyrosine phosphatase (PTPase), which we have termed Fas-associated phosphatase-1 (FAP-1). The FAP-1 protein was biochemically confirmed to bind to the cytosolic tail (C-terminal 15 a.a.) of Fas but not to other members of the TNFR family. FAP-1 expression is highest in tissues and cell lines that are relatively resistant to Fas-mediated cytotoxicity. Furthermore, gene transfer-mediated elevations in FAP-1 partially abolished Fas-induced apoptosis in a T cell line. These findings are consistent with an inhibitory effect of FAP-1 on Fas signal transduction.

Control of the protein phosphorylation on tyrosines is an important mechanism for the regulation of cellular proliferation, differentiation, and cell death. In the future work, the physiological function of FAP-1 will be explored by : (i) gene transfer-mediated modulations of FAP-1 levels in cultured cells (including Breast cancer cell lines) in vitro; (ii) testing the function of mutants of Fas and FAP-1 that fail to interact; (iii) isolate FAP-1 associated proteins and putative signal transducer (a member of TRAF family) on Fas-induced apoptosis; (iv) isolate genomic clones for human FAP-1, map its chromosomal location, and explore the possibility of alterations in FAP-1 gene in human cancers including breast and ovarian cancers.

IV. REFERENCES

1. Cohen, J. J.,Duke, R. C., Fadok, V. A., and Sellins, K. S. (1992). Apoptosis and programmed cell death in immunity. *Annu. Rev. Immunol.* **10**: 267-93.

2. Walker, N. I., Harmon, B. V., Gobe, G. C., and Kerr, J. F. R. (1988). Patterns of cell death. *Methods Achiev. Exp. Pathol.* **13**: 18-54.

3. Wyllie, A. H., Kerr, J. F. R., and Currie, A. R. (1980). Cell death: the significance of apoptosis. *Int .Rev. Cytol.* **68**: 251-306.

4. Tata, J. R., (1966). Requirement for RNA and protein synthesis for induced regression of the tadpole tail in organ culture. *Devl. Biol.* **13**: 77-94.

5. Tata, J. R., (1971). Hormonal regulation of metamorphosis. *Symp. Soc. Exp. Biol.* **25**: 163-181.

6. Smith, C. A., Williams, G. T., Kingston, R., Jenkinson, E. J., and Owen, J. J. T. (1989). Antibodies to CD3/T-cell receptor complex induce death by apoptosis in immature T cells in thymic cultures. *Nature* **337**: 181-184.

7. O'Bryan, M. K., Cheema, S. S., Bartlett, P. F., Murphy, B. F., and Pearse, M. J. (1993). Clusterin levels increase during neuronal development. *J. Neurobiol.* **24**: 421-432.

8. Yonehara, S., Ishii, A., and Yonehara, M. (1989). A cell-killing monoclonal antibody (anti-Fas) to a cell surface antigen codownregulated with the receptor of tumor necrosis factor. *J. Exp. Med.* **169**: 1747-1756.

9. Trauth, B. C., Klas, C., Peters, A. M. J., Matzku, S., Moller, P., Falk, W., Debatin, K.-M., and Krammer, P. H. (1989). Monoclonal antibody-mediated tumor regression by induction of apoptosis. *Science* **245**: 301-305.

10. Itoh, N., Yonehara, S., Ishii, A., Yonehara, M., Mizushima, S-I., Sameshima, M., Hase, A., Seto, Y., and Nagata, Y. (1991). The polypeptide encoded by the cDNA for human cell

surface antigen Fas can mediate apoptosis. *Cell* **66**: 233-243.

11. Rubin, B. Y., Smith, L. J., Hellermann, G. R., Lunn, R. M., Rchardson, N. K., and Anderson, S. L. (1988). Correlation between the anticellular and DNA fragmenting activities of tumor necrosis factor. *Cancer Res.* **48**: 6006-6010.

12. Oehm, A., Behrmann, I., Falk, W., Pawlita, M., Maier, G., Klas, C., Li-Weber, M., Rivhards, S., Dhein, J., Trauth, B. C., Ponsting, H., and Krammer, P. H. (1992). Purification and molecular cloning of the APO-1 cell surface antigen, a member of the tumor necrosis factor/nerve growth factor receptor superfamily. Sequence identity with the Fas antigen. *J.Biol.Chem.* **267**: 10709-10715.

13. Loetscher, H., Pan, Y. C .E., Lahm, H.-W., Gentz, R., Brockhaus, M., Tabuch, H., and Lesslauer, W. (1990). Molecular cloning and expression of the human 55 kd tumor necrosis factor receptor. *Cell* **61**: 351-359.

14. Smith, C. A., Davis, T., Anderson, D., Solam, L., Beckmann, M. P., Jerzy, R., Dower, S. K., Cosman, D., and Goodwin, R. G. (1990). A receptor for tumor necrosis factor defines an unusual family of cellular and viral proteins. *Science* **248**: 1019-1023.

15. Stamenkovic, I., Clark, E. A., and Seed, B. (1989). A B-lymphocyte activation molecule related to the nerve growth factor receptor and induced by cytokines in carcinomas. *EMBO J.* **8**: 1403-1410.

16. Mallett, S., Fossum, S., and Barclay, A. N. (1990). Characterization of the MRC OX40 antigen of activated CD4 positive T lymphocytes-a molecule related to nerve growth factor receptor. *EMBO J.* **9**: 1063-1068.

17. Camerini, D., Watz, G., Loenen, W. A. M., Borst, J., and Seed, B. (1991). The T cell activation antigen CD27 is a member of the nerve growth factor/tumor necrosis factor receptor gene family. *J.Immunol.* **147**: 3165-3169.

18. Smith, C. A., Gruss, H. J., Davis, T ., Anderson, D., Farrah, T., Baker, E., Sutherland, G. R., Brannan, C. I., Copeland, N. G., Jenkins, N. A., Grabstein, K. H., Gliniak, B., McAlister, I. B., Fanslow, W., Ald erson, M., Falk, B., Gimpel, S., Gillis, S., Din, W. S., Goodwin, R. G., and Armitage, R. J. (1993). CD30 antigen, a marker for Hodgkin's lymphoma, is a receptor whose ligand defines an emerging family of cytokines with homology to TNF. *Cell* **73**: 1349-1360.

19. Johnson, D., Lanahan, A., Buck, C. R., Sehgal, S., Morgan, C., Mercer, E., Bothwell, M., and Chao, M. (1986). Expression and structure of the human NGF receptor. *Cell* **47**: 545-554.

20. Inazawa, J., Itoh, N., Abe, T., and Nagata, S. (1992). Assignment of the Human Fas Antigen gene(FAS) to 10q24.1. *Genomics* **14**: 821-822.

21. Lichter, P., Walczak, H., Weitz, S., Behrmann, I., Krammer, P. H. (1992). The human APO-1(APT) antigen maps to 10q23, a region that is syntenic with mouse chromosome 19. *Genomics* **14**: 179-180.

22. Suda, T., Takahashi, T., Golstein, P., and Nagata, S. (1993). Molecular cloning and expression of the Fas ligand, a novel member of the tumor necrosis factor family. *Cell* **75**:1169-1178.

23. Takahashi, T., Tanaka, M., Brannan, C.I., Jenkins, N.A., Copeland, N.G., Suda, T., and Nagata, S. (1994). Generalized lymphoproliferative disease in mice, caused by a point mutation in the Fas ligand. *Cell* **76**:969-976.

24. Watanabe-Fukunaga, R., Brannan, C. I., Itoh, N., Yonehara, S., Copeland, N. G., Jenkins, N. A., and Nagata, S. (1992). The cDNA structure, expression and chromosomal assignment of the mouse Fas Antigen. *J. Immunol.* **148:** 1274-1279.

25. Green E. L. (1987). Catalog of mutant genes and polymorphic loci. In Genetic Variants and Strains of the Laboratory Mouse. Lyon, M. F., and Searle, A. G. eds. Oxford University Press. Oxford, pp. 12-403.

26. Copeland, N. G., and Jenkins, N. A. (1991). Development and application of a molecular genetic linkage map of the mouse genome. *Trends Genet.* **7**: 113-118.

27. Cohen, P. L., and Eisenberg, R. A. (1991). *lpr* and *gld*: Single gene models of systemic autoimmunity and lymphoproliferative disease. *Annu. Rev. Immunl.* **9**: 243-269.

28. Watanabe-Fukunaga, R., Branan, C. I., Copeland, N. G., Jenkins, N. A., and Nagata, S. (1992). Lymphoproliferation disorder in mice explained by defects in Fas antigen that mediates apoptosis. *Nature* **356**: 314-317.

29. Ito, N., and Nagata, S. (1993). A novel protein domain required apoptosis. *J. Biol. Chem.* **268**: 10932-10937.

30. Tartaglia, L. A., Ayres, T. M., Wong, G. H. W., and Goeddel, D. V. (1993). A novel domain with the 55 kd TNF receptor signals cell death. *Cell* **74**: 845-853.

31. Leithäuser, F., Dhein, J., Mechtersheimer, G., Koretz, K., Brüderlein, S., Henne, C., Schmidt, A., Debatin, K.-M., Krammer, P.H., and Möller, P. (1993). Constitutive and induced expression of APO-1, a new member of the nerve growth factor/tumor necrosis factor receptor superfamily, in normal and neoplastic cells. *Lab. Invest.* **69**:415-429.

32. Owen-Schaub, L.B., Radinsky, R., Kruzel, E., Berry, K., and Yonehara, S. (1994). Anti-Fas on nonhematopoietic tumors: levels of Fas/APO-1 and *bcl-2* are not predictive of biological responsiveness. *Cancer Res.* **54**:1580-1586.

33. Mapara, M.Y., Bargou, R., Zugek, C., Döhner, H., Ustaoglu, F., Jonker, R.R., Krammer, P.H., and Dorken, B. (1993). APO-1 mediated apoptosis or proliferation in human chronic B lymphocytic leukemia: correlation with *bcl-2* oncogene expression. *Eur. J. Immunol.* **23**:702-708.

34. Cheng, J., Zhou, T., Liu, C., Shapiro, J.P., Brauer, M.J., Kiefer, M.C., Barr, P.J., and Mountz, J.D. (1994). Protection from Fas-mediated apoptosis by a soluble form of the Fas molecule. *Science* **263**:1759-1762.

35. Liu, Y.-J., Mason, D.Y., Johnson, G.D., Abbot, S., Gregory, C.D., Hardie, D.L., Gordon, J., and MacLennan, I.C.M. (1991). Germinal center cells express *bcl-2* protein after activation by signals which prevent their entry into apoptosis. *Eur. J. Immunol.* **21**:1905-1910.

36. Rabizadeh, S., Oh, J., Zhong, L., Yang, J., Bitler, C.M., Butcher, L.L., and Bredesen, D.L. (1993). Induction of apoptosis by the low-affinity NGF receptor. *Science* **261**:345-348.

37. Ruan, Y., Camerini, D., and Bredesen, D. E. (1995). Expression of CD40 induces neural apoptosis. Neurochemistry, in press.

38. Sato, T., Irie, S., and Reed, J. C. (1995). A novel member of the TRAF family of putative signal transducing proteins binds to the cytosolic domain of CD40. *FEBS Letters*, in press.

39. Hu, H. M., O'Rourke, K., Boguski, M. S., and Dixit, V. M. (1994). A novel RING finger protein interacts with the cytoplasmic domain of CD40. *J. Biol. Chem.* **269**: 30069-30072.

40. Wong, G.H.W. and Goeddel., D.V. (1994). Fas antigen and p55 TNF receptor signal apoptosis through distinct pathways. *Am. Assoc. Immunologists* **152**:1751-1755.

41. Rothe, M., Wong, S. C., Henzel, W. J., and Goeddel, D. V. (1994). A novel family of putative signal transducers associated with the cytoplasmic domain of the 75 kDa tumor necrosis factor receptor. *Cell* **78**: 681-692.

42. Kim, M.-Y., Linardic, C., Obeid, L., and Hannun, Y. (1991). Identification of sphingomyelin turnover as an effector mechanism for the action of tumor necrosis factor a and g-interferon.: Specific role in cell differentiation. *J. Biol. Chem.* **266**:484-489.

43. Dressler, K. A., Mathias, S., and Kolesnik. (1992). Tumor necrosis factor-a activates the sphingomyelin signal transduction pathway in a cell free system. *Science*. **255**:1715-1718.

44. Mathias,- S., Younes, A., Kan, C.-C., Orlow, I., Joseph, C., and Kolesnick, R. N. (1993). Activation of the sphingomyelin signal pathway in intact EL4 cells and in a cell-free system by IL-1b. *Science*. **259**:519-522.

45. Cifone, M. G., Maria, R. D., Roncaioli, P., Rippo, M. R., Azuma, M., Lanier, L. L., Santoni, A., and Testi, R. (1994) Apoptotic signaling through CD95 (Fas/APO-1) activates an acidic sphingomyelinase. *J. Exp. Med.* **177**: 1547-1552.

46. Obeid, L. M., Linardic, C. M., Karolak, L. A., and Hannun, Y. A. (1993). Programmed cell death induced by ceramide. *Science* **259**: 1769-1771.

47. Fields, S., and Song, O. (1989). A novel genetic system to detect protein-protein interactions. *Nature* **340**: 245-246.

48. Vojtek, A. B., Hollenberg, S. M., and Cooper, J. A. (1993). Mammalian Ras interacts directly with the serine/threonine kinase Raf. *Cell* **74**: 205-214.

49. Ito, H., Fukuda, Y., Murata, K., and Kimura, A. (1983). Transformation of intact yeast cells treated with alkaline cations. *J. Bacteriol.* **153**:163-168.

50. Gietz, D., Jean, A.S., Woods, R.A., and Schiestl, R.H. (1992). Improved method for high efficiency transformation of intact yeast cells. *Nucl. Acids Res.* **20**:1425.

51. Schiestl, R.H. and Giest, R.D. (1989). High efficiency transformation of intact cells using single stranded nucleic acids as a carrier. *Curr. Genet.* **16**:339-346.

52. Breeden, L. and Nasmyth, K. (1985). Regulation of the yeast HO gene. *Cold Spring Harbor Symp. Quant. Biol.* **50**:643-650.

53. Maekawa, K., Imagawa, N., Nagamatsu, M., and Harada, S. (1994). Molecular cloning of a novel protein-tyrosine phosphatase containing a membrane-binding domain and GLGF repeats. *FEBS Letters* **337**:200-206.

54. Sato, T., Irie, S., Kitada, S., and Reed, J. C. (1995). FAP-1, a Protein Tyrosine Phosphatase that Associates with Fas. *Science*, in press.

55. Gould, K. L., Bretscher, A., Esch, F. S., and Hunter, T. (1989). cDNA cloning and sequencing of the protein-tyrosine kinase substrate, ezrin, reveals homology to band 4.1. *EMBO J.* **8**: 4133-4142.

56. Funayama, N., Nagafuchi, A., Sato, N., Tsukita, S., and Tsukita, S. (1991). Radixin is a novel member of the band 4.1 family. *J. Cell Biol.* **115**:1039-1048.

57. Lankes, W. T., and Furthmayr, H. (1991). Moesin: a member of the protein 4.1-talin-ezrin family of proteins. *Proc. Natl. Acad. Sci. U.S.A.* **88**:8297-8301.

58. Conboy, J. G., Chan, J. Y., Chasis, J. A., Kan, Y. W., and Mohandas, N. (1991). Tissue- and development-specific alternative RNA splicing regulates expression of multiple isoforms of erythroid membrane protein 4.1. *J. Biol. Chem.* **266**:8273-8280.

59. Yang, Q., and Tonks, N. K. (1991). Isolation of a cDNA clone encoding a human protein-tyrosine phosphatase with homology to the cytoskeletal-associated proteins band 4.1, ezrin, and talin. *Proc. Natl. Acad. Sci. U.S.A.* **88**: 5949-5953.

60. Gu, M. X., York, J. D., Warshawsky, I., and Majerus, P. W. (1991). Identification, cloning, and expression of a cytosolic megakaryocyte protein-tyrosine-phosphatase with sequence homology to cytoskeletal protein 4.1.*Proc. Natl. Acad. Sci. U.S.A.* **88**: 5867-5871.

61. Vogel, W., Lammers, R., Huang, J., and Ullrich, A. (1993). Activation of a phosphotyrosine phosphatase by tyrosine phosphorylation.*Science* **259**: 1611-1614.

62. Woods, D.F. and Bryant, P.J. (1991). The discs-large tumor suppressor gene of Drosophila encodes a guanylate kinase homolog localized at seperate junctions. *Cell* **66**: 451-464.

63. Cho, K.-O., Hunt, C.A., and Kennedy, M.B. (1992). The rat brain postsynaptic density fraction contains a homolog of the

Drosophila discs-large tumor suppressor protein. *Neuron* **9**: 929-942.

64. Gyuris, J., Golemis, E., Chertkov, H., and Brent, R. (1993). Cdil, a human G1 and S phase protein phosphatase that associates with Cdk2. *Cell* **75**: 791-803.

65. Zervous, A.S., Gyuris, J., and Brent, R. (1993). Mix1, a protein that specifically interacts with Max to bind Myc-Max recognition sites. *Cell* **72**:223-232.

66. Gorczyca, W., Bruno, S., Darzynkiewicz, R.J., Gong, J., and Darzynkiewicz, Z. (1992). DNA strand breaks occurring during apoptosis: Their early *in situ* detection by the terminal deoxynucleotidyl transferase and nick translation assays and prevention by serine protease inhibitors. *Int. J. Oncology* **1**: 639-648.

Reprint Series
21 April 1995, Volume 268, pp. 411–415

SCIENCE

FAP-1: A Protein Tyrosine Phosphatase That Associates with Fas

Takaaki Sato, Shinji Irie, Shinichi Kitada, and John C. Reed*

FAP-1: A Protein Tyrosine Phosphatase That Associates with Fas

Takaaki Sato, Shinji Irie, Shinichi Kitada, John C. Reed*

Fas is a cell surface receptor that controls a poorly understood signal transduction pathway that leads to cell death by means of apoptosis. A protein tyrosine phosphatase, FAP-1, capable of interacting with the cytosolic domain of Fas, was identified. The carboxyl terminal 15 amino acids of Fas are necessary and sufficient for interaction with FAP-1. FAP-1 expression is highest in tissues and cell lines that are relatively resistant to Fas-mediated cytotoxicity. Gene transfer–mediated elevations in FAP-1 partially abolished Fas-induced apoptosis in a T cell line. These findings are consistent with an inhibitory effect of FAP-1 on Fas signal transduction.

Fas (also known as APO-1 and CD95) is a cell surface receptor that is expressed on a variety of normal and neoplastic cells. It shares significant amino acid sequence homology with several members of the tumor necrosis factor receptor (TNFR) family, including p55-TNFR, CD40, and the p75–nerve growth factor receptor (NGFR), which have been shown to act as either inhibitors or inducers of cell death (*1*). The ligand for Fas is expressed predominantly on cytolytic T cells (*2*), suggesting that Fas plays a role in the effector branch of cellular immune responses. Mutations in the genes encoding Fas or its ligand have been associated with lymphoproliferative and autoimmune disorders in mice (*3*). Furthermore, alterations in Fas production have been associated with autoimmune disease in humans and susceptibility to induction of apoptosis of T cells in human immunodeficiency virus–infected persons (*4*).

Monoclonal antibodies specific against Fas induce apoptosis in many types of cells (*5*). However, in some cases antibodies to Fas stimulate cell proliferation (*6*, *7*), suggesting that the intracellular signal transduction pathways used by this receptor are subject to regulation. The cytosolic domain of Fas contains no similarity to known kinases or other enzymes that might transduce signals into cells. Deletion mapping analysis has identified a domain that is required for induction of apoptosis, which is called the "death domain." This domain shares homology with sequences located in the cytosolic domains of p55-TNFR1, CD40, and p75-NGFR (*8*). For some cells, apoptosis induced by antibodies to Fas is dependent on protein synthesis inhibitors such as cycloheximide (*8*). This implies either the existence of a labile protein that suppresses Fas-generated signals leading to cell death or the induction of proteins that inhibit the ability of Fas to trigger apoptosis. A negative regulatory domain has been mapped to the COOH-terminal 15 amino acids of Fas that is not homologous to other TNFR-like proteins; deletion of this domain can abrogate the dependence on protein synthesis inhibitors for apoptosis induced by antibody to Fas (*8*).

To identify complementary DNAs (cDNAs) encoding proteins that can potentially modulate the activity of Fas, we used a yeast two-hybrid system for cDNA library screening. We used the cytosolic domain of human Fas fused to a LexA DNA binding domain (*9*, *10*) and random cDNAs fused in frame with a VP16 transactivation domain. Using a His synthetase gene (*HIS3*) under the control of LexA operators as a reporter, we identified 395 His^+ colonies from an initial screen of 3×10^8 transformants. Of these, 84 were also positive when a *lacZ* gene (β-galactosidase) under the control of a LexA operator was used as an alternative reporter. Mating tests were then performed (*11*); only 2 of the 84 candidate clones (numbers 31 and 43) reacted with the cytosolic domain of Fas (Ta-

La Jolla Cancer Research Foundation, Oncogene and Tumor Suppressor Gene Program, La Jolla, CA 92037, USA.

*To whom correspondence should be addressed.

ble 1). These mouse cDNAs represented overlapping independent clones with insert sizes of 381 base pairs (bp) (clone 31) and 351 bp (clone 43); these clones share >95% homology with a human cDNA sequence encoding a protein tyrosine phosphatase (PTP) termed PTP-BAS (*12*).

PTP-BAS was originally cloned from human basophils by a reverse transcriptase–polymerase chain reaction (RT-PCR) method that used degenerate primers targeted against conserved sequences found in PTPs. Three isoforms arising from alternative splicing have been identified by cDNA cloning, the longest of which is predicted to encode a 2485–amino acid protein (*12*). PTP-BAS lacks a transmembrane domain but contains a membrane-binding domain similar to that found in the cytoskeleton-associated proteins ezrin, radixin, moesin, and protein 4.1, as well as in the PTPs PTPH1, PTP-MEG, and PTPD1 (*12*, *13*). In addition to a catalytic domain located near its COOH-terminus, PTP-BAS contains six repeats (Gly-Leu-Gly-Phe; GLGF) (Fig. 1). These structures are thought to mediate intra- and intermolecular interactions among protein domains and may play a role in targeting proteins to the submembranous cytoskeleton or in regulating enzyme activity (*12*). Both Fas-interacting clones 31 and 43 correspond to the third GLGF repeat in PTP-BAS (Fig. 1), suggesting that this domain mediates specific interactions with the cytosolic domain of Fas and implying that PTP-BAS is a Fas-associated phos-

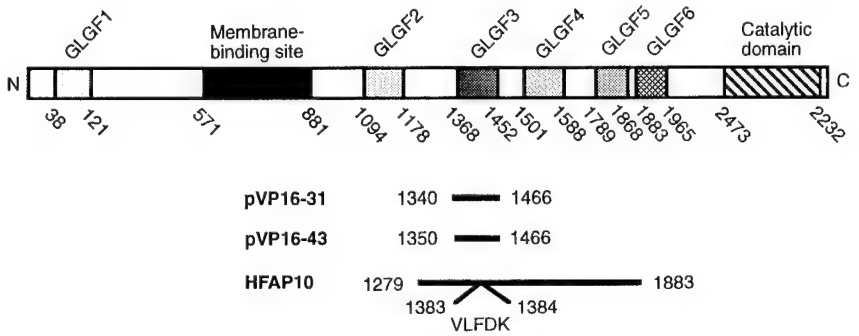

Fig. 1. Diagram of FAP-1 protein and cDNA clones. (**Top**) The structure of the 2485–amino acid human FAP-1 protein (also known as PTP-BAS type-1) (*12*), showing the locations of the catalytic, membrane-binding, and GLGF repeat domains (*12*, *13*). (**Bottom**) The cDNAs identified by two-hybrid screening of a mouse embryo cDNA library: pVP16-31 and pVP16-43 with encoded amino acids relative to the human FAP-1 protein. A human FAP-1 partial cDNA (encoding amino acids 1279 through 1883 of PTP-BAS type-1) from brain was cloned and found to contain a five–amino acid insert in the GLGF3 domain, as compared with the published sequence (*12*). V, Val; L, Leu; F, Phe; D, Asp; and K, Lys. GenBank accession numbers of pVP16-31, pVP16-43, and HFAP10 are L34581, L34582, and L34583, respectively. C, COOH-terminal; N, NH_2-terminal.

Table 1. Specific interaction of FAP-1 with the Fas cytosolic domain. L40 strain cells with pVP16-31 or pVP16-43 were cured of plasmid pBTM116-Fas and then mated with NA87-11A cells transformed with various pBTM116 plasmids as described (*24*). Growth was measured on His-deficient media, and color was measured by a β-galactosidase colorimetric filter assay (*22*).

Proteins	pVP16	Growth	Color
Fas(191–335)	31 and 43	+	Blue
Ras(V12)	31 and 43	–	White
Ras(L35R37)	31 and 43	–	White
CD40(216–277)	31 and 43	–	White
CD40(225–269)	31 and 43	–	White
Bcl-2(83–218)	31 and 43	–	White
Lamin	31 and 43	–	White
Ras(V12)	c-Raf	+	Blue
Lamin	c-Raf	–	White

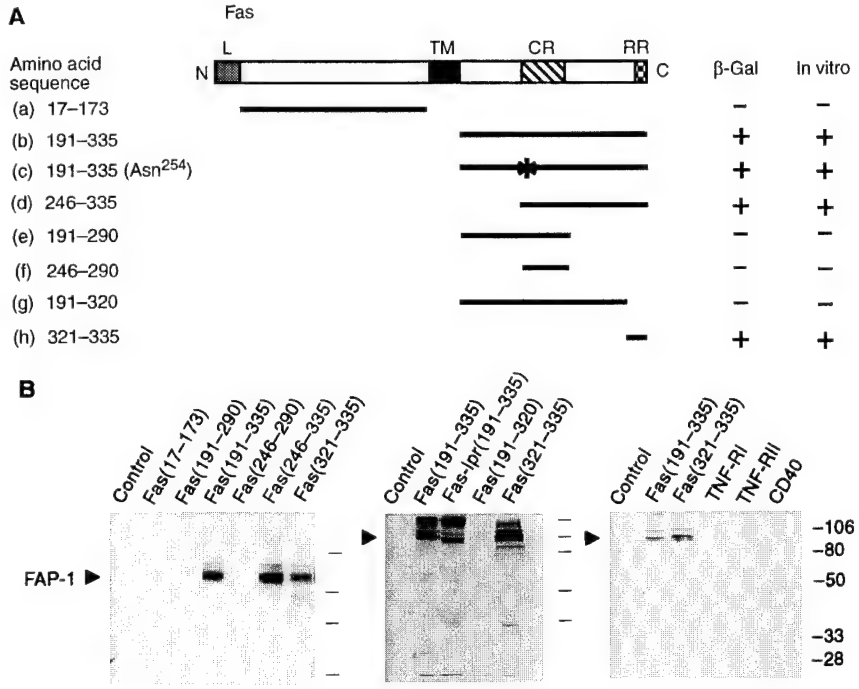

Fig. 2. Mapping of the site on Fas involved in binding to the GLGF3 domain of FAP-1. (**A**) The structure of the Fas protein is depicted with the relative locations of its leader sequence (L), transmembrane domain (TM), conserved cytosolic regions (CR), and unique regulatory region (RR) indicated. A series of Fas deletion mutants were generated (*14*) that contained (a) the extracellular domain of Fas minus its leader sequence (amino acids 17 through 173); (b) the complete cytosolic domain of Fas (191 through 335); (c) a cytosolic domain mutant containing a Val→Asn^{254} mutation (indicated by an asterisk), analogous to an identified mutant allele of Fas in the cg-strain of *lpr* autoimmune mice, which has been shown to be deficient in Fas-mediated induction of apoptosis (*8*); (d) a deletion mutant (246 through 335) lacking the sequences between the TM of Fas and the CR that are required for the induction of apoptosis (*8*); (e) a COOH-terminal deletion mutant (191 through 290) that contains sequences from the TM to the end of the CR; (f) a mutant containing only the CR of Fas (246 through 290); (g) a truncation mutant lacking the COOH-terminal 15 amino acids (191 through 320) that have been shown to constitute a negative RR in Fas (*8*); and (h) a mutant containing only the COOH-terminal 15 amino acids of Fas (321 through 335). They were expressed in L40 strain yeast cells as LexA DNA binding domain fusion proteins with VP16–FAP-1 (clone 31). Protein-protein interactions were detected through the use of a *lacZ* reporter gene under the control of LexA operators with β-galactosidase plate and filter assays (*22*) and scored as positive (blue, +) or negative (white, –). Essentially identical results were obtained in EGY48 strain yeast (*25*). (**B**) These same Fas cDNAs were also subcloned in frame into either pGEX–4T-1 or pGEX–2T-1 and expressed as GST fusion proteins in *E. coli* (*15*). The indicated affinity-purified GST-Fas fusion proteins immobilized on glutathione-Sepharose were incubated with ^{35}S-labeled human FAP-1 protein fragment (1323 through 1883), and specifically bound proteins were detected by SDS-PAGE analysis (*16*) and scored as either positive for binding (+) or negative (–) in (A). Examples of autoradiography results from an SDS-PAGE of samples from the in vitro binding assays are shown. GST nonfusion protein was used as a control. Molecular size markers are shown at right in kilodaltons.

phatase. We therefore called it FAP-1.

To determine the region in the cytosolic domain of Fas that is required for binding to the GLGF3 domain of FAP-1, we prepared a series of Fas deletion mutants that were expressed in yeast as fusion proteins with the LexA DNA binding domain (Fig. 2A) (*14*). When tested in the two-hybrid system, the polypeptide encoded by the longer of the FAP-1 cDNAs (pVP16-31) mediated interactions with LexA fusion proteins containing only the last 15 amino acids of Fas (amino acids 321 through 335) but not with Fas mutants lacking the COOH-terminal 15 amino acids. Thus, the 15–amino acid COOH-terminus of Fas that functionally represents a negative regulatory domain appears to be both necessary and sufficient for interactions with the GLGF3 domain of Fas.

To confirm these two-hybrid results, we performed in vitro binding assays. The Fas deletion mutants were expressed in *Escherichia coli* as glutathione-S-transferase (GST) fusion proteins, affinity-purified on glutathione-Sepharose (*15*), and tested for binding to a ^{35}S-L-Met–labeled fragment of the human FAP-1 protein (amino acids 1323 through 1883) prepared by translation in vitro (*16*). The human FAP-1 partial cDNA used for preparation of in vitro–translated protein was obtained by hybridization screening of a human fetal brain cDNA library (*17*). It contained a five–amino acid insert in the GLGF3 domain, relative to the published PTP-BAS sequence, and presumably therefore represents a different isoform of this PTP that is expressed in brain (Fig. 1). Using this in vitro binding assay approach, we obtained results identical to those with the two-hybrid system: The last 15 amino acids of Fas were found to be both necessary and sufficient for binding to the FAP-1 fragment (Fig. 2B). Moreover, no interaction was detected with GST fusion proteins containing the cytosolic domains of p55-TNFRI, p75-TNFRII, or CD40 (*18*).

The finding that FAP-1 interacts with

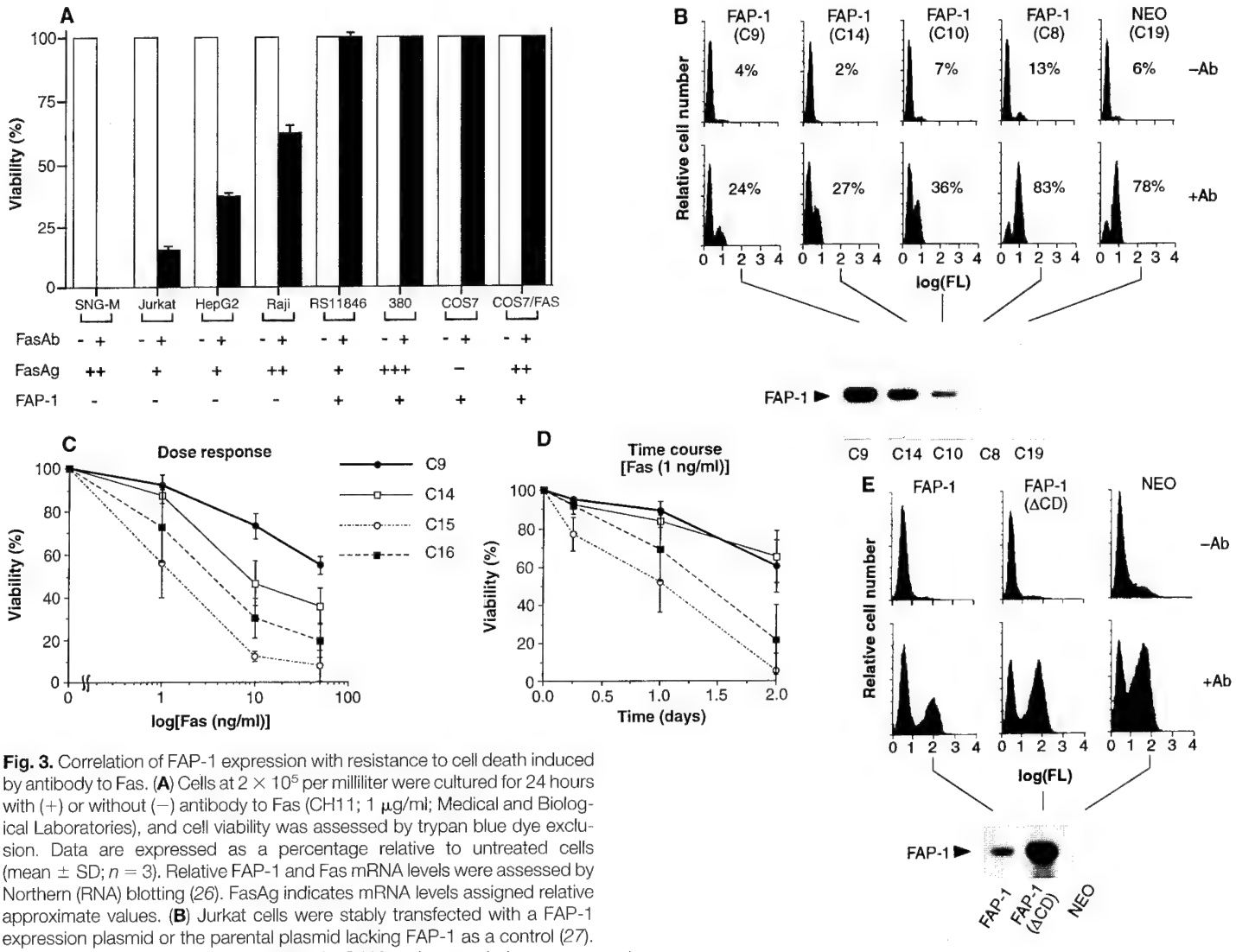

Fig. 3. Correlation of FAP-1 expression with resistance to cell death induced by antibody to Fas. (**A**) Cells at 2×10^5 per milliliter were cultured for 24 hours with (+) or without (−) antibody to Fas (CH11; 1 μg/ml; Medical and Biological Laboratories), and cell viability was assessed by trypan blue dye exclusion. Data are expressed as a percentage relative to untreated cells (mean ± SD; $n = 3$). Relative FAP-1 and Fas mRNA levels were assessed by Northern (RNA) blotting (*26*). FasAg indicates mRNA levels assigned relative approximate values. (**B**) Jurkat cells were stably transfected with a FAP-1 expression plasmid or the parental plasmid lacking FAP-1 as a control (*27*). The relative levels of FAP-1 expression in G418-resistant subclones were then determined by a RT-PCR assay (bottom) (*28*). Data shown are derived from a single exposure of the same blot (lanes reordered for clarity of presentation). Transfected clones were incubated with or without (Ab) CH11 (50 ng/ml), and the TUNEL assay was performed 4 hours later (*19*). Representative histograms are shown (top). Clones C8, C9, C10, and C14 received the FAP-1 plasmid pRc/CMV–FAP-1, whereas clone C19 was transfected with the parental pRc/CMV plasmid (NEO). Data are representative of multiple clones. A control immunoglobin M (IgM) antibody (MOPC-104E; Cappel) did not induce DNA fragmentation and apoptosis in Jurkat cells (*23*). FL, fluorescence. (**C**) FAP-1 transfectant clones C9 and C14 were compared with Neo-transfected control clones C15 and C16 with regards to survival [determined by trypan blue dye exclusion (mean ± SD; $n = 3$)] when cultured for ~1 day with various concentrations of CH11 antibody (zero equals no antibody) (C) or for various times with CH11 antibody (1 ng/ml) (**D**). Cell viability was >95% for cells treated with an IgM control antibody (*23*). (**E**) TUNEL assays and RT-PCR analyses were performed as described in (B) with untransfected Jurkat cells and bulk transfectants that expressed either full-length FAP-1 or a truncated FAP lacking the catalytic domain (ΔCD) (*27*).

the COOH-terminal negative regulatory domain of Fas suggests that this PTP may somehow inhibit Fas-generated signals that lead to apoptosis. To explore this possibility, we correlated the presence or absence of FAP-1 expression with relative sensitivity to apoptosis induced by antibody to Fas in a variety of cell lines that express Fas. Four of four tumor cell lines (SNG-M, Jurkat, HepG2, and Raji) that lacked FAP-1 mRNA, as determined by Northern (RNA) blotting, were sensitive to variable extents to induced cell death caused by antibody to Fas (Fig. 3A). In contrast, all three tumor lines tested which expressed FAP-1 (RS11846, 380, and COS-Fas) were completely resistant to antibody to Fas. This resistance could not be explained by differences in the relative levels of Fas antigen expressed on the surface of the cells, as determined by immunofluorescence flow cytometric analysis.

Next, a cDNA encoding the full-length FAP-1 protein was expressed in a Fas-sensitive clone from the T cell leukemia line Jurkat. Analysis of several independent transfected clones revealed a correlation between the levels of FAP-1 expression and relative resistance to Fas-mediated cytotoxicity. Some representative clones were treated with antibody to Fas for 4 hours and DNA fragmentation indicative of apoptosis was detected by TUNEL assay (*19*); resistance to Fas-mediated apoptosis was demonstrated in clones with higher levels of FAP-1 expression (Fig. 3B). Transfected Jurkat clones with high levels of FAP-1 expression withstood higher concentrations of antibody than control cells did (Fig. 3C) and remained viable for longer periods of time when cultured with antibody to Fas (Fig. 3D). In contrast to Jurkat cells which expressed full-length FAP-1, transfectants expressing a truncated version of FAP-1 lacking the catalytic domain were not protected from Fas-induced DNA degradation (Fig. 3E). Relative levels of Fas expression were equivalent for all subclones shown, on the basis of immunofluorescence flow cytometric assays.

Although other factors besides FAP-1 may contribute to the inhibition of Fas signal transduction events involved in the induction of apoptosis (*7*, *20*), the data presented here support the idea that FAP-1 is a negative regulator of Fas-induced pathways that lead to cell death. This finding therefore implies the involvement of a protein tyrosine kinase (PTK) in some aspect of Fas-mediated cytotoxicity. It has been reported that Fas-induced apoptosis is accompanied by rapid tyrosine phosphorylation of proteins in T cells and can be blocked by pharmacological inhibitors of PTKs (*21*). Presumably, therefore, an antagonistic relation between this unknown PTK and FAP-1 influences the relative sensitivity of cells to apoptosis induced by antibody to Fas.

REFERENCES AND NOTES

1. C. A. Smith, T. Farrah, R. G. Goodwin, *Cell* **76**, 959 (1994).
2. T. Suda, T. Takahashi, P. Golstein, S. Nagata, *ibid.* **75**, 1169 (1993).
3. R. Watanabe-Fukunaga, C. I. Brannan, N. G. Copeland, N. A. Jenkins, S. Nagata, *Nature* **356**, 314 (1992); T. Takahashi *et al.*, *Cell* **76**, 969 (1994); D. H. Lynch *et al.*, *Immunity* **1**, 131 (1994).
4. J. Cheng *et al.*, *Science* **263**, 1759 (1994).
5. S. Yonehara, A. Ishii, M. Yonehara, *J. Exp. Med.* **169**, 1747 (1989); B. C. Trauth *et al.*, *Science* **245**, 301 (1989); N. Itoh *et al.*, *Cell* **66**, 233 (1991).
6. M. R. Alderson *et al.*, *J. Exp. Med.* **178**, 2231 (1993).
7. M. Y. Mapara *et al.*, *Eur. J. Immunol.* **23**, 702 (1993); L. B. Owen-Schaub, R. Radinsky, E. Kruzel, K. Berry, S. Yonehara, *Cancer Res.* **54**, 1580 (1994).
8. N. Itoh and S. Nagata, *J. Biol. Chem.* **268**, 10932 (1993).
9. A. B. Vojtek, S. M. Hollenberg, J. A. Cooper, *Cell* **74**, 205 (1993).
10. Two-hybrid screens were performed essentially as described (*9*) in L40 strain cells [*MATa, trp1, leu2, his3, ade2, LYS2:(lexAop)*^{4}-HIS3, URA3::(lexAop)^8-lacZ] with plasmid pBTM116 containing a human Fas cDNA (amino acids 191 through 335) subcloned in frame with the LexA open reading frame (ORF) and a mouse embryo cDNA library cloned into pVP16. Clones that formed on His-deficient media (His$^+$) were transferred to plates containing X-gal (40 μg/ml), resulting in 84 clones that produced a blue reaction product (β-Gal$^+$) in plate and filter assays (*22*).
11. We cured the 84 His$^+$, β-Gal$^+$ clones of the LexA-Fas plasmid by growing cells in Trp-containing medium and then mating them against a panel of α type yeast, strain NA87-11A (*MATα, leu2, his3, trp1, pho3, pho5*) containing plasmid pBTM116 that produced LexA DNA binding domain fusion protein containing Fas (amino acids 191 through 335), portions of the CD40 cytosolic domain, Bcl-2 protein, lamin, and mutant Ha-Ras proteins (*22*). Mated cells were selected for growth in medium that lacked Trp (pBTM116 plasmid) and Leu (pVP16 plasmid) and tested for the ability to trans-activate a *lacZ* reporter gene by a β-Gal colorimetric filter assay (*22*).
12. K. Maekawa, N. Imagawa, M. Nagamatsu, S. Harada, *FEBS Lett.* **337**, 200 (1994); N. P. H. Moller, *et al.*, *Proc. Natl. Acad. Sci. U.S.A.* **91**, 7477 (1994).
13. The original description of PTP-BAS (*12*) indicated only three GLGF repeat domains, but our analysis with the DNA Strider program (version 1.2) (CEA, France) suggests the presence of six GLGF repeat domains in this PTP.
14. The cDNA sequences encoding various fragments of human Fas were generated by PCR with the following forward (F) and reverse (R) primers containing Eco RI (underlined) and Bcl 1 (italic) sites (bold indicates the stop codon, TCA); F1, 5′-GGAATTCAGATTATCGTCCAAAAGTG-3′; F2, 5′-GGAATTCAAGAGAAAGGAAGTACA-3′; F3, 5′-GGAATTCAAAGGCTTTGTTCGAAAG-3′; R1, 5′-GTGA**TCA**GTTAGATCTGGATCCTTC-3′; R2, 5′-GTGA**TCA**CGCTTCTTTCTTTCCATG-3′; R3, 5′-GTGA**TCA**CTAGACCAAGCTTTGGAT-3′; HFAS-*lpr* (Asn^{254}, 5′-TTCGAAAGAATGGTAACAATGAAGCCAAA-3′; HFAS-15F, 5′-AATTCGACTCAGAAAATTCAAACTTCAGAAATGAAATCCAAAGCTTGGTCTAG-3′; and HFAS-15R, 5′-TCGACTAGACCAAGCTTTGGATTTCATTTCTGAAGTTTGAATTTTCTGAGTCG-3′. We used the following combinations of primers to produce the indicated human Fas cDNA fragments: (a) F1 and R1, amino acids 17 through 173; (b) F2 and R3, 191 through 335; (c) F2 and R3 and Fas-*lpr* (Asn^{254}); (d) F3 and R3, 246 through 335; (e) F2 and R2, 191 through 290; (f) F3 and R2, 246 through 290; (g) Fas/APO-1 (191 through 320), which was generated by restriction endonuclease digestion with Spe I, followed by treatment with T4 DNA polymerase to generate a stop codon; and (h) Fas-15F and Fas-15R, 321 through 335. These Fas deletion mutant cDNAs were subcloned into the Eco RI and Bam HI sites of pEG202 [A. S. Zervous, J. Gyuris, R. Brent, *Cell* **72**, 223 (1993)] in frame with the LexA ORF, the results were confirmed by DNA sequencing, and then the cDNAs were excised with Eco RI and Sal I and subcloned into pBTM116 in frame with LexA.
15. The Fas cDNAs described in (*14*) were subcloned into the Eco RI and Xho I sites of either pGEX-2T-1 or pGEX-4T-1 in frame with the ORF of GST and expressed in DH5αF′ or HB101 cells (BRL/Gibco) by induction with 1 mM isopropyl-β-D-thiogalactopyranoside (IPTG) for 8 to 16 hours at 30°C. GST fusion proteins were purified from bacterial lysates with glutathione–Sepharose 4B (Pharmacia, Piscataway, NJ).
16. The HFAP10 cDNA was subcloned into the Eco RV site of Bluescript pSK-II and in vitro translated from an internal Meth (amino acid 1323) in the presence of [^{35}S]-L-Meth with a coupled transcription-translation system (TNT lysate, Promega) and T7 RNA polymerase, resulting in the production of a human FAP-1/β-Gal fusion protein that was incubated with GST-Fas fusion proteins immobilized on glutathione-Sepharose in 50 mM tris (pH 8.0), 150 mM NaCl, 5 mM dithiothreitol (DTT), 2 mM EDTA, 0.1% NP-40, 1 mM phenylmethylsufonyl fluoride, and leupeptin (1 μg/ml) for 16 hours at 4°C. The beads were then vigorously washed five times in the same solution, pelleted by centrifugation, and boiled in Laemmli sample buffer before analysis by SDS–polyacrylamide gel electrophoresis (PAGE) and fluorography.
17. A human fetal brain cDNA library in λgt11 was screened with the ^{32}P-labeled insert from pVP16-31 used as a hybridization probe, resulting in four independent human Fas partial cDNA clones; HFAP10 is the longest.
18. The cDNA sequences encoding the human CD40 were generated by PCR with the following F and R primers containing Eco RI (underlined) and Bcl I (italic) sites (bold indicates the stop codon, TCA): CD40 (amino acids 216 through 277), 5′-GGAATTCAAAAAGGTGGCCAAG-3′ (F2) and 5′-TGATCA**TCA**CTGTCTCTCCTGCAC-3′ (R2); CD40 (225 through 269), 5′-GGAATTCAAGGCCCCCCACCCCAAG-3′ (F1) and 5′-TGA**TCA**ACTCTCTTTGCCATCCTC-3′ (R1). The PCR products were digested with Eco RI and Bcl I, then directly cloned into the Eco RI and Bam HI site of pBTM116. The Eco RI and Sal I fragments from pBTM116-CD40 were also subcloned into the Eco RI and Sal I sites of pGEX4T-1 (Pharmacia) for the expression of GST-CD40 proteins.
19. W. Gorczyca, J. Gong, Z. Darzynkiewicz, *Cancer Res.* **53**, 1945 (1993).
20. N. Itoh, Y. Tsujimoto, S. Nagata, *J. Immunol.* **151**, 621 (1993); C. L. Klas, K.-M. Debatin, R. R. Jonker, P. H. Krammer, *Int. Immunol.* **5**, 625 (1993); S. Takahashi *et al.*, *Eur. J. Immunol.* **23**, 1935 (1993); S. Takayama *et al.*, *Cell* **80**, 279 (1995).
21. C. M. Eischen, C. J. Dick, P. J. Leibson, *J. Immunol.* **153**, 1947 (1994).
22. T. Sato *et al.*, *Proc. Natl. Acad. Sci. U.S.A.* **91**, 9238 (1994).
23. T. Sato, S. Irie, S. Kitada, J. C. Reed, unpublished data.
24. L40 strain cells containing pVP16-31 or pVP16-43 were cured of plasmid pBTM116-Fas (amino acids 191 through 335) by growth on Trp and then mated with NA87-11A cells transformed with various pBTM116 plasmids producing LexA DNA binding domain fusion proteins containing portions of the Fas, CD40, Bcl-2, lamin, or mutant Ras proteins as indicated (*11*). Interactions of LexA and VP16 fusion proteins were detected by growth on His-deficient media and by a β-galactosidase colorimetric filter assay (*22*) based on the ability to trans-activate HIS3 and *lacZ* reporter genes containing LexA operators. L40 cells producing a VP16-Raf fusion protein served as a positive control when mated with NA87-11A cells containing pBTM116-Ras(V12) (*9*).
25. The Fas cDNAs described in (*14*) in pEG202 was cotransformed with pVP16-31 into EGY48 cells (*MATα trp1 ura3 his3 LEU2::pLexAop6-LEU2*) containing pSH18-34 (Gal1 promoter–*lacZ* with eight LexA operators), and β-galactosidase activity

was assessed by colorimetric plate and filter assays (*22*).

26. Total RNA (20 μg) isolated from various cell lines was subjected to Northern blot assay with ^{32}P-labeled HFAP10 probe, and the results were scored as detectable or undetectable. All cell lines expressed Fas antigen as determined by both flow cytometric immunofluorescence assay with antibody to Fas DX2 (*23*) and by Northern blotting with a ^{32}P-labeled Fas cDNA probe.
27. A cDNA encoding the full-length FAP-1 protein was constructed with a series of four overlapping PCR reactions and DNA derived from a λgt11 fetal brain cDNA library. The 5′- and 3′-flanking primers contained Not I sites that were used for subcloning downstream of the cytomegalovirus (CMV) promoter in pRc/CMV, an expression plasmid that contains a G418 resistance gene (Invitrogen). Jurkat cells were electroporated with 25 μg of pRc/CMV or pRc/CMV–FAP-1, and stable transfectants were obtained by selection in G418 (0.8 mg/ml). Independent clones were obtained by limiting dilution. In addition, a cDNA encoding a COOH-terminal–truncated FAP-1 protein was created by introduction of a stop codon after position 2225. The cDNAs encoding the full-length and truncated FAP-1 proteins were subcloned into pREP-9 (Invitrogen) and expressed in Jurkat cells.
28. Total RNA was isolated from individual transfectant clones and 3 μg was reverse transcribed with a FAP-1–specific primer (5′-AGGTCTGCAGAGAAGCAAGAATAC-3′). PCR amplification was then performed for 25 cycles with the same R and a F primer (5′-GAATACGAGTGTCAGACATGG-3′). The resulting PCR products (607 bp) were subjected to agarose gel electrophoresis and analyzed by Southern (DNA) blotting with a ^{32}P–end-labeled internal FAP-1 oligonucleotide probe (5′-CTAACTCCATTGACAGCTAGGA-3′).

29. We thank P. Krammer for Fas cDNA; C. Ware for GST-TNFRI and TNFRII (University of California at Riverside); S. Hollenberg and E. Golemis for the two-hybrid systems; N. Iwama, H. Kobayashi, and L. Fong for technical assistance; and the Council for Tobacco Research (CTR-3113) for its support. T.S. is fellow of the U.S. Army Medical Research and Development Command, Breast Cancer Research Program. J.C.R. is a Scholar of the Leukemia Society of America.

23 November 1994; accepted 10 January 1995

FEBS Letters 358 (1995) 113–118

A novel member of the TRAF family of putative signal transducing proteins binds to the cytosolic domain of CD40

Takaaki Sato**, Shinji Irie**, John C. Reed*

La Jolla Cancer Research Foundation, Oncogene & Tumor Suppressor Gene Program, 10901 N. Torrey Pines Road, La Jolla, CA 92037, USA

Received 11 November 1994

Abstract **CD40 is a member of the tumor necrosis factor receptor (TNF-R) family that regulates B-lymphocyte proliferation, immunoglobulin class-switching, and apoptosis through poorly defined signal transduction mechanisms. Using a yeast two-hybrid method, cDNAs were obtained that encode a novel protein, CD40-associated protein-1 (CAP-1), which binds specifically to the cytosolic domain of CD40 but not TNF-R1, TNF-R2, or Fas. The CAP-1 protein contains a C-terminal domain that shares strong amino acid sequence homology with a unique domain found recently in two putative signal transducing proteins that bind to the TNF-R2 cytosolic tail, TRAF1 and TRAF2. This C-terminal region of CAP-1 was sufficient to mediate binding to CD40 and homodimerization of CAP-1 proteins. The N-terminal portion of CAP-1 contains a RING finger motif and three zinc finger-like domains similar to those found in several regulatory proteins that interact with DNA or RNA. CAP-1 thus represents a new member of a family of potential signal transducing proteins that contain a conserved domain (the TRAF domain), bind to the cytosolic regions of particular members of TNF-R family proteins, and that can form homo- and heterotypic dimers.**

Key words: CD40; TRAF; Signal transduction

1. Introduction

CD40 is a ~50-kDa glycoprotein receptor that is expressed on the surface of B-lymphocytes, some activated T-cells, monocytes, follicular dendritic cells, basal epithelial cells as well as some epithelial and non-epithelial carcinomas. The functions of this receptor have been most extensively studied in B-cells, where it is believed to play an important role in regulation of proliferation and apoptosis, immunoglobulin class-switching, generation of memory B-cells, modulation of cytokine gene expression, and cell adhesion (reviewed in [1–3]). The ligand for CD40 is expressed on the surface of activated helper T-cells, as well as mast cells and basophils, as a type-II transmembrane glycoprotein [4–6]. CD40-L thus triggers CD40 through a mechanism involving cell–cell contact. The importance of the CD40/CD40-L interaction for the regulation of T-cell-dependent humoral immune responses has been demonstrated by experiments where antibodies to CD40-L were shown to inhibit the generation of primary and secondary humoral immune responses [7]. Moreover, mutations in the CD40-L in humans cause an X-linked immunodeficiency syndrome characterized by excess production of IgM and absence of production of IgG, IgA, and IgE caused by a failure of B-cells to undergo Ig class-switching [8–10]. Thus, CD40-L/CD40 interactions appear to be essential for Ig class switching in vivo. Likewise, transgenic mice with homozygous disruptions of their CD40 genes fail to form germinal centers and do not produce IgG, IgA, and IgE response to thymus-dependent antigens but can mount normal IgM and IgG responses to T-independent antigens [11]. Antibodies to CD40-L prevent collagen-induce arthritis in animal model [12], suggesting that inhibition of CD40-triggering could provide a means of therapeutically intervening in some types of autoimmune dieases. The expression of CD40-L on mast cells and basophils has also been reported to mediate induction of IgE synthesis by B-cells when co-stimulated with IL-4 [6], implying an important role for CD40-L/CD40 interactions in atopic diseases.

CD40 and its ligand are members of the Tumor Necrosis Factor Receptor (TNF-R) family and TNF-family, respectively. The TNF-R family includes the p50/55-TNF-R1, p75/80-TNF-R2, p75-Nerve Growth Factor (NGF) Receptor, CD27, CD30, Fas, among others [13]. The predicted cytoplasmic domain of CD40 contains just 62 amino-acids and bears no resemblance to kinases or other enzymes that might suggest a mechanism by which this protein transduces signals into cells [14]. A region within the cytoplasmic domain of CD40 however has limited homology to a conserved domain found in the cytosolic tails of p75-NGF-R (22%), TNF-R1(31%), and Fas (41%). In TNF-R1 and Fas, this conserved domain is required for induction of signals resulting in cell death [15,16]. Interestingly, though best known for their roles in generating signals that suppress apoptosis, both CD40 and p75-NGF-R have been shown to paradoxically accelerate apoptosis when ectopically expressed in certain neural cell lines in the absence of ligands [17,18]. In these same cells, CD40 and p75-NGF-R can also delay cell death relative to untransfected cells when triggered with appropriate ligands. Thus, it is possible that CD40 and NGF-R (like TNF-R and Fas) can regulate signal transduction pathways leading to cell death under some circumstances. To gain further insights into the mechanisms by which CD40 transduces signals into cells, we used a yeast two-hybrid approach to clone cDNAs that encode proteins capable of specifically binding to the cytosolic domain of this receptor. A novel protein was thus discovered which we have termed CAP-1 for CD40-associated protein-1.

2. Materials and methods

2.1. Plasmid constructions

The cDNA encoding various fragments of CD40 were generated by PCR from the plasmid pCDM8-CD40 (gift of B. Seed) [14] using the following forward (F) and reverse (R) primers containing *Eco*RI (underlined) and *Bcl*I (italic) sites (bold indicates stop codon): CD40 (216–277), 5′-GGAATTCAAAAAGGTGGCCAAG-3′ (F1) and 5′-*TGATCA*TCACTGTCTCTCCTGCAC-3′(R1); and CD40 (225–269),

*Corresponding author. Fax: (1) (619) 455-0181.

**Drs. Sato and Irie contributed equally to the work described herein.

SSDI 0014-5793(94)01406-X

5′-GGAATTCAAGGCCCCCCACCCCAAG-3′ (F2) and 5′-*TGATC*AACTCTCTTTGCCATCCTC-3′ (R2). The PCR products were digested with *Eco*RI and *Bcl*I, then directly cloned into the *Eco*RI and *Bam*HI sites of the yeast two hybrid plasmid pBTM 116 (gift of S. Hollenberg, U. Washington; Seattle) in frame with the upstream LexA DNA-binding domain sequences [19]. For expression of LexA-Fas and LexA-TNF-R2 fusion proteins in yeast, the cytosolic domains of Fas and TNF-R2 were amplified by PCR from the plasmids pBS-APO14.1 (gift of P. Krammer) and pBluescript-p80-TNF-R2 (gift of C. Smith, Immunex, Inc., Seattle, WA), respectively, using the primers 5′-GGAATTCAAGAGAAAGGAAGTACA-3′(forward/Fas) and 5′-*GTGATC*ACTAGACCAAGCTTTGGAT-3′ (reverse/Fas) and 5′-GGAATTCAAAAAGAAGCCCTTGTGCCT-3′ (forward/TNF-R2) and 5′-G*GTCGACTTA*ACTGGGCTTCATCCCA-3′(reverse/TNF-R2). The Fas PCR product was digested with *Eco*RI and *Bcl*I and cloned into *Eco*RI/*Bam*HI-digested pBTM-116, whereas the TNF-R2 PCR product was digested with *Eco*RI and *Sal*I and cloned into *Eco*RI/*Xho*I-digested pBTM 116. Additional pBTM 116 plasmids encoding portions of the Bcl-2, Ha-Ras (V12), and Lamin-C proteins have been described [19,20].

For expression as GST-fusion proteins in *E. coli*, the pBTM 116-CD40 (225–269), Fas, and TNF-R2 plasmids were digested with *Eco*RI and either *Xho*I or *Sal*I and the inserts subcloned in-frame with the upstream GST sequences in pGEX-4T-1. For GST-CD40(220–277), a *Bal*I fragment encoding amino-acids 220–277 was excised from pCDM8-CD40 and subcloned initially into the *Hinc*II site of Bluescript pSKII (Stratagene, Inc., La Jolla, CA). The pSKII-CD40/*Bal*I plasmid was then cut with *Xho*I and *Eco*RI and the CD40 sequences subcloned into a modified verion of pGEX-2T-1 in frame with the GST sequences. For GST-TNF-R1, the cytoplasmic domain of TNF-R1 was PCR amplified from the plasmid pUC19-p55-TNF-R1 (gift of W. Lesslauer; Hoffmann La-Roche Inc., Basal, Switzerland) using the primers 5′-G*GGATCC*GCTACCAACGGTGGAAG-3′ (forward/TNF-R1) and 5′-G*GTCGACT*CATCTGAGAAGACTGGG-3′ (reverse/TNF-R1), digested with *Bam*HI and *Sal*I and subcloned into pGEX-5X-1. For GST-CAP-1, the pACT-2229 cDNA was digested with *Bgl*II, and the CAP-1 cDNA (363–543) was subcloned into pGEX-3X.

2.2. Two-hybrid assays

Library screening by the yeast two-hybrid methods was performed as described [19,21] using a human B-cell library in lambda-ACT (gift of S. Elledge, Baylor; Houston, TX) and L40 strain *S. cerevisiae* [*MATa, trp1, leu2, his3, ade2, LYS2:(lexAop)*^{4}*-HIS3, URA3::(lexAop)*^{8}*-lacZ*]. Cells were grown in either YPD medium with 1% yeast extract, 2% polypeptone, and 2% glucose, or in Burkholder's minimal medium fortified with appropriate amino-acids as described previously [20]. Transformations were performed by a LiCl method using 0.5 mg of pACT-cDNA library DNA, 1 mg of denatured salmon sperm carrier DNA, and ~5×10^9 L40-strain cells. The mating strain was NA87–11A (*MATα, leu2, his3, trp1, pho3, pho5*) which had been transformed with pBTM116 plasmids producing CD40 cytoplasmic domain or various control proteins and selected on tryptophan-minus media. To confirm the specificity of interactions, 5 μg of various pBTM116 plasmids and 5 μg of either pACT-121 or pACT-2229 were transformed into L40 cells and plated on semi-solid media lacking tryptophan and leucine. Colonies were then transfered to histidine-deficient plates or histidine-containing media with X-gal. β-Galactosidase plate assays were performed ~12 h later and filter assays hrs later as described previously [20].

2.3. In vitro protein-binding assays

The CAP-1 cDNA was PCR amplified using a forward primer containing a T7 promoter (5′-TAATACGACTCACTATAGGGAGACCACATGGATGATGTATATAACTATCATTTC-3′) and a reverse primer (5′-CTACCAGAATTCGGCATGCCGGTAGAGGTGTGGTCA-3′) from 1 μg of pACT-2229 plasmid DNA. One-tenth of the resulting PCR product (~0.1 μg) was then directly transcribed and translated in vitro in the presence of [^{35}S]methionine using 12.5 μl of reticulocyte lysate (TNT-Lysate; Promega, Inc.; Madison, WI). Glutathione-Sepharose bead containing 5 μg of GST fusion proteins were incubated with 10 μl of in vitro translated protein in 50 mM Tris (pH 8.0), 150 mM NaCl, 5 mM DTT, 2 mM EDTA, 0.1% NP-40, 1 mM PMSF, and 1 μg/ml leupeptin for 16 h at 4°C. The beads were washed vigorously 5× in the same solution, pelleted by centrifugation, and boiled in Laemmli sample buffer before analysis by SDS-PAGE and fluorography.

For experiments with cell lysates, 2×10^7 RS11846 B-cell lymphoma cells were lysed in 0.25 ml of ice-cold 10 mM Tris (pH 7.4), 150 mM NaCl, 5 mM EDTA, 1% Triton X-100, with protease inhibitors (PMSF, aprotinin, leupeptin, benzamidine, and pepstatin) and nuclei and debris were removed by centrifugation as described. The resulting supernatants were then incubated with 5 μg of affinity-purified GST-CAP-1 (363–543) or GST-control protein immobilized on 50 μl of glutathione-Sepharose beads for ~16 h at 4°C, then washed × 10 in 50 mM Tris (pH 7.4), 150 mM NaCl, 5 mM EDTA, 0.1% NP-40, 1 mM PMSF, 1 μg/ml leupeptin. Proteins adsorbed to beads were then boiled in Laemmli sample buffer and analyzed by SDS-PAGE (12% gels) and transfered to nitrocellulose. The resulting blots were preblocked in Tris-buffered saline (pH 7.4) containing 5% non-fat milk and 3% bovine serum albumin (BSA) and then incubated with 2 μl/ml of anti-human CD40 monoclonal antibody B-B20 (Biosource, Inc.; Camarillo, CA) followed by horseradish peroxidase-conjugated goat anti-mouse IgG and detection using an ECL method (Amersham, Inc.).

2.4. Screening of cDNA libraries and RT-PCR

The insert from pACT-2229 was excised with *Xho*I, ^{32}P-labeled by a random primer method, and used to screen a human fetal brain cDNA library (Clonetech, Inc.) in λ-gt11. Two cDNA clones were obtained, PCR amplified using primers flanking the cloning site in λ-gt11, and the resulting PCR products were subcloned into a *Eco*RV-digested, T-tailed pSK-II plasmid and their DNA sequence determined by the dideoxynucleotide method.

For 5′-RACE, 10 μg of total RNA from Raji B-cell lymphoma cells was reverse-transcribed using a specific primer 5′-GCGTTAACTGCTCTGCACAA-3′ and recombinant Moloney murine leukemia virus reverse transcriptase (Gibco/BRL, Inc.; Gaitherburg, MD). The resulting cDNA was subjected to homopolymeric tailing using dCTP and terminal deoxynucleotidyl transferase using a kit from BRL/GIBCO, and then PCR amplified using a universal 5′-anchor primer provided by the manufacturer and a CAP-1-specific reverse primer 5′-GTACATTTTGGACTTGAAGA-3′. The final PCR product was subcloned into T- tailed pSK-II and sequenced.

3. Results

3.1. Cloning of cDNAs encoding a CD40-binding protein by yeast two-hybrid method

A yeast two hybrid approach was employed to attempt to clone cDNAs encoding proteins capable of binding to the cytoplasmic domain of CD40. For these experiments, the entire cytoplasmic tail of CD40 (amino-acids 216–277) was expressed in yeast as a fusion protein with an NH_2-terminal LexA DNA binding domain. Yeast were then transformed with a human B-cell cDNA library in an plasmid that expresses random cDNAs as fusion proteins with a Gal4 *trans*-activation domain. Positive interactions between the LexA-CD40 bait protein and Gal-4-fusion proteins were detected using either a *HIS3* gene or *lacZ* gene under the control of *lexA* operators. From an initial screen of ~3×10^7 transformants, 2,640 clones were identified that *trans*-activated the *HIS3* reporter gene based on ability to grow on histidine-deficient media. Of these, 166 were also produced β-galactosidase. These 166 candidate transformants were then cured of the LexA/CD40 bait plasmid by growth in media containing tryptophan and then mated with each of 4 different indicator strains of cells containing one of the following LexA bait proteins: cytosolic domain of CD40 (amino-acids 216–277), cytoplasmic domain of Fas (191–335), Bcl-2 (83–218), or Lamin-C. This resulted in just two clones that grew on histidine-deficient media and produced β-galactosidase when expressed in combination with the LexA-CD40 bait protein but not the other 3 control LexA fusion proteins.

DNA sequencing demonstrated that these represented identical cDNAs, presumably arising during library amplification. An open reading frame of 543 bp (181 amino-acids) followed by a stop codon and a ~457 bp 3′-untranslated region was identified fused with the upstream Gal4 *trans*-activation domain sequences (hereafter termed CAP-1).

3.2. *CAP-1 interacts with a subregion of the CD40 cytoplasmic domain that is conserved in some other members of the TNF receptor family*

The Gal4/CAP-1 plasmids identified through the cDNA library screening experiment described above were isolated and retransformed into yeast cells with various LexA fusion proteins to confirm their ability to bind to the cytoplasmic domain of CD40 in two-hybrid assays. As summarized in Table 1, the CAP-1 protein fragment interacted with LexA fusion proteins containing not only the complete cytosolic domain of CD40 (amino-acids 216–277), but also a smaller portion of this domain (amino-acids 225–269) that has homology to a conserved domain found in the cytosolic domains of TNF-R1, Fas, and the p75 subunit of the NGF receptor [22]. CAP-1, however, failed to interact with the cytoplasmic domains of Fas and TNF-R2 in these two-hybrid experiments, as well as a variety of other proteins, including Ha-Ras, Bcl-2, and Lamin-C.

3.3. *Interactions of CAP-1 with CD40 cytoplasmic domain demonstrated by in vitro binding assays*

To confirm the interaction of CAP-1 with the cytoplasmic domain of CD40, in vitro binding assays were performed using in vitro translated CAP-1 and affinity-purified GST-CD40 fusion proteins. For these experiments, the CAP-1 cDNAs identified by library screening were transcribed and translated in vitro using rabbit reticulocyte lysates in the presence of [^{35}S]L-methionine. The resulting ^{35}S-labeled CAP-1 protein was then incubated with various GST-fusion protein, as indicated in Fig. 1A. Using this in vitro binding assay, CAP-1 was shown to interact specifically with GST-fusion proteins containing the nearly full-length CD40 cytoplasmic domain (220–277) as well as the conserved subregion of the CD40 cytosolic domain (225–269). No interactions were detected in vitro between ^{35}S-labeled CAP-1 and GST-fusion protein containing the cytosolic domains of Fas, TNF-R1, or TNF-R2 (Fig. 1A). CAP-1 also did not interact with a GST non-fusion protein but did interestingly

Table 1
Specific interaction of CAP-1 with CD40 cytoplasmic domain

pBMT116 (LexA)	pACT (Gal4)	His	β-Gal
CD40 (216–277)	2229	+	+
CD40 (225–269)		+	+
TNFR2 (288–461)		−	−
Fas (191–335)		−	−
Ras (V12)		−	−
Bcl-2 (83–218)		−	−
Lamin-C		−	−

pBTM116 plasmids producing LexA DNA-binding domain fusion proteins (listed at left) were co-transformed with pACT-CAP-1 (clone 2229) which encodes the C-terminal 181 amino-acids of CAP-1 fused to a Gal-4 *trans*-activation domain (5 μg each) into L40 stain yeast. Transformed cells were grown on semi-solid media lacking histidine or containing histidine as a control. Plasmid combinations that resulted on growth on histidine-deficient media were scored as positive (+). β-galactosidase activity of each colony was tested by filter assay and scored as blue (+) versus white (−).

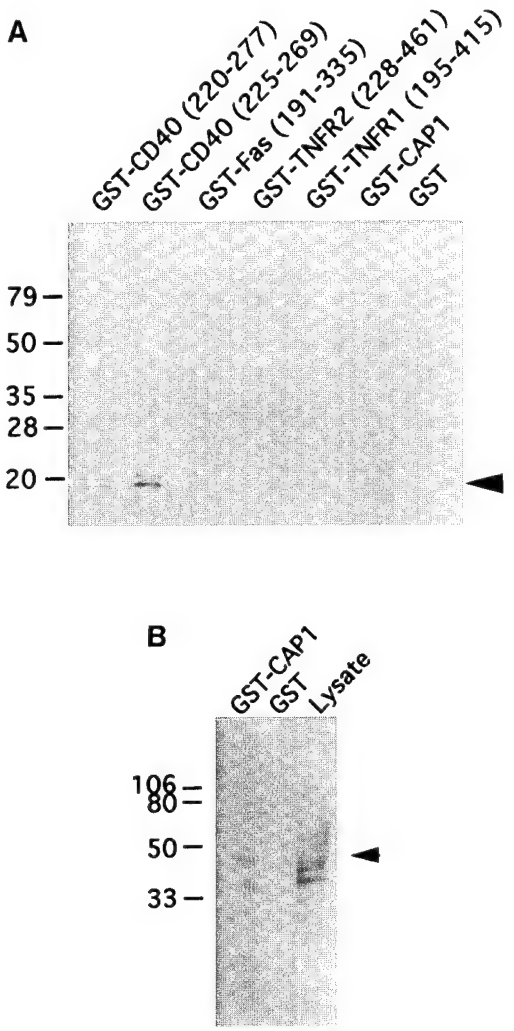

Fig. 1. In vitro binding of CAP-1 to CD40 cytoplasmic domain and CAP-1 C-terminal domain. In (A), various GST-fusion proteins as indicated were affinity-purified on glutathione-Sepharose. Beads containing ~5 μg of GST-proteins were incubated with ^{35}S-L-methionine-labeled in vitro translated CAP-1 (C-terminal 181 amino-acids). After extensive washing, beads were boiled in Laemmli buffer and the eluted proteins were subjected to SDS-PAGE followed by fluorographic detection of ^{35}S-CAP-1 protein (bold arrow) which migrated as a doublet here, presumably due to translation from both the first AUG of Gal-4 in pACT-2229 as well as an internal start codon located either 4 or 15 residues downstream (from multiple cloning site of pACT). In (B), GST-CAP-1 (C-terminal 181 amino-acids) and GST control proteins were immobilized on glutathione-Sepharose and incubated with detergent lysates prepared from RS11846 B-cell lymphoma cells. Beads were washed extensively, and associated proteins were eluted by boiling in Laemmli buffer followed by SDS-PAGE and transfer to nitrocellulose filters. RS11846 cell lysates were also run directly in the gel as a positive control (far right lane). The resulting blot was incubated with anti-CD40 monoclonal antibody B-B20 , which was detected subequently by an ECL method using 10 min exposed to X-ray film. The position of CD40 is indicated by the bold arrow.

interact with GST-CAP-1, implying that CAP-1 can homodimerize. The specificity of these results was further confirmed by experiments where a variety of other ^{35}S-labeled in vitro translated proteins including Bcl-2, Bax, Lyn were tested and found not to bind to GST-CD40 fusion proteins under the same conditions used here of ^{35}S-CAP-1 (not shown).

```
CAP-1       MESSKKMDSP GALQTNPPLK LHTDRSAGTP VFVPEQGGYK EKFVKTVEDK   50
TRAF2       MAAA-SVTSP GSLELLQP-G FSKTLLGTRL EAKYLCSACK NILRRPFQAQ   48
TRAF1       MASS-S--AP DENE-FQF-G CPPAPCQDPS EPRVLC--CT ACLSENLRDD   43
Consensus   MASS-S..SP G.LE..QP-G .......... E...LC..CK ..L.....D.   50

CAP-1       YKCEKCHLVL CSPKQTECGH RFCESCMAAL LSSSSPKCTA CQESIVKDKV  100
TRAF2       CGHRYCS--F CLTSILSSGP QNCAACVYEG LYEEG---IS ILESSS---A   90
TRAF1       -EDRICP--K CRADNLHPVS PGSP--LTQE KVHSD---VA EAEIMC---P   82
Consensus   ...R.C.--. C....L..G. ..C..C.... L..S.----.A ..ES..---.  100

CAP-1       FKDNCCKREI LALQIYCRNE SRGCAEQLTL GHLLVHLKND CHFEELPCVR  150
TRAF2       FPDNAARREV ESLPAVCPND --GCTWKGTL KEYESCHEGL CPF--LLTEC  136
TRAF1       FAG------- ----VGCSFK --GSP--QSM QEHEATSQSS HLY--LL---  112
Consensus   F.DN...RE. ..L...C.N. --GC....TL .E.E..... C.F--LL...  150

CAP-1       PDCKEKVLRK DLRDHVEKAC KYREATCSHC KSQVPMIALQ KHEDTDCPCV  200
TRAF2       PACKGLVRLS EKEHHTEQEC PKRSLSCQHC RAPCSHVDLE VHYEV-CPKF  185
TRAF1       -----LAVL- -KEW---KSS PGSNLG---- SAP---MALE RNL----SEL  141
Consensus   P.CK.LV.L. .KE.H.EK.C P.R.L.C.HC .AP....ALE .H...-CP..  200

CAP-1       VVSCPHKCSV QTLLRSEGTN QQIKAHEASS AVQHVNLLKE WSNSLEKKVS  250
TRAF2       PLTC-DGCGK KKIPR-ETFQ DHVRACSKCR VLCRFHTVG- -CSEMVETEN  231
TRAF1       QL-------- -QAAV-EATG DLEVDC--YR APC------- -C------ES  165
Consensus   .L.C-..C.. ....R-E.T. D...AC...R A.C......- -C......ES  250

CAP-1       LLQNESVEKN KSIQSLHNQI CSFEIEIERQ KEMLRNNESK ILHLQRVIDS  300
TRAF2       -LQDHELQRL REHLAL--LL SSF-LEAQAS PGTLNQVGPE LLQRCQILE-  276
TRAF1       -QEELALQHL ---------- ---------- ------VKEK LLAQ---LE-  184
Consensus   -LQ...LQ.L .....L--.. .SF-.E.... ...L..V..K LL.....LE-  300

CAP-1       QAEKLKELDK EIRSFRQNWE EADSMKSSVE SLQNRVTELE SVDKSAGQVA  350
TRAF2       --QKIATFEN IVCVLNRE-V ERVAVTAEAC SRQHRL-DQD KIEA------  316
TRAF1       --EKLRVFAN IVAVLNKE-V EASHLALAAS IHQSQL-DRE HLLS------  224
Consensus   --EKL..F.N IV.VLN.E-V EA......A. S.Q.RL-D.E ....------  350

CAP-1       RNTGLLESQL SRHDQMLSVH DIRLADMDLR FQVLETASYN GVLIWKIRDY  400
TRAF2       -----LSNKV QQLERSIGLK DLAMADLEQK VSELEVSTYD GVFIWKISDF  361
TRAF1       -----LEQRV VELQQTLAQK DQVLGKLEHS LRLMEEASFD GTFLWKITNV  269
Consensus   -----LE..V ..L.Q.L..K D..LADLE.. ...LE.ASYD GVFIWKI.D.  400

CAP-1       KRRKQEAVMG KTLSLYSQPF YTGYFGYKMC ARVYLNGDGM GKGTHLSLFF  450
TRAF2       TRKRQEAVAG RTPAIFSPAF YTSRYGYKMC LRVYLNGDGT GRGTHLSLFF  411
TRAF1       TKRCHESVCG RTVSLFSPAF YTAKYGYKLC LRLYLNGDGS GKKTHLSLFI  319
Consensus   TRR.QEAV.G RT.SLFSPAF YT..YGYKMC LRVYLNGDG. GKGTHLSLFF  450

CAP-1       VIMRGEYDAL LPWPFKQKVT LMLMDQGSSR RHLGDAFKPD PNSSSFKKPT  500
TRAF2       VVMKGPNDAL LQWPFNQKVT LMLLDH-NNR EHVIDAFRPD VTSSSFQRPV  460
TRAF1       VIMRGEYDAL LPWPFRNKVT FMLLDQ-NNR EHAIDAFRPD LSSASFQRPQ  368
Consensus   VIMRGEYDAL LPWPF.QKVT LMLLDQ-NNR EH.IDAFRPD ..SSSFQRP.  500

CAP-1       GEMNIASGCP VFVAQTVLE- -NGTYIKDDT IFIKVIVDTS DLPDP       543
TRAF2       SDMNIASGCP LFCPVSKME- AKNSYVRDDA IFIKAIVD-- -LTGL       501
TRAF1       SETNVASGCP LFFPLSKLQS PKHAYVKDDT MFLKCIVD-- --TSA       409
Consensus   SEMNIASGCP LF.P.SKLE- .K..YVKDDT IFIK.IVD-- -LT..       545
```

Fig. 2. Alignment of predicted amino-acids sequences of CAP-1 with TRAF1 and TRAF2. An alignment of the predicted amino-acids sequences of the human CAP-1, TRAF2, and TRAF1 proteins is shown. Residues that are identical in all three proteins are shown in bold type. A concensus sequence is provided below in italics, with residues that are shared among two of the three proteins in plain type and residues that are identical in all three proteins in bold type.

As another approach to examining the interaction of CAP-1 with CD40, in vitro binding experiments were performed using cell lysates derived from an CD40-expressing human B-cell lymphoma cell line RS11846. GST control protein or GST-CAP-1 fusion protein were immobilized on glutathione-Sepharose beads and mixed with detergent-lysates from RS11846 cells. After thorough washing, the beads were pelleted by centrifugation and associated proteins were subjected to SDS-PAGE/immunoblot assays with anti-CD40 antibody, demonstrating the presence of CD40 in samples containing the GST-CAP-1 protein but not the GST control protein (Fig. 1B).

3.4. Determination of the complete open reading frame of the CAP-1 protein reveals a new member of the TRAF family of putative signal transducing proteins

A human fetal brain cDNA library was screened and two additional overlapping clones having insert sizes of ~2.0 kbp and 0.1 kbp were obtained. The DNA sequence of the longer

of these extended the coding region in the 5′-direction by another 282 amino-acids but suggested that the complete ORF had still not been obtained. A 5′-RACE (rapid amplification of cDNA ends) procedure was then used to obtain an additional ~378 bp of DNA sequence. Taken together these cDNA cloning results demonstrated the presence of a continuous ORF predicted to encode a 543 amino-acid protein, having an estimated molecular mass of ~62 kDa (Fig. 2). The predicted translation initiation site conforms well to the Kozak consensus sequence, with 6 of 7 matches. Stop codons were found in all three reading-frames upstream of the longest ORF (nucleotide sequence submitted to Genbank).

A search of the CAP-1 nucleotide sequence against the available databases using the BLAST program revealed 26% and 30% overall amino-acid sequence homology with TRAF1 and TRAF2, two putative signal transducing proteins that have recently been shown to bind to the cytosolic domain of TNF-R2 [23]. The strongest homology was located in the C-terminal regions of these proteins, corresponding to the 'TRAF' domains of TRAF1 and TRAF2 (Fig. 2). The TRAF domain of CAP-1 is located between residues 384 to 540, and has 57% and 59% amino-acid identity to the analogous domains in TRAF1 and TRAF2, respectively.

Like TRAF2, the CAP-1 protein contains a RING finger domain near its NH_2-terminus (residues 53–91) having the consensus motif C-X_2-C-X_{11-12}-C-X_{1-3}-H-X_2-C-X_2-C-X_{10-13}-C-X_2 -C. This sequence is believed to form a structure that binds two zinc atoms and is found in several regulatory proteins that can bind to either DNA or RNA, including the DNA repair genes RAD18 of *S. cerevisiae* and UVS-2 of *Neurospora crassa*, the human SS-A/Ro ribonucleoprotein, the Bmi-1, C-dbl, Pml, and RET proto-oncogenes, the recombinase RAG-1, and the human RING-1 protein (reviewed in [24]). The RING finger domains of CAP-1 and TRAF2 are 42% identical.

Following the RING finger motif are two zinc finger domains in CAP-1 that contain the consensus sequence C/H-X_{2-4} -C/H-X_{2-15}-C/H-X_2-C/H which is found in several DNA-binding proteins including the *Xenopus* transcription factor TFIIIA [25] as well as some RING-finger proteins such as RAD18, and UVS-2 (reviewed in [24]). A third zinc-finger-like domain is found in CAP-1 (between residues 117–141), but the spacing between the first two cysteines is longer than usual in this case (6 instead of usual 2 to 4). The TRAF2 protein also contains four zinc finger motifs downstream of its RING finger domain [23]. Taken together, these data indicate that CAP-1 is a novel homolog of TRAF2 and a new member of the family of putative signal transducing proteins that contain TRAF-domains.

4. Discussion

Using a yeast two-hybrid approach, cDNAs encoding a novel protein CAP-1 that binds specifically to the cytosolic domain of CD40 were obtained. The region in the cytosolic domain of CD40 that is sufficient for CAP-1 binding constitutes a 45 amino-acid domain (residues 225–269) that is weakly homologous (22–41%) to domains found in the cytosolic portions of TNF-R1, Fas, and p75-NGF-R. This domain has been shown to be required for TNF-R1- and Fas-based cytotoxicity [15,16], suggesting that it plays an important role in some aspect of signal transduction mediated by these receptors. Conceivably, therefore, other TRAF-domain proteins could interact with these homologous domains in Fas, TNF-R1, and p75-NGF-R.

Previous analysis of the TRAF1 and TRAF2 proteins that bind to TNF-R2 failed to delineate the significance of the conserved C-terminal TRAF domain. Since the CAP-1 cDNA originally cloned during two-hybrid-based cDNA library screening encodes little more than the TRAF domain and given that this portion of CAP-1 (residues 384–540) is sufficient for interactions with the cytoplasmic domain of CD40 both in vitro and in two-hybrid assays, this finding suggests that one function of the TRAF domain is to mediate interactions with TNF-R family receptors. In addition, we showed that this same region in CAP-1 is sufficient to mediate dimerization of CAP-1 fusion proteins, suggesting yet another role for the TRAF domain. Previously it was shown that TRAF1 and TRAF2 can form homotypic and heterotypic dimers [23]. It is presently unknown whether CAP-1 can dimerize with TRAF1 or TRAF2. By analogy, however, it seems likely that CAP-1 will be able to participate in heterodimer formation with at least some other known or unknown members of the TRAF family, since the TRAF-domain in CAP-1 appears to be sufficient for dimerization with itself. This possibility for various combinations of homo- and heterotypic dimers could then create opportunities for specificity in signal transduction response which might be controlled both at the level of gene expression in terms of which members of the TRAF-domain gene family that are expressed in any particular cell-type and at the level of protein-protein interactions between TRAF-domain-containing proteins and specific members of the TNF-R family. With regards to the former, preliminary results suggest that CAP-1 is widely expressed (our unpublished data), like TRAF2, but unlike TRAF-1 which appears to be expressed in only spleen, lung, and testes [23]. However, specificity in the involvement of CAP-1 in signal transduction presumably can be achieved through its ability to interact with CD40 but not several other members of the TNF-R family, including TNF-R1, TNF-R2, and Fas.

CAP-1 and TRAF-2 both contain RING finger domains near their N-termini. This cysteine-rich structure represents a unique zinc-binding motif that has been found in over 40 proteins to date (reviewed in [24]). Though RING-fingers may have other roles, in at least some circumstances they have been shown to bind to DNA [26–28]. Moreover, several viral transcriptional regulators including the Herpes Simplex virus immediate-early genes IEHBV, IEEHV, and IE110 contain RING fingers and deletion of this domain in IE110 has been reported to abolish its function as a *trans*-activator [29,30]. These findings raise the possibility that CAP-1 and TRAF2 may participate directly in signal transduction from membrane to nucleus by analogy to the Stat proteins, which associate with the cytoplasmic domains of many cytokine receptors, dissociate from the receptor at the membrane upon ligand-induced phosphorylation, and translocate into the nucleus where they bind to specific DNA sequences and participate in the regulation of gene expression (reviewed in [31]). Interestingly, CAP-1 also contains three and TRAF2 has two zinc-finger domains similar to those first found in the *Xenopus* transcription factor TFIIIA [25], thus further suggesting a potential role for these proteins in transcriptional regulation. However, at present it is unknown whether RING-finger domains constitute sequence-specific DNA-binding elements, and other potential functions for proteins that contain this structure are clearly possible, including

participation in protein-protein and protein-lipid interactions [24]. Though the precise role that CAP-1 plays in CD40-mediated signal transduction responses remains to be determined, the identification of CAP-1 and the demonstration of its homology with other TRAF-domain-containing proteins nevertheless represent significant advances in our understanding of the mechanisms by which CD40 and some other members of the TNF-R family exert their potent biological effects in cells.

Acknowledgements: We thank S. Elledge for the B-cell two-hybrid library, E. Golemis and S. Hollenberg for other two-hybrid reagents, I. Stamenkovic and B. Seed from CD40 cDNAs, and C. Stephens for manuscript preparation. Dr. Sato is a recipient of a fellowship from the US Army Medical Research Development Command/Breast Cancer Research Inititative. Dr. Reed is a Scholar of the Leukemia Society of America.

References

[1] Clark, E.A. and Ledbetter, J.A. (1994) Nature 367, 425–428.
[2] Noelle, R.J., Ledbetter, J.A. and Aruffo, A. (1992) Immunol. Today 13, 431–433.
[3] Lederman, S., Yellin, M.J., Covey, L.R., Cleary, A.M., Callard, R. and Chess, L. (1993) Curr. Opin. Immunol. 5, 439–444.
[4] Armitage, R.J., Fanslow, W.C., Strockbine, L., Sato, T.A., Clifford, K.N., Macduff, B.M., Anderson, D.M., Gimpel, S.D., Davis-Smith, T., Maliszewski, C.R., Clark, E.A., Smith, C.A., Grabstein, K.H., Cosman, D. and Spriggs, M.K. (1992) Nature 357, 80–82.
[5] Hollenbaugh, D., Grosmaire, L.S., Kullas, C.D., Chalupny, N.J., Braesch-Anderson, S., Noelle, R.J., Stamenkovic, I., Ledbetter, J.A. and Aruffo, A. (1992) EMBO J. 11, 4313–4321.
[6] Gauchat, J.-F., Henchoz, S., Mazzel, G., Aubry, J.-P., Brunner, T., Blasey, H., Life, P., Talabot, D., Flores-Romo, L., Thompson, J., Kishi, K., Butterfield, J., Dahinden, C. and Bonnefoy, J.-Y. (1993) Nature 365, 340–343.
[7] Foy, T.M., Shepherd, D.M., Durie, F.H.,m Aruffo, A., Ledbetter, J.A. and Noelle, R.J. (1993) J. Exp. Med. 178, 1567–1575.
[8] Allen, R.C., Armitage, R.J., Conley, M.E., Rosenblatt, H., Jenkins, N.A., Copeland, N.G., Bedell, M.A., Edelhoff, S., Disteche, C.M., Simoneaux, D.K., Fanslow, W.C., Belmont, J. and Spriggs, M.K. (1993) Science 259, 990–993.
[9] DiSanto, J.P., Bonnefoy, J.Y., Gauchat, J.F., Fischer, A. and de Saint Basile, G. (1993) Nature 361, 541–543.
[10] Korthäuer, U., Graf, D., Mages, H.W., Briére, F., Padayachee, M., Malcolm, S., Ugazio, A.G., Notarangelo, L.D., Levinsky, R.J. and Kroczek, R.A. (1993) Nature 361, 539–543.
[11] Kawabe, T., Naka, T., Yoshida, K., Tanaka, T., Fujiwara, H., Suematsu, S., Yoshida, N., Kishimoto, T. and Kikutani, H. (1994) Immunity 1, 167–178.
[12] Durie, F.H., Fava, R.A., Foy, T.M., Aruffo, A., Ledbetter, J.A. and Noelle, R.J. (1993) Science 261, 1328–1330.
[13] Smith, C.A., Farrah, T. and Goodwin, R.G. (1994) Cell 76, 959–962.
[14] Stamenkovic, I., Clark, E.A. and Seed, S. (1989) EMBO J. 8, 1403–1410.
[15] Itoh, N. and Nagata, S. (1993) J. Biol. Chem. 268, 10932–10937.
[16] Tartaglia, L.A., Ayres, T.M., Wong, G.H.W. and Goeddel, D.V. (1993) Cell 74, 845–853.
[17] Rabizadeh, S., Oh, J., Zhong, L., Yang, J., Bilter, C., Butcher, L. and Bredesen, D. (1993) Science 261, 345–348.
[18] Ruan, Y., Camerini, D. and Bredesen, D.E. (1994) Neurochemistry, in press.
[19] Vojtek, A.B., Hollenberg, S.M. and Cooper, J.A. (1993) Cell 74, 205–214.
[20] Sato, T., Hanada, M., Bodrug, S., Irie, S., Iwama, N., Boise, H.L., Thompson, B.C., Golemis, E., Fong, L., Wang, H.-G. and Reed, J.C. (1994) Proc. Natl. Acad. Sci. USA 91, 9238–9242.
[21] Durfee, T., Becherer, K., Chen, P.-L., Yeh, S.-H., Yang, Y., Kilburn, A.E., Lee, W.H. and Elledge, S.J. (1993) Genes Dev. 7, 555–569.
[22] Itoh, N., Yonehara, S., Ishii, A., Yonehara, M., Mizushima, S.-I., Sameshima, M., Hase, A., Seto, Y. and Nagata, S. (1991) Cell 66, 233–243.
[23] Rothe, M., Wong, S.C., Henzel, W.J. and Goeddel, D.V. (1994) Cell 78, 681–692.
[24] Freemont, P.S. (1993) in: Ann. NY Acad. Sci. p. 174–192.
[25] Berg, J.M. (1990) J. Biol. Chem. 265, 6513–6516.
[26] Lovering, R., Hanson, I.M., Borden, K.L.B., Martin, S., O'Reilly, N., Evan, G.I., Rahman, D., Pappin, D.J.C., Trowsdale, J. and Freemont, P.S. (1993) Proc. Natl. Acad. Sci. USA 90, 2112–2116.
[27] Tagawa, M., Sakamoto, T., Shigemoto, K., Matsubara, H., Tamura, Y., Ito, T., Nakamura, I., Okitsu, A., Imai, K. and Taniguchi, M. (1990) J. Biol. Chem. 265, 20021–20026.
[28] Reddy, B., Kloc, M. and Etkin, L.D. (1991) Dev. Biol. 148, 107–116.
[29] Everett, R.D. (1988) J. Mol. Biol. 202, 87–96.
[30] Zhu, X., Chen, J., Young, C.H.S. and Silverstein, S. (1990) J. Virol. 64, 4489–4498.
[31] Darnell, J.E., Kerr, I.M. and Stark, G.R. (1994) Science 264, 1415–1412.

Cell, Vol. 80, 279–284, January 27, 1995, Copyright © 1995 by Cell Press

Cloning and Functional Analysis of BAG-1: A Novel Bcl-2-Binding Protein with Anti-Cell Death Activity

Shinichi Takayama, Takaaki Sato, Stanislaw Krajewski, Kristine Kochel, Shinji Irie, Juan A. Millan, and John C. Reed
The La Jolla Cancer Research Foundation
La Jolla, California 92037

Summary

Using a protein interaction cloning technique, we identified cDNAs that encode a novel Bcl-2-binding protein, termed BAG-1. The BAG-1 protein shares no significant homology with Bcl-2 or other Bcl-2 family proteins, which can form homo- and heterodimers. In gene transfer experiments using a human lymphoid cell line, Jurkat, coexpression of BAG-1 and Bcl-2 provided markedly increased protection from cell death induced by several stimuli, including staurosporine, anti-Fas antibody, and cytolytic T cells, relative to cells that contained gene transfer–mediated elevations in either BAG-1 or Bcl-2 protein alone. BAG-transfected 3T3 fibroblasts also exhibited prolonged cell survival in response to an apoptotic stimulus. The findings indicate that *bag-1* represents a new type of anti–cell death gene and suggest that some routes of apoptosis induction previously ascribed to Bcl-2-independent pathways may instead reflect a need for the combination of Bcl-2 and BAG-1.

Introduction

Cell death plays an important role in a wide variety of physiological circumstances in essentially all complex multicellular organisms (reviewed by Ellis et al., 1991). Several genes have been identified that participate as either inducers or repressors of programmed cell death. Among these is *bcl-2* (for B cell lymphoma 2), a blocker of cell death that was first discovered by virtue of its involvement in the t(14;18) chromosomal translocations found in the majority of non-Hodgkin's B cell lymphomas (Tsujimoto and Croce, 1986). Gene transfer–mediated elevations in Bcl-2 protein levels have been shown to render cells relatively more resistant to induction of apoptosis by an impressive variety of stimuli and insults, suggesting that this protein regulates a distal step in a final common pathway for apoptotic cell death (reviewed by Reed, 1994). Furthermore, elements of this pathway appear to be well conserved throughout evolution (Vaux et al., 1992b; Hengartner and Horvitz, 1994).

The biochemical mechanism of action of the Bcl-2 protein remains enigmatic, principally because its predicted amino acid sequence shares no significant homology with other proteins whose functions are known. For this reason, we have attempted to identify proteins that can bind to Bcl-2. Here we describe the molecular cloning and functional characterization of cDNAs encoding a novel protein that interacts physically and functionally with the Bcl-2 protein. Gene transfer–mediated elevations in the levels of this Bcl-2-binding protein can prolong cell survival in some circumstances and also can cooperate with Bcl-2 in the suppression of apoptosis. These properties suggest that the gene encoding this protein represents a novel type of anti–cell death gene, which we have termed BAG-1, for Bcl-2-associated athanogene 1 (from the Greek word athanos, which refers to anti-death).

Results

Molecular Cloning of cDNAs for BAG-1

To identify cDNAs encoding proteins that can bind to Bcl-2, a mouse embryo cDNA library in a λ phage expression vector was screened with recombinant human Bcl-2 protein. Phage clones that produced proteins capable of binding to recombinant Bcl-2 protein were then detected by incubation of filters with a human-specific anti-Bcl-2 monoclonal antibody, resulting in a single positive clone from a screen of ~10^6 phage clones. DNA sequencing revealed an 830 bp insert, containing a 630 bp coding region in-frame with the upstream T7/10 protein sequences derived from the λEX-lox cloning vector.

BAG-1 Protein Specifically Interacts with Bcl-2 In Vitro

An immobilized protein interaction (Far Western blot) assay was performed to confirm the ability of recombinant Bcl-2 protein to bind to BAG-1 protein. The *bag-1* partial cDNA described above was subcloned into the plasmid pGEX-3X and expressed in Escherichia coli as a GST–BAG-1 fusion protein. GST–BAG-1 and GST nonfusion protein were compared with regards to binding of baculovirus-produced Bcl-2, using the same filter binding assay employed for library screening. As shown in Figure 1A, Bcl-2 bound to GST–BAG-1 but not to GST protein. In this experiment, cell lysates from a murine lymphoid cell, S49.1, that had been stably infected with a recombinant retrovirus encoding human Bcl-2 protein (S49.1-BCL-2) or a control retrovirus (S49.1-NEO) (Miyashita and Reed, 1992) were also included. The prominent ~26 kDa band seen in S49-BCL-2 cell lysates represents direct binding of the anti-human Bcl-2 monoclonal antibody 4D7 to human Bcl-2 protein in the S49.1-BCL-2 cells, thus serving as a control for the antibody detection system. In addition, however, a faint band at ~28–30 kDa was also seen in both S49.1-BCL-2 and S49.1-NEO cells that may represent binding of recombinant Bcl-2 protein to endogenous BAG-1 protein (see below). As a control, Far Western blot analysis was performed using Sf9 lysates derived from cells infected with a β-galactosidase (β-gal)-expressing baculovirus (Figure 1A, right).

To determine whether the interaction of BAG-1 with Bcl-2 can also take place in solution, soluble GST–BAG-1 and GST control proteins were immobilized on glutathione–Sepharose and then incubated with lysates prepared from Sf9 cells that had been infected with either Bcl-2-

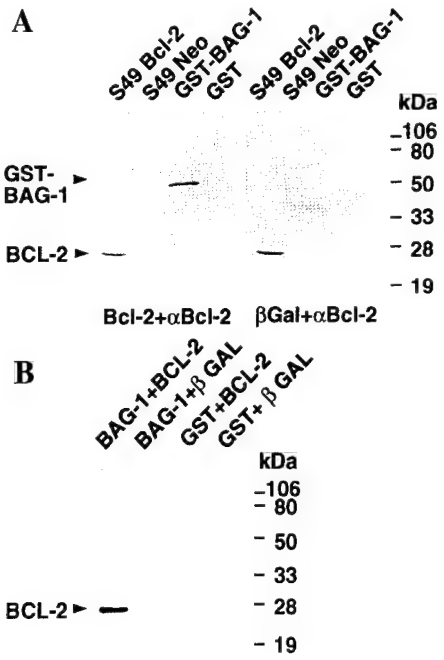

Figure 1. Interaction of Bcl-2 with BAG-1 Fusion Proteins

(A) Purified GST–BAG-1 (amino acids 8–219) fusion and GST nonfusion proteins (1 μg) and detergent lysates prepared from 10^6 S49-NEO and S49-BCL-2 cells were subjected to SDS–PAGE and transferred to nitrocellulose. The resulting filters were incubated with 1% (v/v) Sf9 lysates derived from cells infected with either Bcl-2 (left) or β-gal (right) baculoviruses, followed by anti-Bcl-2 antibody, which was detected by using an alkaline phosphatase–conjugated secondary antibody.

(B) GST–BAG-1 fusion and GST nonfusion proteins were immobilized on glutathione–Sepharose (~2.5 μg) and mixed with 500 μg of detergent lysates prepared from Sf9 cells infected with either Bcl-2 or β-gal-producing baculoviruses. The Sepharose beads were then washed extensively and associated proteins analyzed by SDS–PAGE/immunoblot assay using a Bcl-2-specific antiserum.

producing or control β-gal baculovirus. After the beads were washed, associated proteins were analyzed by immunoblotting using a Bcl-2-specific antibody (Reed et al., 1991). As shown, Bcl-2 protein was specifically recovered from Sf9 cell lysates on GST–BAG-1 Sepharose but not on beads that contained GST control protein (Figure 1B). Though the data are not presented here, Bcl-2 also did not associate with several other control GST fusion proteins. The interaction of BAG-1 with Bcl-2 was also confirmed by a yeast two-hybrid method (data not shown).

Predicted Amino Acid Sequence of BAG-1 Reveals a Novel Protein

Using the partial *bag-1* cDNA as a hybridization probe for cDNA library screening, we obtained additional *bag-1* cDNAs, thus deducing the complete open reading frame for the 219 amino acid mouse BAG-1 protein (Figure 2). BAG-1 is novel and shares no similarity with Bcl-2 or its homologous proteins. The BAG-1 protein is acidic (predicted pI, 4.81) and contains multiple glutamic acid residues (31 of 219). Although this raised the possibility of Ca^{2+} binding, no clear homology was observed with other

```
MAKTEEMVQT EEMETPRLSV IVTHSNERYD     30
LLVTPQQGNS EPVVQDLAQL VEEATGVPLP     60
FQKLIFKGKS LKEMETPLSA LGMQNGCRVM     90
LIGEKSNPEE EVELKKLKDL EVSAEKIANH    120
LQELNKELSG IQQGFLAKEL QAEALCKLDR    150
KVKATIEQFM KILEEIDTMV LPEQFKDSRL    180
KRKNLVKKVQ VFLAECDTVE QYICQETERL    210
QSTNLALAE                           219
```

Figure 2. Predicted Amino Acid Sequence of BAG-1 Protein

The predicted amino acid sequence of the encoded BAG-1 protein is presented.

Ca^{2+}-binding proteins of either the EF-hand or non-EF-hand type. A region in the mouse BAG-1 protein (residues 37–73) shows as much as 50% amino acid sequence identity (66% similarity) with several ubiquitin and ubiquitin-like proteins. The region from amino acid ~100 to amino acid ~212 is predicted to assume a largely α-helical conformation and contains segments that on Edmundson wheel plots are predicted to be amphipathic in nature and thus good candidates for participation in coiled-coil interactions with other proteins. Kyte–Doolittle plots failed to reveal any hydrophobic domains in BAG-1 that would suggest the presence of a transmembrane domain or hydrophobic leader sequence.

Gene Transfer Analysis of BAG-1 Function Reveals Anti-Cell Death Activity

A cDNA encoding full-length BAG-1 protein was subcloned into a mammalian expression plasmid, pCEP-4, that contains a hygromycin phosphotransferase gene and was introduced into Jurkat T cell lines that had previously been stably transfected with either a *bcl-2* (pZip–Bcl-2) or a control (pZip–NEO) expression plasmid (Torigoe et al., 1994a, 1994b). After selection in hygromycin, the BAG-1 transfectant cells were analyzed by immunoblotting using BAG-1- and Bcl-2-specific anti-peptide antisera. Elevated levels of BAG-1 protein were detected in the Jurkat–Bcl-2 and Jurkat–NEO transfectants that received the pCEP–4–BAG-1 plasmid but not those that were transfected with pCEP-4 parental control plasmid (Figure 3, left). Despite a predicted molecular mass of ~24.5 kDa, note that the BAG-1 protein migrates as a ~29–30 kDa protein, presumably owing to its acidic nature. As expected, Bcl-2 protein levels were markedly elevated in the Jurkat–Bcl-2 cells as compared with Jurkat–NEO cells (Figure 3, right).

We next explored the relative sensitivity of these doubly transfected T cells to induction of apoptosis by several stimuli. As shown in Figure 4, Jurkat T cells with gene transfer–mediated elevations in Bcl-2 protein were partially resistant to cytotoxicity induced by 1 μg/ml anti-Fas antibody. In contrast with Bcl-2, gene transfer–mediated elevations in BAG-1 by themselves had essentially no effect on the relative sensitivity of Jurkat T cells to anti-Fas-induced cytotoxicity. In combination with Bcl-2, however, elevations in BAG-1 protein levels resulted in markedly enhanced resistance to anti-Fas-induced apoptosis. Similar conclusions were reached on the basis of experiments where the protein kinase inhibitor staurosporine was employed to induce apoptosis in Jurkat T cells. As shown in

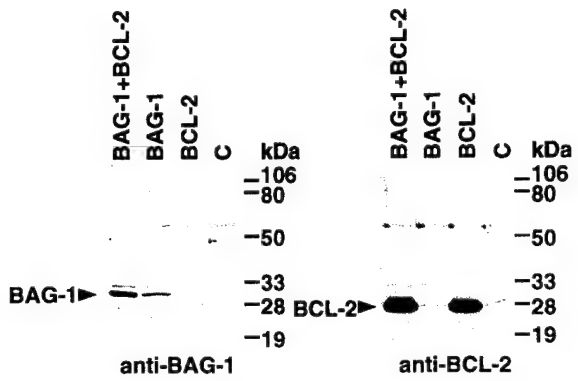

Figure 3. Immunoblot Analysis of BAG–1-Transfected Jurkat T Cells

Protein from cell lysates (50 μg) was subjected to SDS–PAGE/immunoblot analysis using either anti-BAG-1 (left) or anti-Bcl-2 antiserum (right). The arrows indicate the positions of the BAG-1 and Bcl-2 proteins. Control-transfected Jurkat cells (C) contained the pZip–NEO and pCEP-4 plasmids without inserted *bcl-2* or *bag-1* cDNAs.

Figure 4, BAG-1 alone provided only slightly enhanced protection from staurosporine-induced cell death. Bcl-2 was partially protective, with less than half of the cells still alive after 2 days. In contrast, the combination of BAG-1 and Bcl-2 afforded marked resistance to staurosporine-induced cell death, with ~80% of the cells surviving a

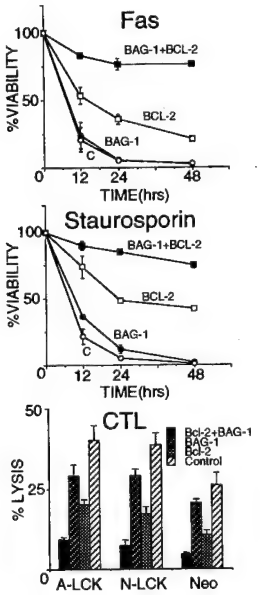

Figure 4. BAG-1 Cooperates with Bcl-2 to Increase Resistance to Cell Death in Jurkat T Cells

Transfected Jurkat cells were cultured at 5×10^5 cells/ml in complete medium containing either 1 μg/ml of anti-Fas monoclonal antibody 2D1 (top) or 10 μM staurosporine (middle). The percentage viable cells were then determined at various times thereafter by trypan blue dye exclusion. Equivalent data were obtained using MTT assays (data not shown). Jurkat cells were labeled with ^{51}Cr (bottom) and mixed with CTLL-2 cytolytic T cells that had been transfected with expression plasmids, producing constitutively activated Lck kinase (Tyr→Phe505), normal Lck kinase, or neo control plasmid alone. Specific Cr release was measured 4 hr later. All data represent mean ± standard deviation (n = 3).

2 day treatment with 10 μM staurosporine. The differential survival of these Jurkat T cell transfectants was not attributable to variations in rates of spontaneous cell death, since cell viability was >95% for all four cell lines when cultured for up to 3 or 4 days without anti-Fas antibody or other stimuli. Comparable results were obtained when several independent clones of tranfected Jurkat cells were evaluated (data not shown).

Next, Jurkat cells were labeled with ^{51}Cr and then cocultured with cloned cytolytic T cells. Specific cytotoxic T lymphocyte (CTL)-induced ^{51}Cr release was then monitored in standard 4 hr cytotoxicity assays. These cloned T cells were previously shown to exhibit lymphokine-activated killer (LAK)-like cytolytic activity against Jurkat and certain other tumor cell lines through a CD3- and major histocompatibility complex–independent mechanism (Torigoe et al., 1994a, 1994b). Some of these cytolytic T cells had been stably transfected with expression plasmids encoding normal Lck kinase (N-Lck) or a constitutively active mutant version of Lck (A-Lck), since our previous investigations demonstrated that elevated levels of Lck kinase activity can enhance cytolytic T cell killing by increasing secretion of cytotoxic granules and expression of cell adhesion proteins (Torigoe et al., 1994a). Jurkat cells with elevations in BAG-1 protein exhibited some slight but reproducible (n = 3) resistance to lysis induced by CTLs. Jurkat cells with elevated levels of Bcl-2 protein were relatively more resistant than the BAG-1 transfectants, but not as resistant as Jurkat cells that contained gene transfer–mediated elevations in both Bcl-2 and BAG-1 proteins. Depending on the particular CTL clone examined, Jurkat cells overexpressing the combination of Bcl-2 and BAG-1 experienced only 16%–23% as much lysis as control-transfected Jurkat cells, compared with 76%–79% for the BAG-1 single transfectants and 40%–50% for the Bcl-2 single transfectants. Taken together, these data indicate that BAG-1 can augment the anti–cell death function of Bcl-2.

Analysis of BAG-1 Function in 3T3 Fibroblasts

In contrast with Jurkat T cells where BAG-1 alone only marginally enhanced cell survival, gene transfer studies using BALB/c 3T3 fibroblasts suggested that BAG-1 can have significant anti–cell death activity in some cells even when transfected without Bcl-2 expression plasmids. In these experiments, 3T3 cells were stably transfected either with the BAG-1 expression plasmid pRc/CMV–BAG-1 or with the pRc–CMV plasmid lacking an inserted *bag-1* cDNA. For comparison, 3T3 cells were also transfected with a Bcl-2 expression plasmid. Initially, a polyclonal line of G418-resistant BAG-1 transfectants was obtained but found to contain BAG-1 protein at levels not detectably above those seen in control-transfected 3T3 cells (lanes 1 and 2 of Figure 5). Individual clones from this bulk-transfected line were therefore obtained and some identified that had elevations in BAG-1 protein, presumably reflecting integration of the plasmid DNA into sites favorable for expression. The clone shown in Figure 5 (lane 3; clone number 19), for instance, contained ~3-fold higher levels of BAG-1 than the NEO control transfectants (lane 2). In

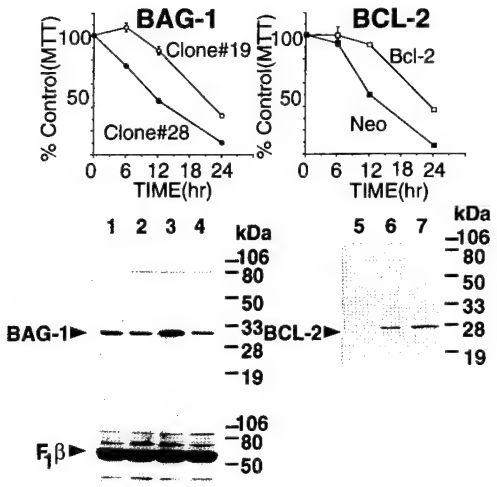

Figure 5. Expression and Function of BAG-1 in BALB/c 3T3 Cells

BALB/c 3T3 cells were stably transfected with pRc/CMV–BAG-1 (lane 1), pRc/CMV (lane 2), pZip–NEO (lane 5), or pZip–Bcl-2 (lane 6) plasmid DNAs. In some cases, independent clones were isolated from the pRc/CMV–BAG-1-transfected line: clones number 19 (lane 3) and number 28 (lane 4). Immunoblot analysis was performed (30 μg of cellular proteins) using antibodies specific for either the BAG-1 (lanes 1–4) or human Bcl-2 (lanes 5–7) proteins and using an ECL method. The t(14; 18)-containing line RS11846 was included as a positive control (lane 7) for Bcl-2. The blot (lanes 1–4) was subsequently incubated with an antiserum specific for F_1–β-ATPase (detected by a colorimetric assay) to verify loading of equal amounts of protein.

At top, 3T3 transfectants were cultured at 10^4 cells/well (50%–70% confluent) for various times with 1 μM staurosporine, and the relative number of viable cells was determined by MTT assay and expressed as a control relative to untreated cells at the initiation of the experiment (mean ± standard deviation; n = 3).

many other G418-resistant clones, however, the levels of BAG-1 protein were essentially unchanged from baseline (clone number 28, for example; lane 4 of Figure 5).

Previously we showed that the protein kinase inhibitor staurosporine is a potent inducer of apoptosis in fibroblast cell lines (Jacobson et al., 1993), often producing more synchronous and reproducible cell death kinetics than serum withdrawal. We therefore challenged BAG-1 and control-transfected 3T3 cells with 1 μM staurosporine and monitored cell survival at various times thereafter. As shown, for example, by the results obtained with the BAG-1-overexpressing clone 19, gene transfer–mediated elevations in BAG-1 protein prolonged the survival of BALB/c 3T3 cells relative to other clones, such as clone 28, which had been transfected with the same *bag-1* cDNA–containing plasmid but failed to produce higher levels of BAG-1 protein (Figure 5). This prolongation of cell survival was typically similar to that seen for 3T3 cells that had been stably transfected with a Bcl-2-encoding expression plasmid.

Discussion

Using a protein interaction cloning technique, we have identified cDNAs encoding a novel Bcl-2-binding protein. With the exception of a ubiquitin-like domain, the predicted amino acid sequence of BAG-1 has no clear similarity to other known proteins and contains no motifs that would indicate a biochemical function for this protein. BAG-1 therefore may represent the prototype of a novel type of anti–cell death gene. Although Bcl-2 has been shown to bind to several homologous proteins, including Bax (for Bcl-2-associated x protein), Bcl-x_L, Bcl-x_S, and Mcl1 (Sato et al., 1994; Oltvai et al., 1993), BAG-1 lacks sequence homology with Bcl-2 and its related proteins. All Bcl-2 homologs identified thus far contain significant amino acid similarity in at least one of three well-conserved domains, which we have previously designated Bcl-2 domains A, B, and C (Sato et al., 1994). The BAG-1 protein lacks similarity to all three of these conserved domains, indicating that it is not a member of the Bcl-2 protein family.

BAG-1 contains a domain located at residues 37–73 that has sequence similarity with several ubiquitin and ubiquitin-like proteins, including the human and mouse Gdx-1 protein (50%, 43%), baculovirus ubiquitin-like protein (46%), and the mouse *Nedd8* gene (36%). Ubiquitin is a small 76 amino acid protein that is well conserved throughout evolution and that becomes covalently attached to proteins, typically as part of a nonlysosomal, ATP-dependent protein degradation pathway (reviewed by Hershko and Ciechanover, 1992; Rechsteiner, 1991). Ubiquitins contain a conserved lysine at position 48 that provides an ε amino acceptor group for covalent ligation to the carboxyl group of the C-terminal glycine of other ubiquitin molecules during the formation of branch chain ubiquitin–ubiquitin conjugates on target proteins. Interestingly, a lysine is found at position 67 within the ubiquitin-like domain of BAG-1 that corresponds to lysine 48 of ubiquitin. Internal lysines have also been shown to be the sites of ubiquitin conjugation in some other proteins that become polyubiquitinated and thereby targeted for degradation. Thus, one possible role of the ubiquitin-like domain in BAG-1 may be to serve as a site for attachment of ubiquitin and subsequent proteolytic degradation. In this regard, ubiquitin conjugation has been shown to regulate the turnover of other proteins that are either known or thought to play a role in cell death regulation in mammals, including the tumor suppressor p53 and some cyclins (Rechsteiner, 1991; Hershco and Ciechanover, 1992). In addition, previous studies using antisense approaches have documented a requirement for ubiquitin for apoptosis induced by γ-radiation in thymocytes (Delic et al., 1993). Inasmuch as this ubiquitin-like domain may be involved in targeting BAG-1 for degradation, it may be relevant that Jurkat cells cotransfected with Bcl-2 and BAG-1 consistently contained higher relative levels of BAG-1 protein than cells transfected with BAG-1 alone, suggesting that the interaction of BAG-1 with Bcl-2 potentially could stabilize the BAG-1 protein (Figure 3; data not shown). Unlike the protein ubiquitin, the function of the ubiquitin-like domains found in Gdx-1, Nedd-8, and other ubiquitin-like proteins is unknown. It has been speculated, however, that they may mediate protein–protein recognition (Toniolo et al., 1988), and thus, the ubiquitin-like domain in BAG-1 theoretically may participate in the binding of BAG-1 to Bcl-2 or other proteins. Recent studies indicate that proteases

can be essential for induction of programmed cell death and apoptosis in a variety of physiological and pathological circumstances (Yuan et al., 1993; Miura et al., 1993; Sarin et al., 1994; Gagliardini et al., 1994). By analogy to the known role of covalent addition of ubiquitin in rendering target proteins recognizable by subunits of a large 26S proteasome, it is tempting to speculate that the BAG-1 protein plays a role in bringing Bcl-2 or other Bcl-2-binding proteins into contact with a protease-containing protein complex that participates in cell death regulation.

Previously it has been suggested that there exist both Bcl-2-dependent and Bcl-2-independent pathways for suppression of apoptosis, largely on the basis of gene transfer experiments where elevated levels of Bcl-2 protein production were shown to be insufficient to protect cells from induction of cell death by some kinds of stimuli. In particular, it has been controversial whether high levels of Bcl-2 protein correlate with resistance to apoptosis induced by anti-Fas antibodies and cytolytic T cells, with Bcl-2 apparently providing protection in some cell lines but not others (Itoh et al., 1993; Owen-Schaub et al., 1994; Vaux et al., 1992a; Strasser et al., 1991; Torigoe et al., 1994b). The gene transfer experiments presented here, however, suggest that the failure of Bcl-2 to promote cell survival in at least some of these scenarios may have an explanation other than invoking the presence of a Bcl-2-independent pathway. In Jurkat T cells, for example, cotransfection of Bcl-2 and BAG-1 expression plasmids rendered these cells relatively more resistant to induction of cell death by staurosporine, anti-Fas antibody, and cytolytic T cells, whereas either Bcl-2 or BAG-1 alone was comparatively ineffective at providing protection from cell death. Clearly, therefore, the context in which Bcl-2 is overexpressed is vitally important to its ability to block cell death. To the extent that partner proteins such as BAG-1 are present at insufficient levels or dominant inhibitors such as Bax or Bcl-x_S are produced at excessive levels, a mere increase in Bcl-2 protein levels may be inadequate to protect some types of cells from some kinds of cell death stimuli. In these cases, the cell death pathway utilized may nevertheless directly involve a Bcl-2-regulable step.

Experimental Procedures

cDNA Library Screening

A mouse embryo DNA library in λEX-lox (Novagen, Incorporated) was plated on BL21(DE3) cells and induced with isopropyl-β-D-thiogalactopyranoside (IPTG) according to the protocol of the manufacturer. Filters were preblocked in Hyb75 solution (20 mM HEPES [pH 7.7], 75 mM KCl, 2.5 mM $MgCl_2$, 2 mM EDTA, 1 mM dithiothreitol [DTT], 0.1% Triton X-100) containing 5% nonfat milk for 30 min and then incubated overnight at 4°C in Hyb75 containing 1 mM phenylmethylsulfonyl fluoride (PMSF), 1% milk, and 1% lysate from *bcl-2*–baculovirus-infected Sf9 cells (Reed et al., 1992; Newmeyer et al., 1994). After one wash for 5 min in Hyb75, filters were incubated for 2 hr at 4°C in the same solution containing 1% nonfat milk and 0.1% (v/v) ascites from the anti-Bcl-2 antibody–producing hybridoma 4D7.4 (Reed et al., 1992). Antibody detection was accomplished by using 0.14 μg/ml alkaline phosphatase–conjugated rabbit anti-mouse IgG (Promega, Incorporated) in Hyb75 with 1% milk followed by 5-bromo-4-chloro-3-indolylphosphate toluidinium–nitroblue tetrazolium chloride (BCIP–NBT). To convert this phage to plasmid, BM25.8 cells that contain P1 *cre* recombinase (Palazzolo et al., 1990) were infected and plated on ampicillin-containing LB plates.

In addition, a mouse kidney cDNA library in λgt10 (Clontech, Incorporated) was screened using the original *bag-1* cDNA clone (pS33–1) as a ^{32}P-labeled hybridization probe to obtain additional cDNA clones, of which λSN-245-9 contained nucleotides −82 to +843 bp.

BAG-1 Fusion Proteins

For GST–BAG-1 fusion protein, the *bag-1* cDNA (pS33–1) was excised from pEX/*ox*–BAG-1 by digestion with EcoRI and HindIII and subcloned into the EcoRI site of pGEX-3X (Pharmacia, Incorporated) by use of a HindIII–EcoRI adapter. The pGEX-3X and pGEX-3X–BAG-1 plasmids were transformed into XL1-blue cells (Stratagene, Incorporated). Overnight cultures were diluted 1:10 into LB medium containing 50 μg/ml ampicillin, and 2 hr later, 0.1–0.2 mM IPTG was added prior to incubating cultures 12–18 hr at 30°C with aeration. Cells were recovered from 250 ml cultures by centrifugation, resuspended in ~10 ml of phosphate-buffered saline (PBS; pH 7.4) containing 1% Triton X-100, 1 mM PMSF, and 1 mg/ml lysozyme, and sonicated on ice by using five bursts of 30 s each from a 1.6 mm tip (Ultrasonicator model XL-2020; Heat Systems, Incorporated). After centrifugation at 16,000 × g for 15–30 min, the supernatant was mixed with ~1 ml of glutathione–Sepharose-4B (Pharmacia, Incorporated) for 1 hr at 4°C. The beads were then washed two times in PBS containing 1% Triton X-100, and the GST–BAG-1 and GST proteins were eluted by using 5 vol of 5 mM glutathione, 50 mM Tris [pH 8.0].

Filter binding assays were performed using ~0.25 μg of purified GST–BAG-1 and GST control proteins. After size fractionation of proteins by SDS–polyacrylamide gel electrophoresis (PAGE) and transfer to nitrocellulose, filters were processed as described above for library screening. For binding of Bcl-2 to GST–BAG-1 protein in solution, GST control or GST–BAG-1 proteins were immobilized on glutathione–Sepharose-4B (~0.25 μg of protein/1 μl of beads) that had been preblocked in 0.5% nonfat milk and 0.05% bovine serum albumin (BSA), and ~10–20 μl was incubated for 1 hr on a rotator at 4°C with 50 μl of Sf9 cell lysates in 0.4 ml of binding buffer (20 mM Tris [pH 7.5], 100 mM NaCl, 2 mM EDTA, 0.1% Nonidet P-40 [NP-40], 2 mM DTT, 0.05% BSA, 5% glycerol). Sepharose beads were then washed three times in 1 ml of TENNS buffer (2.5 mM Tris [pH 7.4], 2.5 mM EDTA, 250 mM NaCl, 1% NP-40, 2.5% sucrose), then resuspended in 20 μl of Laemmli buffer, and 10 μl was analyzed by SDS–PAGE/immunoblot assay (12% gels) using 0.2% (v/v) of an anti-Bcl-2 rabbit antiserum (Reed et al., 1991) and alkaline phosphatase–conjugated goat anti-rabbit IgG (Promega, Incorporated), followed by NBT–BCIP in 0.1 M Tris [pH 9.5], 0.1 M NaCl, 5 mM $MgCl_2$.

Antibodies and Immunoblotting

Antisera were prepared in rabbits essentially as described previously (Reed et al., 1991) by using a synthetic peptide corresponding to the C-terminal 16 amino acids of BAG-1 (NH_2–CQETERLQSTNLALAE-COOH) that was conjugated to maleimide-activated keyhole limpet hemocyanin (KLH) (Pierce, Incorporated). For SDS–PAGE/immunoblot assays, blots were preblocked in Tris-buffered saline (TBS; 20 mM Tris [pH 7.5], 150 mM NaCl) containing both 3% BSA and 5% nonfat milk, and washes were performed using TBS containing 0.05% Triton X-100. Primary antibodies were used at 0.1%–0.2% (v/v), and detection was with 0.05% horseradish peroxidase–conjugated goat anti-rabbit IgG (Amersham, Incorporated) in TBS with 3% BSA by the enhanced chemiluminescence (ECL) method (Amersham, Incorporated).

Gene Transfections

For BALB/c 3T3 cells, the *bag-1* cDNA SN-245-9 was subcloned into the HindIII and XbaI sites of pRc/CMV (Invitrogen, Incorporated). ScaI-linearized DNA (25 μg) was mixed with 2.5 × 10^6 BALB/c 3T3 cells in 0.8 ml of Hanks' balanced salt solution (HBSS; 20 mM HEPES [pH 7.05], 137 mM NaCl, 5 mM KCl, 0.7 mM Na_2HPO_4, 6 mM dextrose) on ice. Electroporations were performed in 0.4 cm (diameter) cuvettes with platinum electrodes using 270 V and 1500 μF (Cell Ject; EquiBio, Incorporated). Selections were begun 2 days later using medium containing 1 mg/ml geneticin (GIBCO BRL, Incorporated), and individual clones were isolated using cloning cylinders.

For Jurkat T cells, the *bag-1* cDNA SN-245-9 in pSK-II was excised by use of HindIII and BamHI and subcloned into pCEP (Invitrogen, Incorporated). Jurkat cells (5 × 10^6) were mixed with 25 μg of plasmid

DNA in 0.8 ml of HBSS and electroporated using 270 V and 900 μF. After 2 days, cells were seeded at 10^5 cells/ml in medium containing 1 mg/ml hygromycin (Calbiochem, Incorporated).

Cytotoxicity Assays

Jurkat cells were cultured for various times at 5 × 10^5 cells/ml in 96-well flat-bottomed plates (Falcon, Incorporated) (0.2 ml/well) containing 1 μg/ml 2D1 antibody (Takahashi et al., 1993), 10 μM staurosporine (Sigma, Incorporated), or none of these reagents. BALB/c 3T3 cells were cultured with or without 1 μM staurosporine at 10^4 cells per flat-bottomed well. Relative numbers or percentages of viable cells were determined by trypan blue dye exclusion or 3[4,5-dimethylthiazol-2-yl]-2,5-diphenyltetrazolium bromide (MTT) dye reduction assay as described previously (Kitada et al., 1994). For CTL experiments, Jurkat cells were labeled with ^{51}Cr and cultured for 4 hr with CTLs at an E/T ratio of 20/1. The percentage specific ^{51}Cr release was then calculated by correction for spontaneous release and normalization for total release induced by 1% NP-40 as described (Torigoe et al., 1994a, 1994b).

Acknowledgments

Correspondence should be addressed to J. C. R. We thank S. Huang for helpful discussions, J. Smith for the β-gal virus, S. Takahashi and K. Kikuchi for the 2D1 antibody, and the National Institutes of Health (CA-60181) and American Cancer Society (IM-414) for research support. J. C. R. is a Scholar of the Leukemia Society of America. T. S. has a fellowship from the United States Army Medical Research Development Command, Breast Cancer Research Program. S. T. is the recipient of a RAAM fellowship.

Received September 21, 1994; revised November 3, 1994.

References

Delic, J., Morange, M., and Magdelenat, H. (1993). Ubiquitin pathway involvement in human lymphocyte γ-irradiation-induced apoptosis. Mol. Cell. Biol. *13*, 4875–4883.

Ellis, R. E., Yuan, J., and Horvitz, H. R. (1991). Mechanisms and functions of cell death. Annu. Rev. Cell Biol. *7*, 663–668.

Gagliardini, V., Fernandez, P. A., Lee, R. K., Drexler, H. C., Rotello, R. J., Fishman, M. C., and Yuan, J. (1994). Prevention of vertebrate neuronal death by the *crmA* gene. Science *263*, 826–828.

Hengartner, M. O., and Horvitz, H. R. (1994). C. elegans cell survival gene *ced-9* encodes a functional homolog of the mammalian proto-oncogene *bcl-2*. Cell *76*, 665–676.

Hershko, A., and Ciechanover, A. (1992). The ubiquitin system for protein degradation. Annu. Rev. Biochem. *61*, 761–807.

Itoh, N., Tsujimoto, Y., and Nagata, S. (1993). Effect of *bcl-2* on Fas antigen–mediated cell death. J. Immunol. *151*, 621–627.

Jacobson, M. D., Burne, J. F., King, M. P., Miyashita, T., Reed, J. C., and Raff, M. C. (1993). Apoptosis and Bcl-2 protein in cells without mitochondrial DNA. Nature *361*, 365–368.

Kitada, S., Takayama, S., DeRiel, K., Tanaka, S., and Reed, J. C. (1994). Reversal of chemoresistance of lymphoma cells by antisense-mediated reduction of *bcl-2* gene expression. Antisense Res. Dev. *4*, 71–79.

Miura, M., Zhu, H., Rotello, R., Hartwieg, E. A., and Yuan, J. (1993). Induction of apoptosis in fibroblasts by IL-1β-converting enzyme, a mammalian homolog of the C. elegans cell death gene *ced-3*. Cell *75*, 653–660.

Miyashita, T., and Reed, J. C. (1992). *bcl-2* gene transfer increases relative resistance of S49.1 and WEHI7.2 lymphoid cells to cell death and DNA fragmentation induced by glucocorticoids and multiple chemotherapeutic drugs. Cancer Res. *52*, 5407–5411.

Newmeyer, D. D., Farschon, D. M., and Reed, J. C. (1994). Cell-free apoptosis in Xenopus egg extracts: inhibition by bcl-2 and requirement for an organelle fraction enriched in mitochondria. Cell *79*, 353–364.

Oltvai, Z., Milliman, C., and Korsmeyer, S. J. (1993). Bcl-2 heterodimerizes in vivo with a conserved homolog, Bax, that accelerates programmed cell death. Cell *74*, 609–619.

Owen-Schaub, L. B., Radinsky, R., Kruzel, E., Berry, K., and Yonehara, S. (1994). Effects of anti-Fas on nonhematopoietic tumors: levels of Fas/APO-1 and *bcl-2* are not predictive of biological responsiveness. Cancer Res. *54*, 1580–1586.

Palazzolo, M. J., Hamilton, B. A., Ding, D., Martin, C. H., Mead, D. A., Mierendorf, R. C., Raghavan, K. V., Meyerowitz, E. M., and Lipshitz, H. D. (1990). Phage lambda cDNA cloning vectors for subtractive hybridization, fusion-protein synthesis and Cre–loxP automatic plasmid subcloning. Gene *66*, 25–36.

Rechsteiner, M. (1991). Natural substrates of the ubiquitin proteolytic pathway. Cell *66*, 615–618.

Reed, J. C. (1994). Bcl-2 and the regulation of programmed cell death. J. Cell Biol. *124*, 1–6.

Reed, J., Meister, L., Cuddy, M., Geyer, C., and Pleasure, D. (1991). Differential expression of the Bcl-2 proto-oncogene in neuroblastomas and other human neural tumors. Cancer Res. *51*, 6529–6538.

Reed, J. C., Tanaka, S., Cuddy, M., Cho, D., Smith, J., Kallen, R., Saragovi, H. U., and Torigoe, T. (1992). A strategy for generating monoclonal antibodies against recombinant baculovirus–produced proteins: application to the Bcl-2 oncoprotein. Anal. Biochem. *205*, 70–76.

Sarin, A., Clerici, M., Blatt, S. P., Hendrix, C. W., Shearer, G. M., and Henkart, P. A. (1994). Inhibition of activation-induced programmed cell death and restoration of defective immune responses of HIV^+ donors by cysteine protease inhibitors. J. Immunol. *153*, 862–872.

Sato, T., Hanada, M., Bodrug, S., Irie, S., Iwama, N., Boise, L. H., Thompson, C. B., Golemis, E., Fong, L., Wang, H.-G., and Reed, J. C. (1994). Interactions among members of the *bcl-2* protein family analyzed with a yeast two-hybrid system. Proc. Natl. Acad. Sci. USA *91*, 9238–9242.

Strasser, A., Harris, A. W., and Cory, S. (1991). *bcl-2* transgene inhibits T cell death and perturbs thymic self-censorship. Cell *67*, 889–899.

Takahashi, S., Sato, N., Takayama, S., Ichimiya, S., Satoh, M., Hyakumachi, N., and Kikuchi, K. (1993). Establishment of apoptosis-inducing monoclonal antibody 2D1–resistant variants of human T cell lines. Eur. J. Immunol. *23*, 1935–1941.

Toniolo, D., Persico, M., and Alcalay, M. (1988). A "housekeeping" gene on the X chromosome encodes a protein similar to ubiquitin. Proc. Natl. Acad. Sci. USA *85*, 851–855.

Torigoe, T., Millan, J. A., Chan, K. W. H., Taichman, R., Brian, A. A., and Reed, J. C. (1994a). Protein tyrosine kinase p56–lck regulates lymphocyte function–associated 1 adhesion molecule expression, granule exocytosis, and cytolytic effector function in a cloned T cell. J. Exp. Med. *180*, 1115–1127.

Torigoe, T., Millan, J. A., Takayama, S., and Reed, J. C. (1994b). Bcl-2 inhibits T-cell-mediated cytolysis of leukemia cell line. Cancer Res. *54*, 4851–4854.

Tsujimoto, Y., and Croce, C. M. (1986). Analysis of the structure, transcripts, and protein products of *bcl-2*, the gene involved in human follicular lymphoma. Proc. Natl. Acad. Sci. USA *83*, 5214–5218.

Vaux, D. L., Aguila, H. L., and Weissman, I. L. (1992a). Bcl-2 prevents death of factor-deprived cells but fails to prevent apoptosis in targets of cell mediated killing. Int. Immunol. *4*, 821–824.

Vaux, D. L., Weissman, I. L., and Kim, S. K. (1992b). Prevention of programmed cell death in *Caenorhabditis elegans* by human *bcl-2*. Science *258*, 1955–1957.

Yuan, J., Shaham, S., Ledoux, S., Ellis, H. M., and Horvitz, H. R. (1993). The C. elegans cell death gene *ced-3* encodes a protein similar to mammalian interleukin-1β-converting enzyme. Cell *75*, 641–652.

GenBank Accession Number

The accession number for the sequence reported in this paper is U17162.

Proc. Natl. Acad. Sci. USA
Vol. 91, pp. 9238–9242, September 1994
Cell Biology

Interactions among members of the Bcl-2 protein family analyzed with a yeast two-hybrid system

TAKAAKI SATO*, MOTOI HANADA*, SHARON BODRUG*, SHINJI IRIE*, NATSUKO IWAMA*, LAWRENCE H. BOISE†, CRAIG B. THOMPSON†, ERICA GOLEMIS‡, LINDA FONG*, HONG-GANG WANG*, AND JOHN C. REED*§

*La Jolla Cancer Research Foundation, Oncogene and Tumor Suppressor Gene Program, 10901 North Torrey Pines Road, La Jolla, CA 92037; †University of Chicago School of Medicine, Howard Hughes Medical Institute, Chicago, IL 60637; and ‡The Fox Chase Cancer Center, 7701 Burholme Avenue, Philadelphia, PA 19111

Communicated by Peter C. Nowell, May 27, 1994

ABSTRACT **Interactions of the Bcl-2 protein with itself and other members of the Bcl-2 family, including Bcl-X-L, Bcl-X-S, Mcl-1, and Bax, were explored with a yeast two-hybrid system. Fusion proteins were created by linking Bcl-2 family proteins to a LexA DNA-binding domain or a B42 trans-activation domain. Protein–protein interactions were examined by expression of these fusion proteins in *Saccharomyces cerevisiae* having a *lacZ* (β-galactosidase) gene under control of a LexA-dependent operator. This approach gave evidence for Bcl-2 protein homodimerization. Bcl-2 also interacted with Bcl-X-L and Mcl-1 and with the dominant inhibitors Bax and Bcl-X-S. Bcl-X-L displayed the same pattern of combinatorial interactions with Bcl-2 family proteins as Bcl-2. Use of deletion mutants of Bcl-2 suggested that Bcl-2 homodimerization involves interactions between two distinct regions within the Bcl-2 protein, since a LexA protein containing Bcl-2 amino acids 83–218 mediated functional interactions with a B42 fusion protein containing Bcl-2 amino acids 1–81 but did not complement a B42 fusion protein containing Bcl-2 amino acids 83–218. In contrast to LexA/Bcl-2 fusion proteins, expression of a LexA/Bax protein was lethal to yeast. This cytotoxicity could be abrogated by B42 fusion proteins containing Bcl-2, Bcl-X-L, or Mcl-1 but not those containing Bcl-X-S (an alternatively spliced form of Bcl-X that lacks a well-conserved 63-amino acid region). The findings suggest a model whereby Bax and Bcl-X-S differentially regulate Bcl-2 function, and indicate that requirements for Bcl-2/Bax heterodimerization may be different from those for Bcl-2/Bcl-2 homodimerization.**

The *bcl-2* gene becomes dysregulated in a wide variety of human cancers and contributes to neoplastic cell expansion by prolonging cell survival rather than by accelerating rates of cellular proliferation. Specifically, *bcl-2* blocks programmed cell death, a physiological process that normally ensures a homeostatic balance between cell production and cell turnover in most tissues with self-renewal capacity and which often involves characteristic changes in cell morphology termed apoptosis. In fact, Bcl-2 can prevent or delay apoptosis induced by a wide variety of stimuli, including growth factor deprivation, alterations in Ca^{2+}, free radicals, cytotoxic lymphokines, some types of viruses, radiation, and most chemotherapeutic drugs, suggesting that this oncoprotein controls a common final pathway involved in cell death regulation (reviewed in refs. 1 and 2).

The mechanism by which Bcl-2 prevents cell death remains enigmatic, as the predicted amino acid sequence of the 26-kDa human Bcl-2 protein (239 aa) has no significant homology with other proteins whose biochemical activity is known. Recently, however, Bcl-2 has been shown to interact with a low molecular weight GTPase member of the Ras family, p23-R-Ras (3), and also can be coimmunoprecipitated with the serine/threonine-specific protein kinase Raf-1 (4). Thus, Bcl-2 may somehow regulate a signal transduction pathway involving R-Ras and Raf-1. In addition, p26-Bcl-2 has been shown to form heterodimers (or possibly heterooligomers) with a 21-kDa protein, Bax. The Bax-α protein has ≈21% amino acid identity with Bcl-2 and is topographically similar to Bcl-2 in that both proteins contain a stretch of hydrophobic amino acids near their C termini (5). Gene transfer studies in lymphokine-dependent hemopoietic cells indicate that Bax antagonizes Bcl-2 function, abrogating the ability of Bcl-2 to prolong cell survival in the setting of growth factor withdrawal (5). It is unclear, however, which of these two proteins, Bcl-2 or Bax, is the active effector and which is the regulator. In this regard, two non-mutually exclusive possibilities exist: (*i*) Bcl-2 could induce a pathway that actively maintains cell survival, with Bax serving as a negative regulator of Bcl-2, or (*ii*) Bax could directly or indirectly generate death signals, with Bcl-2 serving in this case as a dominant inhibitor of Bax.

In addition to *bax*, several other cellular genes have been reported that encode proteins which share sequence homology with Bcl-2. Among these is *bcl-X*, which can generate two proteins through an alternative splicing mechanism: Bcl-X-L (longer form), a 241-aa protein which has 43% sequence identity with Bcl-2 and which suppresses cell death, and Bcl-X-S (shorter form), a 178-aa protein that is missing a 63-aa region (aa 126–188) found in Bcl-X-L and which functions as a dominant inhibitor of Bcl-2 (6). Another of these Bcl-2 homologs is Mcl-1, which shares ≈35% sequence identity with Bcl-2 over a region of ≈140 aa (7). The function of Mcl-1 with regard to regulation of cell death has not been reported, nor has the issue of whether Bcl-X-L, Bcl-X-S, or Mcl-1 can interact with either Bcl-2 or Bax been addressed. Using a yeast two-hybrid system (8–10), we explored interactions among various Bcl-2 family proteins.

MATERIALS AND METHODS

Yeast Strains, Media, and Transformations. *Saccharomyces cerevisiae* strain EGY191 (*MATα trp1 ura3 his3 LEU2::pLexAop1–LEU2*) was grown in YPD medium containing 1% yeast extract, 2% polypeptone, and 2% glucose. Burkholder's minimal medium (11) fortified with appropriate amino acids was used for preparation of high-phosphate medium (0.15% KH_2PO_4) unless otherwise specified. Plasmid DNA transformations were done by the LiCl method (12); cells were grown in complete minimal medium lacking uracil,

The publication costs of this article were defrayed in part by page charge payment. This article must therefore be hereby marked "*advertisement*" in accordance with 18 U.S.C. §1734 solely to indicate this fact.

Abbreviation: X-Gal, 5-bromo-4-chloro-3-indolyl β-D-galactopyranoside.

§To whom reprint requests should be addressed.

tryptophan, or histidine as necessary to select for the presence of various plasmids. Yeast cell extracts were prepared by a spheroplast method (13), and production of LexA and B42 fusion proteins was verified by immunoblot assays using a LexA-specific polyclonal antiserum (14) or a hemagglutinin (HA1)-specific monoclonal antibody (clone 12CA5; Boehringer Mannheim).

Reverse Transcription–PCR Cloning of *mcl-1* cDNA. To obtain cDNAs for human *mcl-1*, total RNA from U-937 human monocytic cells was reverse-transcribed with recombinant Moloney murine leukemia virus reverse transcriptase (Superscript) (GIBCO/BRL) and a combination of random oligodeoxynucleotide hexamers and a *mcl-1*-specific primer complementary to a region 3′ of the open reading frame (5′-CATAATCCTCTTGCCACTTGC-3′). The first-strand cDNA was amplified by PCR using Vent polymerase (New England Biolabs), a 5′ primer containing a *Sac* I site (underlined) flanking the initiation codon (5′-CAGAGCTCGCAATGTTTGGCCTCA-3′), and a reverse primer complementary to sequences downstream of the *mcl-1* stop codon (5′-GAAGTTACAGCTTGGAGTCC-3′). The 1.1-kb PCR product was digested with *Sac* I and *Hin*cII and cloned into the plasmid pBluescript SKII (Stratagene). The *mcl-1* cDNA was confirmed by DNA sequencing to be free of errors that would alter the Mcl-1 protein.

Plasmid Constructions. The cDNAs encoding Mcl-1, mouse Bax (15), human Bcl-2 (16), human Bcl-X-L and Bcl-X-S (6), and human Fas/APO-1 (17) were modified by a PCR mutagenesis approach (18) for subcloning in-frame into the two-hybrid plasmids pEG202 (a derivative of pLex202-PL containing an expanded polylinker) and pJG4-5 (8–10). To avoid problems with targeting of proteins to the nucleus, sequences corresponding to the transmembrane domains of Bcl-2, Bcl-X-L, Bcl-X-S, Bax, and Mcl-1 were omitted and a stop codon was inserted. The pEG202 plasmid utilizes an *ADH* promoter to constitutively drive expression of fusion proteins containing an N-terminal LexA DNA-binding domain (aa 1–202). All cDNAs for testing were subcloned between the *Eco*RI and *Bam*HI sites of pEG202, in frame with the upstream *lexA* sequences. Forward and reverse primers (*Eco*RI site underlined, *Bcl* I site overlined, and stop codons in bold type) included (*i*) for Bcl-2 (aa 1–218), 5′-GGAATTCATGGCGCACGCTGGGAGAAC-3′ and 5′-TGATCACTTCAGAGACAGCCAC-3′; (*ii*) for Bcl-X-L (aa 1–212) and Bcl-X-S (aa 1–149), 5′-GGAATTCATGTCTCAGAGCAACCGG-3′ and 5′-CTGATCAGCGGTTGAAGCGTTCCTG-3′; (*iii*) for Bax (aa 1–171), 5′-GGAATTCGCGGTGATGGACGGGTCCGG-3′ and 5′-GGAATTCTCAGCCCATCTTCTTCCAGA-3′; (*iv*) for human Fas/APO-1 (aa 191–335), 5′-GGAATTCAAGAGAAAGGAAGTACAG-3′ and 5′-TGATCACTAGACCAAGCTTTGGAT-3′. (*v*) For Mcl-1 (aa 1–329), the PCR-generated "full-length" *mcl-1* cDNA described above was first subcloned into pUC18 to pick up an *Eco*RI site at the 5′ end and then was digested with *Xho* I and *Hin*cII, and the resulting 0.34-kb fragment representing the 3′ portion of the *mcl-1* open reading frame containing the transmembrane region was replaced with a 0.28-kb *Xho* I–*Sma* I fragment (lacking the transmembrane region) that was derived by reverse transcription–PCR from U-937 mRNA by using the primers 5′-AGAATTCACCTTACGACGGGTTGG-3′ and 5′-CGAATTCACCTGATGCCACCTTCTAG-3′. The resulting plasmid was digested with *Eco*RI, and the 1.0-kb fragment representing *mcl-1* (aa 1–329) was subcloned into the *Eco*RI sites of pEG202 and pJG4-5.

The pJG4-5 plasmid utilizes a galactose-dependent promoter from the *GAL1* gene to inducibly drive expression of fusion proteins containing an N-terminal B42 trans-activation domain, simian virus 40 nuclear localization signal sequence, and hemagglutinin (HA1) epitope tag (8–10). All cDNAs for testing were liberated from the pEG202 plasmids described above by cleavage with *Eco*RI and *Xho* I and then subcloned between the *Eco*RI and *Xho* I sites of pJG4-5, in frame with the upstream B42 sequences. The plasmids pEG202-c-raf-1, pEG202-laminC, and pJG4-5-laminC were constructed from pBMT116-c-raf-1 and pBMT116-laminC (19) generously provided by S. Hollenberg (University of Washington).

For construction of Bcl-2 deletion mutants, pEG202-Bcl-2-(1–81) and pJG4-5-Bcl-2-(1–81), the pEG202-Bcl-2 and pJG4-4-Bcl-2 plasmids were digested with *Sac* II/*Bam*HI and *Sac* II/*Xho* I, respectively. The ends of these digested plasmids were intramolecularly ligated after blunting with T4 DNA polymerase. The pEG202-Bcl-2-(1–81) and pJG4-5-Bcl-2-(1–81) plasmids contain an additional 3 codons and 38 codons of plasmid-derived coding sequences before the stop codon, respectively. For construction of pEG202-Bcl-2-(83–218) and pJG4-5-Bcl-2-(83–218) plasmids, both pEG202-Bcl-2 and pJG4-5-Bcl-2 were digested with *Sac* II and *Eco*RI, and the ends were made blunt with T4 DNA polymerase and then intramolecularly ligated. The structure of the regions of Bcl-2, Bax, Bcl-X, and Mcl-1 subcloned into yeast expression plasmids is diagrammed in Fig. 1. Proper construction of all plasmids and absence of PCR-generated errors were verified in every case by DNA sequence analysis.

β-Galactosidase Assays. EGY191 cells were stably transformed with the LexA operator–*lacZ* reporter gene plasmid SH18-34 (gifts of S. Hanes, Massachusetts General Hospital, Boston) and selected for growth on uracil-deficient medium. For plate assays, yeast were spotted onto SD minimal medium plates lacking uracil, tryptophan, and histidine and containing 2% glucose or 2% galactose and the chromogenic substrate 5-bromo-4-chloro-3-indolyl β-D-galactopyranoside (X-Gal) (20). Filter assays were performed with X-Gal as a substrate, essentially as described (21), except that Pall nylon membranes were used instead of nitrocellulose filters. Z-buffer (13) containing X-Gal (25 μg/ml) in *N,N*,-dimethylformamide was used for measurements of β-galac-

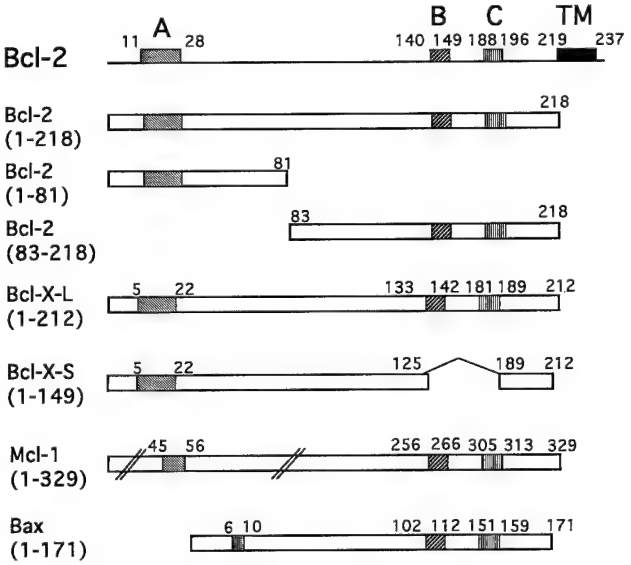

FIG. 1. Schematic depiction of regions of Bcl-2 and related proteins expressed as LexA or B42 fusion proteins. The structure of the human Bcl-2 protein is presented in linear form, indicating the three regions that are conserved among many of the family members (domains A, B, and C) and the corresponding amino acid positions. The transmembrane (TM) domain was excluded from all fusion proteins by introduction of a stop codon. The Bcl-X-S protein has a 63-aa deletion relative to Bcl-X-L because of a splicing event. The Mcl-1 protein is the longest of the family members (denoted by slashes).

tosidase activity. Filters were monitored for blue reaction products at 0.5, 1, 2, 4, and 24 hr.

RESULTS

Interactions Among Members of the Bcl-2 Protein Family. A LexA/Bcl-2 fusion protein containing aa 1–218 of the human Bcl-2 protein (lacking the C-terminal region, aa 219–239, which includes the transmembrane domain of Bcl-2) resulted in trans-activation of a *lacZ* reporter gene containing LexA operators when coexpressed with a fusion protein representing the B42 trans-activation domain fused with Bcl-2-(1–218) (Table 1). Furthermore, trans-activation of the *lacZ* reporter occurred only when cells were grown on galactose-containing plates but not on glucose plates, consistent with the galactose dependency of the *GAL1* promoter used to drive expression of the B42/Bcl-2-(1–218) expression plasmid. Expression of the LexA/Bcl-2 protein also resulted in *lacZ* reporter activation when combined with B42/Bcl-X-L, B42/Bcl-X-S, B42/Mcl-1, or B42/Bax protein in this assay (Table 1), implying that Bcl-2 can interact not only with itself but also with Bcl-X-L, Bcl-X-S, Bax, and Mcl-1. The interactions of Bcl-2 with itself and other members of the Bcl-2 family as revealed by the two-hybrid approach were specific, based on the use of control proteins including LexA/Raf, LexA/Fas, LexA/laminC, B42/Ha-Ras, and other B42 fusion proteins.

As with Bcl-2, expression of a LexA/Bcl-X-L fusion protein also resulted in *lacZ* reporter activation when combined with B42/Bcl-2, B42/Bcl-X-L, B42/Bcl-X-S, B42/Bax, or B42/Mcl-1 fusion protein but not with the B42/Ras, B42/5-1, or B42/5-2 protein (Table 1 and data not shown). Thus, Bcl-X-L appears to be capable of mediating the same spectrum of interactions among these members of the Bcl-2 protein family as that observed for Bcl-2. Interestingly, expression of a B42/Bcl-X-S protein in combination with either LexA/Bcl-2 or LexA/Bcl-X-L resulted in particularly high levels of *lacZ* reporter activation, as indicated by the more intense blue color produced in these colonies when grown on plates containing the β-galactosidase colorimetric substrate X-Gal, relative to cells expressing B42/Bcl-2 or B42/Bcl-X-L protein (Table 1). Immunoblot analysis revealed comparable levels of all B42 fusion proteins (data not shown), thus excluding quantitative differences in the amounts of B42/Bcl-X-S, B42/Bcl-2, and B42/Bcl-X-L protein production as an explanation for this phenomenon and suggesting that the interaction of Bcl-X-S with Bcl-2 and Bcl-X-L may be of higher affinity than the interactions of the Bcl-2 and Bcl-X-L proteins with themselves or each other. Confirmation of this suspicion, however, must await formal determination of the dissociation constants for Bcl-2 with itself and Bcl-X-S using purified proteins.

Structural Requirements for Bcl-2 Homodimerization. As a preliminary attempt to delineate the subregions within Bcl-2 that are required for Bcl-2/Bcl-2 homodimerization, constructs were prepared that encoded either LexA or B42 fusion proteins containing an N-terminal truncation mutant of Bcl-2 (aa 83–218). The LexA/Bcl-2-(83–218) protein interacted with a "full-length" B42/Bcl-2(1–218) protein but not the "truncated" B42/Bcl-2(83–218) fusion protein in the two-hybrid system (Table 2). Conversely, the B42/Bcl-2-(83–218) truncation mutant interacted with full-length LexA/Bcl-2-(1–218) but not with LexA/Bcl-2-(83–218). Taken together, these results exclude insufficient levels of B42/Bcl-2-(83–218) and LexA/Bcl-2-(83–218) protein production as an explanation for the failure of these N-terminal truncation mutants to interact with each other.

The finding that the Bcl-2 N-terminal deletion mutant was capable of mediating interactions with "full-length" Bcl-2-(1–218) but could not homodimerize with itself implies that amino acid sequences located between residues 1 and 82 of the Bcl-2 protein are required for interactions with the Bcl-2-(83–218) region. To test this hypothesis, a construct was prepared that encoded a B42 fusion protein containing aa 1–81 of human Bcl-2. The B42/Bcl-2-(1–81) protein interacted with LexA/Bcl-2-(1–218) and LexA/Bcl-2-(83–218) in the two-hybrid system, consistent with a model involving interaction of an N-terminal domain of Bcl-2 with the C-terminal region of Bcl-2 in a head-to-tail fashion. LexA/Bcl-2-(83–218) also resulted in *lacZ* reporter expression in a galactose-dependent manner when coexpressed with B42 fusion proteins containing Bcl-X-L, Bcl-X-S, or Mcl-1 (Table 2), implying that amino acid sequences sufficient for association with the 83–218 region of Bcl-2 are conserved within all of these proteins. The interactions mediated by the B42/Bcl-2-(1–81) protein appeared to be specific, since B42/Bcl-2-(1–81) failed to interact with LexA/laminC, LexA/CD40, LexA/Fas, and LexA/Raf negative control proteins (Table 2).

Bax Exhibits a Lethal Phenotype in Yeast That Is Neutralized by Bcl-2, Bcl-X-L, and Mcl-1. When Bax was expressed in yeast as a B42 fusion protein in pJG5.4 under the control of a galactose-inducible *GAL1* gene promoter, growth upon replica plating from glucose to galactose-containing plates was retarded in many cases (Tables 1 and 2). Moreover, expression of Bax as a LexA fusion protein in pEG202 under the control of the *ADH* promoter—a stronger, constitutive promoter—resulted in nearly complete absence of colony formation on glucose plates (Table 3). In contrast, transformation of cells with the same expression vector, pEG202, containing the *bax* cDNA in reverse (antisense) orientation produced colonies on glucose-containing medium at approx-

Table 1. Summary of yeast two-hybrid assay results for Bcl-2 and Bcl-X-L proteins

	B42							
LexA	Bcl-2	Bcl-X-L	Bcl-X-S	Mcl-1	Bax	Clone 1	Clone 2	[Val^{12}]Ras
Bcl-2	+	+	+++	+	+	−	−	−
Bcl-X-L	+	+	+++	+	+	−	−	−
c-Raf	−	−	−	−	−	−	−	++
Lamin	−	−	−	−	−	−	−	−
Fas	−	−	−	−	−	−	−	−

Versions of the pEG202 expression plasmids producing either LexA DNA-binding-domain fusion proteins (listed at left) or derivatives of pJG4-5 that encode B42 trans-activation-domain fusion proteins (listed at top) were introduced into EGY191 cells (5 μg each) and the resulting transformants were grown on plates containing X-Gal and either galactose or glucose as a carbon source. Combinations of two-hybrid plasmids that resulted in galactose-dependent production of blue colored colonies are indicated as +, ++, or +++ depending on the relative strength of the blue color reaction. All positive combinations produced discernible blue color within 4 hr in filter assays. Data were in agreement in all cases for both plate and filter assays. Some plasmid combinations failed to result in blue color production on either galactose or glucose-containing medium (−). Clones 1 and 2 are random cDNAs from a HeLa cell library (8).

Table 2. Analysis of interactions of Bcl-2 deletion mutants by two-hybrid assay

	B42								
LexA	Bcl-2	Bcl-2-(83–218)	Bcl-2-(1–81)	Bcl-X-L	Bcl-X-S	Bax	Mcl-1	Clone 1	Clone 2
Bcl-2	+	++	+	+	+++	+	+	−	−
Bcl-2-(83–218)	++	−	++	++	++	− (PG)	+	−	−
Bcl-X-L	+	++	+	+	+++	+	+	−	−
Fas	−	−	−	−	−	− (PG)	−	−	−
CD40	ND	ND	−	ND	ND	ND	ND	−	−
c-raf	−	−	−	−	−	− (PG)	−	−	−
Lamin	−	−	−	−	−	− (PG)	−	−	−

Experiments were performed as in Table 1. Transformants that grew poorly are indicated (PG). ND, not done.

imately normal efficiencies (Table 3). Additional experiments (data not shown) indicated that expression of the LexA/Bax protein was lethal to EGY191 yeast cells and not merely growth inhibitory.

In contrast, when EGY191 cells that had been cotransformed with the LexA/Bax vector and galactose-inducible B42/Bcl-2, B42/Bcl-X-L, or B42/Mcl-1 plasmid were plated directly on galactose-containing medium, colony formation occurred. Coexpression of B42/Bcl-X-S, however, did not nullify the inhibitory activity of LexA/Bax. The deletion mutant forms of Bcl-2, B42/Bcl-2-(1–81), and B42/Bcl-2-(83–218), as well as the control proteins B42/laminC and B42/5-1, also failed to abrogate the suppressive effects of LexA/Bax on colony formation (Table 3). Immunoblot analysis demonstrated comparable levels of all B42 fusion proteins in EGY191 cells (data not shown), suggesting that quantitative differences in the amounts of B42 fusion protein production cannot account for the failure of the B42/Bcl-X-S, B42/Bcl-2-(1–81), and B42/Bcl-2-(83–218) proteins to nullify the inhibitory effects of LexA/Bax.

DISCUSSION

Using a yeast two-hybrid system, we have obtained evidence for combinatorial interactions among several members of the Bcl-2 protein family. In addition to the previously reported interaction of Bcl-2 with Bax (5), the data presented here suggest that the following additional interactions can occur among Bcl-2 family proteins: (*i*) Bcl-2 with Bcl-2, (*ii*) Bcl-2 with Bcl-X-L, (*iii*) Bcl-2 with Bcl-X-S, (*iv*) Bcl-2 with Mcl-1, (*v*) Bcl-X-L with Bcl-X-L, (*vi*) Bcl-X-L with Bax, (*vii*) Bcl-X-L with Bcl-X-S, (*viii*) Bcl-X-L with Mcl-1, and (*ix*) Bax with Mcl-1. Of course, interpretation of results obtained by use of the two-hybrid approach must take into consideration several caveats. First, the results do not exclude the possibility that the interactions detected among members of the Bcl-2 family are indirect, requiring an additional bridging protein(s) that is conserved from yeast to humans. Second, the stoichiometry of these interactions can also not be inferred from these data, and while it is attractive to view the results as consistent with a homo/heterodimerization model, one cannot exclude other possibilities. Third, though the data presented here reveal the array of protein–protein interactions that are theoretically possible, they do not guarantee that these interactions occur in physiologically relevant contexts in mammalian cells.

The finding that LexA/Bax has an apparently lethal effect in *S. cerevisiae* strongly suggests that Bax is a cell-death effector protein, as opposed to merely a repressor of proteins (e.g., Bcl-2) that may be necessary for cell survival. However, it is possible that the lethal effects of Bax in yeast reflect its ability to bind to and neutralize an endogenous yeast homolog of Bcl-2—though we favor the alternative interpretation, given our previous lack of success with cloning of Bcl-2 homologs from yeast (unpublished data). While ectopic expression of mammalian proteins in yeast can sometimes be nonspecifically toxic, the lethal effect of Bax appeared to be specific, inasmuch as it was partially abrogated by Bcl-2 and Bcl-X-L, two known suppressors of apoptotic cell death, but not by Bcl-X-S, a dominant inhibitor of Bcl-2. To the extent that the cell-death pathways in mammalian cells and yeast are conserved, our discovery of an apparently lethal phenotype for Bax in *S. cerevisiae* suggests possibilities for using the power of yeast genetics to map this pathway and delineate several of the proteins involved.

Our preliminary attempts to map the regions within Bcl-2 that are necessary for homodimerization suggest a head-to-tail model for this protein–protein interaction (Fig. 2). This model is consistent with the observation that a LexA/Bcl-2-(83–218) fusion protein was able to complement a B42/Bcl-2-(1–81) fusion protein whereas it did not interact with a B42/Bcl-2-(83–218) protein. Unfortunately, it was not possible to perform the converse experiment using a LexA/Bcl-2-(1–81), because of nonspecific reporter gene activation. The explanation for this phenomenon is unclear, but the nonspecific activation could be due to a short stretch of acidic residues at positions 28–34 of the human Bcl-2 protein which may become unmasked in the deletion mutant LexA/Bcl-2-(1–81) and thus be able to function directly as a transactivating sequence (10). When the Bcl-2-(1–81) region was expressed as B42 fusion, however, no problems with nonspecific reactivity were encountered. For example, while the B42/Bcl-2(1–81) protein complemented LexA/Bcl-2-(1–218) ("full-length" Bcl-2) and LexA/Bcl-2-(83–218) proteins in the two-hybrid system, it displayed absolutely no reactivity

Table 3. Neutralization of Bax activity by Bcl-2, Bcl-X-L, and Mcl-1

		B42							
LexA	Medium	Bcl-2	Bcl-X-L	Bcl-X-S	Mcl-1	Bcl-2-(83–218)	Bcl-2-(1–81)	Clone 1	Lamin
Bax	Gal	2.8×10^2	3.0×10^2	− (10)	2.9×10^2	− (16)	− (19)	− (9)	− (8)
(sense)	Glc	− (1)	− (5)	− (3)	− (1)	− (10)	− (10)	− (15)	− (7)
Bax	Gal	1.2×10^3	ND	ND	ND	ND	ND	ND	2.2×10^3
(antisense)	Glc	6.6×10^2	ND	ND	ND	ND	ND	ND	2.2×10^3

EYG191 cells were cotransformed with 5 μg each of pEG202- and pJG4-5-based expression plasmids and plated onto semisolid medium containing either galactose (Gal) or glucose (Glc). The number of visible colonies that formed is indicated; for plates scored as negative (−) for growth, the number of visible colonies is given in parentheses. ND, not done. Data are representative of three of three experiments.

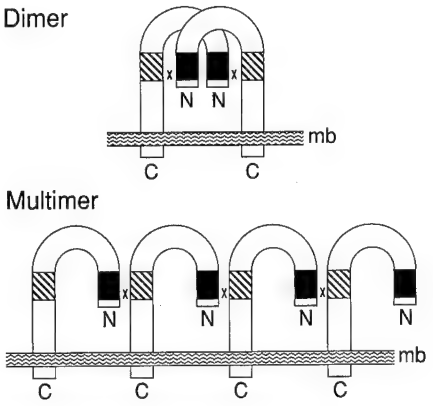

FIG. 2. Head-to-tail model for Bcl-2 protein interaction. The Bcl-2 protein contains a hydrophobic C-terminus that anchors it in membranes (mb). Interaction (X) between an N-terminal domain (black boxes) and a C-terminal domain (striped boxes) is required for formation of protein dimers or multimers.

with a variety of negative control LexA fusion proteins, including LexA/laminC, LexA/CD40, LexA/Raf-1, and LexA/Fas. Though our data are consistent with homodimerization of Bcl-2 proteins occurring via intermolecular interactions between two distinct regions within the protein, these results could instead reflect an intramolecular interaction of the 1–81 region of Bcl-2 with the 83–218 region. However, the ability of "full-length" Bcl-2-(1–218) fusion proteins to interact in the two-hybrid system with Bcl-2-(1–81) and Bcl-2-(83–218) fusion proteins tends to argue against this alternative interpretation. The precise amino acid residues within Bcl-2 involved in this multimerization are a matter for future investigations, but likely candidates are the three domains that are highly conserved among many members of this multigene family (22) [referred to as Bcl-2 domains (BD) A–C in Fig. 1]. Of note, however, is the finding that the Bcl-X-S protein, which lacks BD-B and BD-C because of an alternative splicing event, can still interact with Bcl-2 and Bcl-X-L in the two-hybrid system. This result suggests that BD-B and BD-C are not required for interaction of Bcl-X-S with Bcl-2 and Bcl-X-L and is consistent with the idea of a head-to-tail interaction where an N-terminal domain in Bcl-X-S can interact with a C-terminal domain or domains in Bcl-2 and Bcl-X-L—which could include, however, BD-B or BD-C within Bcl-2 and Bcl-X-L. It is interesting, therefore, that Bcl-X-S did not neutralize Bax-mediated cytotoxicity in yeast whereas Bcl-2 and Bcl-X-L did (Table 3). This result implies that the 63-aa region missing from Bcl-X-S, which contains BD-B and BD-C, is important either for heterodimerization of Bax with Bcl-2 and Bcl-X-L, or for neutralization of Bax function, or both.

Although the two-hybrid data indicate that both Bax and Bcl-X-S can bind to Bcl-2, our data derived from *S. cerevisiae* suggest that these dominant inhibitors abrogate Bcl-2 function through different mechanisms. For example, Bax was lethal to EGY191 cells when expressed at high levels as a fusion protein with LexA, whereas LexA/Bcl-X-S did not produce similar results and, in fact, LexA/Bcl-X-S-expressing cells appeared to have a slight growth advantage relative to other transformants (unpublished data). These results therefore suggest a model that proposes different mechanisms by which the dominant inhibitors Bax and Bcl-X-S abrogate Bcl-2 function. In this model (Fig. 3), Bax is envisioned as a cell-death effector whose activity is neutralized by binding of Bcl-2. The binding of Bcl-X-S to Bcl-2 we hypothesize prevents Bcl-2 from interacting with Bax and thus leaves Bax unopposed in its cell-death effector function. It may be of further relevance that the interaction of Bcl-X-S

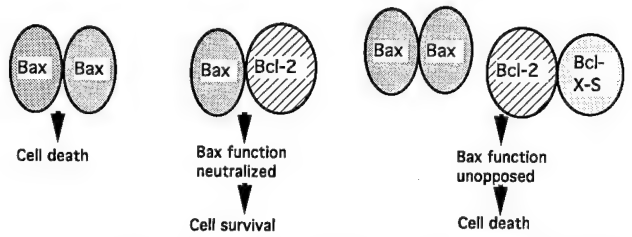

FIG. 3. Model for differential regulation of cell death by Bax and Bcl-X-S. In this speculative model, Bax is theorized to form a homodimer with itself that generates cell-death "signals" (*Left*). Heterodimerization of Bcl-2 and Bax abrogates Bax function (*Center*). Bcl-X-S binding to Bcl-2 prevents Bcl-2 from binding to and neutralizing Bax (*Right*).

with Bcl-2 in two-hybrid assays appeared to be more potent than the interaction of Bcl-2 with itself, suggesting that Bcl-X-S/Bcl-2 heterodimers represent higher-affinity protein–protein interactions than Bcl-2/Bcl-2 homodimers. Though highly speculative, this model provides a reasonable starting point for future investigations and is consistent with all of the data available to date.

Note Added in Proof. A recent paper by Yin *et al.*. (23) confirmed portions of this work in mammalian cells.

This work was supported in part by National Institutes of Health Grants CA60181 and CA47956 and by a grant from the Council for Tobacco Research (CTR-3113). J.C.R. is a Scholar and L.H.B. is a Fellow of the Leukemia Society of America. T.S. is a Fellow of the U.S. Army Medical Research Development Command, Breast Cancer Research Program. S.B. is a Fellow of the Medical Research Council of Canada.

1. Reed, J. C. (1994) *J. Cell Biol.* **124,** 1–6.
2. Wyllie, A. H., Kerr, J. F. R. & Currie, A. R. (1980) *Int. Rev. Cytol.* **68,** 251–306.
3. Fernandez-Sarabia, M. J. & Bischoff, J. R. (1993) *Nature (London)* **366,** 274–275.
4. Wang, H.-G., Miyashita, T., Takayama, S., Sato, T., Torigoe, T., Krajewski, S., Tanaka, S., Hovey, L., III, Troppmair, J., Rapp, U. R. & Reed, J. C. (1994) *Oncogene* **9,** 2751–2756.
5. Oltvai, Z., Milliman, C. & Korsmeyer, S. J. (1993) *Cell* **74,** 609–619.
6. Boise, L. H., Gonzâalez-Garcia, M., Postema, C. E., Ding, L., Lindsten, T., Turka, L. A., Mao, X., Nunez, G. & Thompson, C. B. (1993) *Cell* **74,** 597–608.
7. Kozopas, K. M., Yang, T., Buchan, H. L., Zhou, P. & Craig, R. W. (1993) *Proc. Natl. Acad. Sci. USA* **90,** 3516–3520.
8. Zervous, A. S., Gyuris, J. & Brent, R. (1993) *Cell* **72,** 223–232.
9. Gyuris, J., Golemis, E., Chertkov, H. & Brent, R. (1993) *Cell* **75,** 791–803.
10. Golemis, E., Gyuris, J. & Brent, R. (1994) in *Current Protocols in Molecular Biology*, eds. Ausubel, F. M., Brent, R., Kingston, R. E., Moore, D. D., Seidman, J. G., Smith, J. A. & Struhl, K. (Wiley, New York), in press.
11. Tohe, A., Ueda, Y., Kakimoto, S.-I. & Oshima, Y. (1973) *J. Bacteriol.* **113,** 727–738.
12. Schiestl, R. H. & Giest, R. D. (1989) *Curr. Genet.* **16,** 339–346.
13. Smith, D. B. & Corcoran, L. M. (1989) in *Current Protocols in Molecular Biology*, eds. Ausubel, F. M., Brent, R., Kingston, R. E., Moore, D. D., Seidman, J. G., Smith, J. A. & Struhl, K. (Wiley, New York), pp. 13.13.1–13.13.7.
14. Brent, R. & Ptashne, M. (1984) *Nature (London)* **312,** 612–615.
15. Miyashita, T., Krajewski, S., Krajewska, M., Wang, H.-G., Lin, H. K., Hoffman, B., Lieberman, D. & Reed, J. C. (1994) *Oncogene* **9,** 1799–1805.
16. Tanaka, S., Saito, K. & Reed, J. C. (1993) *J. Biol. Chem.* **268,** 10920–10926.
17. Itoh, N., Yonehara, S., Ishii, A., Yonehara, M., Mizushima, S.-I., Sameshima, M., Hase, A., Seto, Y. & Nagata, S. (1991) *Cell* **66,** 233–243.
18. Higuchi, R. (1990) in *PCR Protocols*, eds. Innis, M. A., Gelfard, D. H., Sivinsky, J. J. & White, T. J. (Academic, San Diego), pp. 177–183.
19. Vojtek, A. B., Hollenburg, S. M. & Cooper, J. M. (1993) *Cell* **74,** 205–214.
20. Chien, C.-T., Bartel, P. L., Sternglanz, R. & Fields, S. (1991) *Proc. Natl. Acad. Sci. USA* **88,** 9578–9582.
21. Breeden, L. & Nasmyth, K. (1985) *Cold Spring Harbor Symp. Quant. Biol.* **50,** 643–650.
22. Sato, T., Irie, S., Krajewski, S. & Reed, J. C. (1994) *Gene* **140,** 291–292.
23. Yin, X.-M., Otlvai, Z. N. & Korsmeyer, S. J. (1994) *Nature (London)* **369,** 321–323.

Trophinin and tastin, a novel cell adhesion molecule complex with potential involvement in embryo implantation

Michiko N. Fukuda,[1,4] Takaaki Sato,[1] Jun Nakayama,[1] George Klier,[1,3] Mikio Mikami,[1,2] Daisuke Aoki,[2] and Shiro Nozawa[2]

[1]La Jolla Cancer Research Foundation, La Jolla, California 92037 USA; [2]Department of Gynecology and Obstetrics, Keio University School of Medicine, Tokyo, Japan

Two human epithelial cell lines, trophoblastic teratocarcinoma HT-H and endometrial adenocarcinoma SNG-M cells, adhere to each other at their respective apical cell surfaces in a divalent cation-independent manner. Two novel molecules responsible for the adhesion between these two cell types were identified by expression cDNA cloning. One, named trophinin, is an intrinsic membrane protein and mediates homophilic self-binding. Another, named tastin, is a cytoplasmic protein and is necessary for trophinin to function as a cell adhesion molecule. Trophinin and tastin appear to be associated with the cytoskeleton in HT-H and SNG-M cells. These molecules are normally not expressed in various types of human cells in tissues, with the exception of macrophages. Strong expression of these molecules was detected in the trophectoderm surface of monkey blastocyst. These molecules are also expressed in human endometrial surface epithelium on day 16/17 at the early secretory phase of human endometrium, the time consistent with that expected for the "implantation window."

[*Key Words*: Trophoblast; polarized epithelium; cytoskeleton; molecular cloning; embryo]

Received February 14, 1995; revised version accepted March 30, 1995.

Although the precise morphological events of implantation vary from species to species, one essential feature is the formation of allogeneic and heterotypic cell-to-cell contacts between embryonic and maternal cells. The early events of implantation are an initial apposition of the trophoblast to the uterus and subsequent adhesion of the trophoblast to the endometrial epithelium (Sclafke and Enders 1975; Enders et al. 1981; Kaufman 1985; Ringler and Strauss 1990; Aplin 1991). The initial attachment of the trophoblast to the endometrial epithelium is unusual in that this cell-to-cell contact occurs via their respective apical cell membranes. In general, the apical surface of the epithelium is not adhesive, whereas the basolateral surface supports adhesion. One hypothesis is that the apical surfaces of the trophectoderm and uterine epithelium express a "basolateral" character that promotes adhesion between the blastocyst and the uterine epithelium (Leivo et al. 1980; Armant et al. 1986; Farach et al. 1987; Sutherland et al. 1988). Alternatively, the apical plasma membranes of the trophoblast and endometrial epithelia express unique cell adhesion molecules that mediate an initial attachment between these cells (Kliman et al. 1989).

[3]Present address: Department of Cell Biology, Scripps Research Institute, La Jolla, California 92037 USA.
[4]Corresponding author.

Attempts to identify molecules involved in embryo implantation have been conducted both in vivo and in vitro (Leivo et al. 1980; Armant 1986; Farach et al. 1987; Kimber et al. 1988; Lindenberg et al. 1988; Sutherland et al. 1988; Romagnano and Babiartz 1990; Yamagata and Yamazaki 1991). Analysis of implantation at the molecular level, however, has been difficult because of the lack of tractable model systems, particularly if the human embryo is the subject to be analyzed.

In vivo, human endometrium is under strict hormonal controls and is generally not permissive to implantation (Yoshinaga 1988). During a relatively short time in the menstrual cycle, the surface epithelium of the endometrium becomes receptive to trophoblast attachment (Harper 1992). It is difficult to reproduce such an "implantation window" using endometrial epithelia in tissue culture. However, recent studies using several endometrial adenocarcinoma cell lines suggest that some of the adenocarcinoma cells interact with trophoblastic cells at their apical cell surfaces (John et al. 1993; Rohde and Carson 1993).

Morphological studies of human embryo implantation indicate that trophoblasts of the blastocyst that are in contact with the endometrial epithelia are binucleated, suggesting early syncytia formation at the implantation stage (Lindenberg et al. 1986). We have shown previously that HT-H human teratocarcinoma cells (Ducibella et al.

1982) spontaneously differentiate into syncytiotrophoblast-like cells (Izhar et al. 1986). Because cell lines established from teratocarcinoma tumors often show characteristics of cells at early embryonic stages (Martin 1980; Andrew et al. 1983), HT-H cells were thought to exhibit both embryonic and syncytiotrophoblastic properties.

In this paper we describe the adhesion of HT-H cells (Izhar et al. 1986) to endometrial adenocarcinoma SNG-M cells (Ishiwata et al. 1977) and identify the molecules responsible for the cell adhesion between these two cell types. The expression pattern of the cloned molecules in vivo and activity of the cloned proteins support the possibility that they mediate the adhesion of the blastocyst to the endometrial epithelium at the time of implantation.

Results

Trophoblastic teratocarcinoma HT-H cells adhere to the upper surface of endometrial adenocarcinoma SNG-M cells

The adhesion of HT-H cells to several human endometrium epithelial cells was examined (Table 1). The HT-H cells attached to the SNG-M, Hec1A, KLE, and RL95-2 cells but did not adhere to the AN3CA cells. Because HT-H cells adhere to SNG-M cells most efficiently in the presence of EDTA, adhesion between these two cell lines was analyzed further.

HT-H cells adhered efficiently to the SNG-M cells (Table 1). SNG-M cells also adhered to their own cell type (Fig. 1A), suggesting that the adhesion between these two cell types is mediated by a homophilic adhesion mechanism rather than ligand receptor-type heterophilic adhesion mechanism. COS-1 cells adhered poorly to a monolayer of SNG-M cells (Fig. 1A). Other types of epithelial cells, HeLa, HepG2, SW480, and A431, did not adhere to monolayers of the SNG-M cells.

Similar results were obtained when HT-H cell monolayers were tested for adhesion (not shown), indicating that adhesion between the HT-H and SNG-M cells is homophilic and cell type-specific and occurs at their respective upper cell surfaces.

Morphological characterization of HT-H and SNG-M cells at contact

Attachment of HT-H and SNG-M cells was examined under an electron microscope. At 10 min after contact, HT-H cells were seen with their upper surfaces facing the upper surface of SNG-M cells (Fig. 2A,B). There are many microvilli between these two cell types. Electron microscopy of the cells after 6 hr of coculture shows closer adhesive interactions between these two cell types (Fig. 2C). After 4 days of coculture, the microvilli disappeared completely from the surfaces of both cell types and desmosome-like adherent junctions were formed between the HT-H and SNG-M cells (Fig. 2D).

Morphological studies of human embryo implantation in vivo (Knoth and Larsen 1972) and in vitro (Lindenberg et al. 1986) demonstrate similar characteristics shown in Figure 2, except that the trophoblasts intrude between endometrial epithelia in vivo and HT-H cells do not intrude between SNG-M cells.

Table 1. *Adhesion of HT-H cells on the upper surfaces of endometrial adenocarcinoma cells*

Endometrial Adenocarcinoma Cells[a]	HT-H Cells Attached[b] (%)	
	EDTA$^-$	EDTA$^+$
SNG-M	56.9 ± 8.2	49.7 ± 7.3
Hec1A	29.6 ± 10.2	24.2 ± 8.3
KLE	32.5 ± 8.5	27.3 ± 4.8
RL95-1	83.5 ± 9.7	20.4 ± 12.1
AN3CA	4.2 ± 0.8	2.1 ± 0.6

[a]All assays were performed by using live ^{35}S-labeled HT-H cells suspended in HBS (10 mM HEPES buffer at pH 7.4 containing 0.12 M NaCl). Twenty minutes after adding HT-H cells on the monolayers, nonadherent HT-H cells were washed with HBS with or without 1 mM EDTA. Numbers are expressed as percent radioactivity remaining on the monolayer relative to the total radioactivity of ^{35}S-labeled HT-H cells added. The results were obtained by each triplicate experiment.

[b]Unfixed monolayers of endometrial adenocarcinoma cells were used in these adhesion assays. Trophoblastic HT-H cells were separated from undifferentiated HT-H cells as described, subcloned, and used in the present study. Endometrial adenocarcinoma cell lines Hec1A, RL95-2, and AN3CA were obtained from the American Tissue Culture Collection. All cells lines were cultured in DMEM containing 10% fetal bovine serum, 2 mM glutamine, 100 U/ml of penicillin and 100 μg/ml of streptomycin. HT-H cells were metabolically labeled with ^{35}S-Label (New England Nuclear) in methionine- and cysteine-free RPMI medium for 20 min and chased with complete medium for 2 hr. The ^{35}S-labeled HT-H cells were detached from the bottom of the tissue culture dishes using cell dissociation solution (Specialty Media, Lavalette, NJ). The cells (0.2 ml, 5 × 10^5 cells) were suspended in HBS and added to the monolayers of endometrial adenocarcinoma cells that had been grown on the bottom of a 24-well tissue culture plate. After 20 min, the monolayers were washed three times with HBS with or without 1 mM EDTA. The cells remaining in each well were solubilized with 0.5 ml of 0.5 N NaOH and 1% SDS, and radioactivity was counted.

Expression cloning of molecules mediating adhesion between HT-H and SNG-M cells

As COS-1 cells do not adhere to a monolayer of SNG-M cells (Fig. 2A), it was expected that if COS-1 cells were transfected by cDNAs encoding an appropriate adhesion molecule, they would acquire the ability to adhere to a SNG-M cell monolayer.

A cDNA library of the HT-H cells was constructed in the mammalian expression vector pcDNAI, and COS-1 cells were transfected with the library. After two rounds of screening (see Materials and methods for details), COS-1 cells transfected with a mixture of cDNA clones

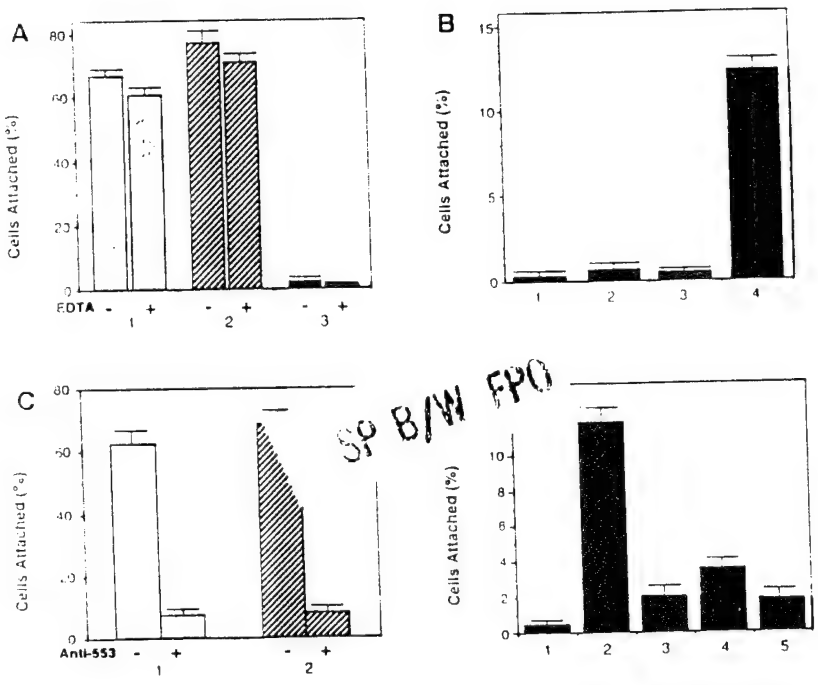

Figure 1. Binding of HT-H, SNG-M, and COS-1 cells to monolayers of SNG-M cells or transfected COS-1 cells. Adhesion assays were conducted as shown in Table 1, except that monolayers were prefixed with 1% paraformaldehyde at room temperature for 15 min. Numbers presented are the averages obtained by triplicate experiments. (*A*) Binding of HT-H (*1*), SNG-M (*2*), and COS-1 (*3*) cells to monolayers of SNG-M cells. (*B*) Adhesion of COS-1 cells to monolayers of SNG-M cells. COS-1 cells were transfected with pcDNAI vector alone (*1*), tastin cDNA alone (*2*), trophinin cDNA alone (*3*), or a mixture of tastin and trophinin cDNAs (*4*). (*C*) Effect of anti-trophinin antibodies on cell adhesion. Each monolayer of the SNG-M cells was pretreated either with anti-trophinin (GST553) antiserum or with preimmune serum for 1 hr at room temperature. After washing the monolayers, HT-H (*1*) or SNG-M (*2*) cells were added to the monolayers. (*D*) Self-binding of COS-1 cells to monolayers of trophinin- and tastin-expressing COS-1 cells. COS-1 cells were transfected with pcDNAI vector alone (*1*) or a mixture of tastin and trophinin cDNAs (*2–5*). Monolayers of COS-1 cells were pretreated with anti-GST551 (*3*), anti-GST552 (*4*), or anti-GST553 (*5*) antisera for 1 hr at room temperature. In *B–D*, adhesion assays were conducted in the presence of 1 mM EDTA.

adhered to a monolayer of SNG-M cells. Surprisingly, however, COS-1 cells transfected with each clone individually failed to adhere to the SNG-M cells. Two clones necessary for cell adhesion were then identified (Fig. 1B). One cDNA clone is named trophinin, as it was cloned from trophoblastic cells. The second cDNA clone is named tastin, as this encodes a trophinin assisting protein.

Characterization of trophinin

The trophinin cDNA clone covers 2524 nucleotides with an open reading frame encoding 749 amino acids (Fig. 3A). Searches through the data base have shown no significant homology between trophinin and other known nucleotide or peptide sequences.

In vitro translation of this cDNA showed a major product at 61 kD (Fig. 3B), which is in approximate agreement with the predicted molecular mass of 69 kD. Hydropathy analysis (Kyte and Doolittle 1982) predicted eight transmembrane domains (Fig. 3A,C). No cleavable signal sequence was found in trophinin. The presence of arginine residues at positions 43, 48, and 54 upstream of the predicted first transmembrane domain (Fig. 3A) suggests the possibility that these basic amino acid residues function as stop transfer during translocation of trophinin in the endoplasmic reticulum (ER) and that the amino-terminal segment (residues 1–66) localizes in the cytoplasm. Polyclonal antibodies against the amino-terminal region did not stain unpermeabilized cells but did stain cells after they were permeabilized (see Fig. 5A, below), supporting the hypothesis that the amino-terminal region localizes in the cytoplasm. In this region, there are three serine and threonine residues in a context that makes them potential phosphorylation sites for protein kinases (Fig. 3A,C; Kemp and Pearson 1990).

The most striking structural feature of trophinin is that >90% of this molecule is made of tandem repeats of decapeptide sequences (Fig. 3D). There are a total of 69 such repeats. Within the repeats are three relatively long hydrophilic domains. Three glutathione *S*-transferase (GST) fusion proteins, each having the peptide sequences of the first, second, and third hydrophilic domains, designated GST551, GST552, and GST553, respectively, were produced in bacteria. Antibodies against these fusion proteins were raised (see Fig. 3C and Materials and methods for details). These antibodies stained unpermiabilized COS-1 cells transfected with trophinin cDNA (see staining with anti-GST553 antibodies in Fig. 4A,B, below). These antibodies also stained unpermeabilized HT-H cells and SNG-M cells, showing staining patterns very similar to those given by anti-trophinin antibodies raised against the amino-terminal domain of trophinin (Fig. 5A,B, below), suggesting that these three regions of trophinin are exposed on the cell surface.

To examine further whether trophinin is a plasma membrane protein, cell surface-labeling experiments were performed. Intact HT-H cells were labeled with biotin–maleimide, a reagent that reacts with the sulfhy-

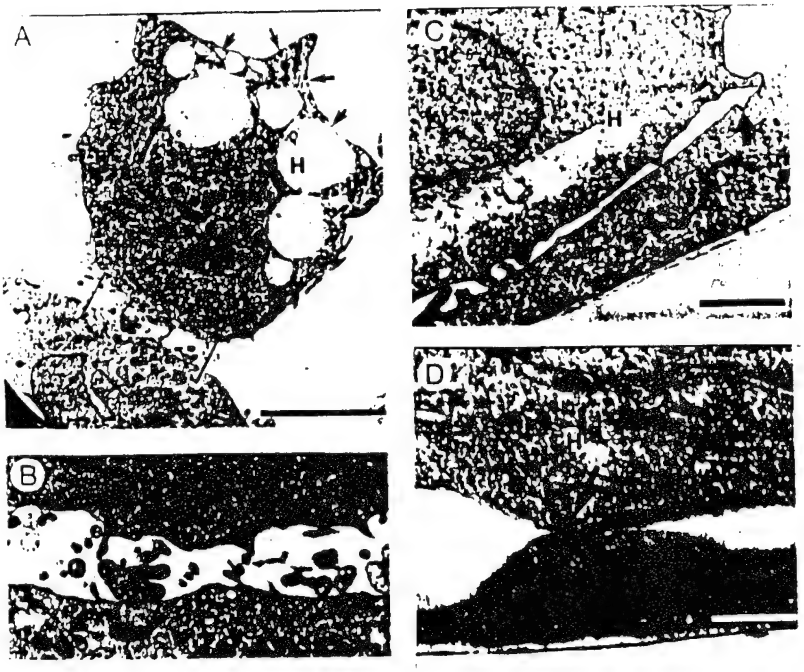

Figure 2. Electron micrographs of the HT-H cells cocultured on a SNG-M cell monolayer. HT-H cells were added to a monolayer of SNG-M cells, and both cell types were cocultured for up to 4 days. The micrographs show the boundary of the two cell types at 10 min (*A*,*B*) 6 hr (C), and 4 days (*D*). (*A*) An HT-H cell (H, upper cell) attached on a SNG-M cell (S) grown on a tissue culture plate. The HT-H cell has microvilli on the lower side (presumably an apical surface originally) facing the upper surface of the SNG-M cell. The basal surface of the HT-H cell is indicated by arrows. Bar, 5 μm. (*B*) Higher magnification of the area shown indicated by brackets in *A*). Note that these two cell types contact via microvilli. (H) HT-H cell; (S) SNG-M cell. (*C*) HT-H (H, upper) and SNG-M (S, lower) cells at 6 hr of coculture. Closer contact between the two cell types is seen. Note that the microvilli are flattened in both cell types. Tips of microvilli extended from one cell type appear to attach directly to the plasma membrane of the other cell type. The SNG-M cells at this stage of contact often show invagination activity (arrow). Bar, 1 μm. (*D*) An HT-H cell cocultured on a monolayer of the SNG-M cells for 4 days. Note the absence of microvilli on the surface of both the HT-H (H, upper) and SNG-M (S, lower) cells. The contact between these two cell types is mostly focal, and occasional development of an adherent junction (arrow) is detected. Bar, 0.5μm.

dryl group of cysteine.[1] Biotinylated cells were solubilized with NP-40. NP-40-insoluble material was solubilized further with SDS. Biotinylated (presumably cell surface proteins) were then recovered by avidin–agarose beads. Both avidin-bound and -unbound fractions were resolved by SDS-PAGE and were subjected to Western blot analysis with anti-trophinin antibodies. Western blots with anti-GST553 antibodies show three bands with apparent molecular masses of 90, 120, and 140 kD in HT-H cells (Fig. 3E).[2] The majority of trophinins were recovered in the avidin-bound fraction (lanes 2,4), suggesting that trophinin is exposed at the cell surface. Furthermore, a significant amount of trophinin was insoluble in NP-40 (lanes 1,2) and was extracted with SDS (lanes 3,4), suggesting that trophinin is associated with the cytoskeleton in HT-H cells. Similar results were obtained when SNG-M cells were analyzed by surface labeling and Western blot. These results collectively indicate that trophinin is an intrinsic plasma membrane protein. However, predicted topology of trophinin shown in Figure 3, A and C, is tentative. Further analysis is needed to define each cytoplasmic membrane and cell surface domain of trophinin.

[1]There are three cysteine residues in the predicted cell surface domain of trophinin that an be labeled with biotin–maleimide, whereas no lysine residues exist for labeling with biotin–succinimide.

[2]Because these molecular masses are much larger than the expected 69 kD, Western blot was performed with another antibody directed against the amino-terminal region of trophinin (see anti-peptide antibodies in legend to Fig. 5). Western blot analysis with the anti-peptide antibodies detected the same three bands, whereas preimmune sera did not detect them. Therefore, we conclude that the bands shown in Figure 3E are trophinin. Although it is possible that alternative splicing of the trophinin gene in HT-H and SNG-M cells results in the production of altered trophinin polypeptides, the cause of differences in molecular weights and in the three bands of trophinin reains unknown.

Involvement of trophinin in homophilic cell adhesion

The antibodies raised against the predicted cell surface domains of trophinin were examined for their effect on cell adhesion. Adhesion of HT-H or SNG-M cells to SNG-M cell monolayers was reduced significantly by pretreatment with Fab' fragment (not shown) as well as intact anti-GST553 antibodies (Fig. 1C). Preimmune sera of these antibodies or antibodies raised against the amino-terminal region of trophinin did not show any effect on cell adhesion.

If trophinin mediates homophilic cell adhesion, COS-1 cells that are cotransfected with trophinin and tastin should be self-adhesive. COS-1 cells transfected with a mixture of trophinin and tastin cDNAs aggregated when they were left in suspension. These COS-1 cells adhered to monolayers of cotransfected COS-1 cells, and this binding was reduced significantly by pretreatment with the antibodies raised against predicted cell surface domains of trophinin (Fig. 1D).

Direct binding of trophinin to the cell surfaces of trophinin-expressing cells was examined. Fusion proteins (GST551, GST552, and GST553) were labeled with bi-

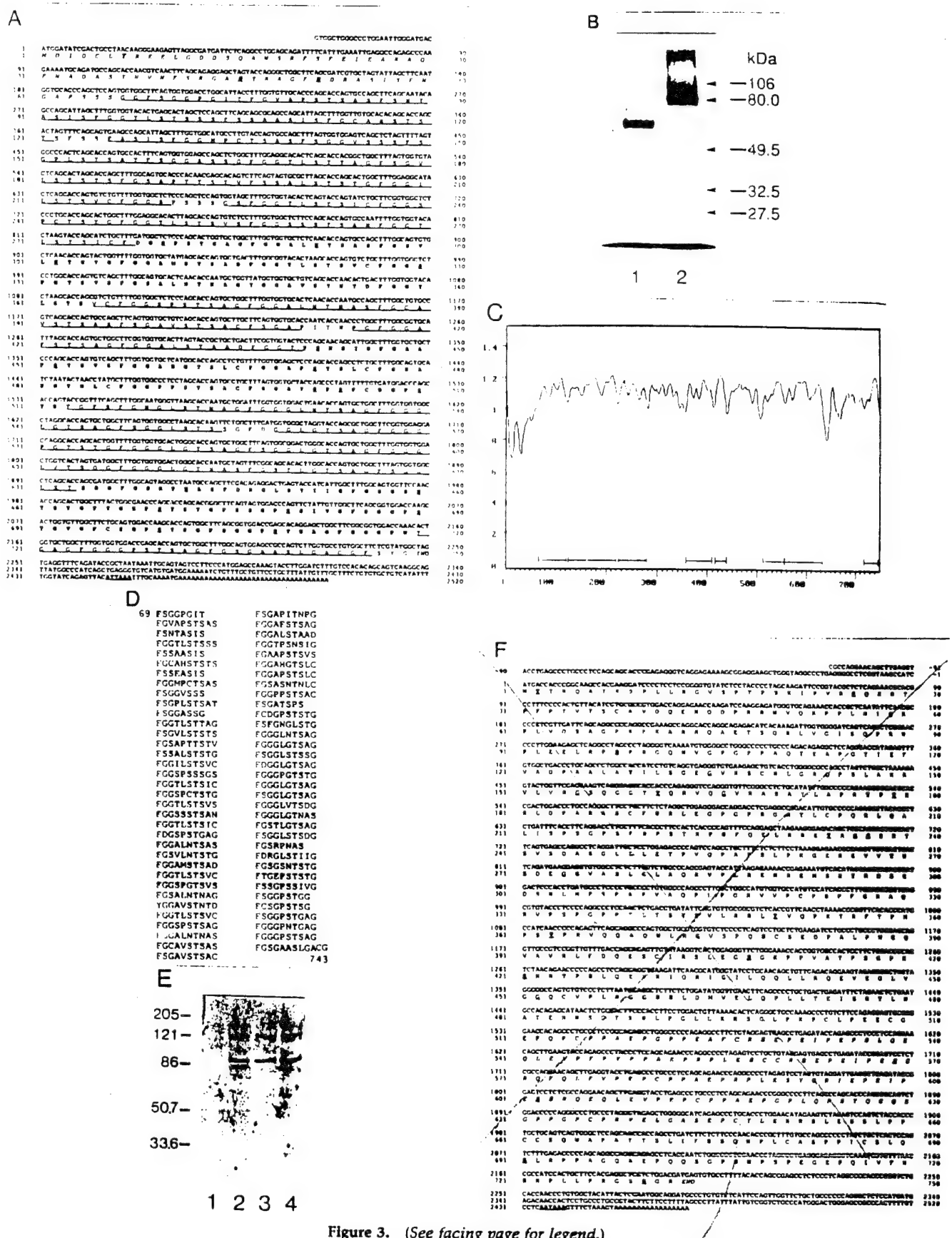

Figure 3. (*See facing page for legend.*)

→ and tyrosine /

Figure 3. Structure and characterization of trophinin and tastin. (*A*) Nucleotide and deduced amino acid sequences of the trophinin cDNA clone. Single-letter amino acid symbols are used. The putative transmembrane domains are underlined, putative cytoplasmic domains are shown in italics, and putative cell surface domains are shown by boldface letters. Potential amino-linked and *O*-linked glycosylation sites are underlined. Potential site of serine and threonine residues for phosphorylation by casein kinase II and protein kinase C are shown by shadowed and underlined/shadowed letters, respectively. These sequence data are available from EMBL/GenBank/DDBJ under accession number U04811. (*B*) SDS–polyacrylamide gel electrophoresis analysis of in vitro-translated products from trophinin and tastin cDNA. Numbers at *right* show positions of molecular mass markers. (Lane *1*) Translated products of trophinin cDNA; (lane 2) translated products of tastin cDNA. (*C*) A hydropathy plot of trophinin polypeptide. Settings of the parameters (peak minimal value, baseline value), including minimum length (16 amino acid residues) of a transmembrane helix, are identical to those proposed previously (Kyte and Doolittle 1982). Bars at the *bottom* indicate regions predicted for transmembrane helices. (*D*) Tandem decapeptide repeats in trophinin. The amino acid sequence of trophinin from residue 69 to 743 is comprised of decapeptide repeats. (*E*) Cell surface labeling and Western blot analysis of trophinin in HT-H cells. Intact HT-H cells were labeled with biotin–maleimide and subsequently solubilized with 1% NP-40. NP-40-insoluble material was solubilized further with 0.1% SDS. Each extract was incubated with avidin–agarose beads, separated into avidin-bound and -unbound fractions, and subjected to Western blot analysis using anti-trophinin (GST553) antibodies. (Lane 2) NP-40 extracted, and avidin-bound fractions; (lane *1*) unbound fractions. (Lane 4) SDS-extracted and avidin-bound fractions; (lane 3) unbound fractions. Numbers at *left* show positions of prestained molecular mass markers. (*F*) Nucleotide and deduced amino acid sequence of tastin cDNA clone. Single-letter amino acid symbols are used. Potential sites of serine and threonine residues for phosphorylation by protein kinase C, cAMP/cGMP-dependent protein kinase, casein kinase II, and MAP kinase are shown by underlined boldface, underlined, boldface, and shadowed letters, respectively. Potential sites of glycine residues for myristoylation are underlined. The region from amino acid residues 504 to 687 is rich in cysteines. Within this region, the peptide segment from residues 516 to 647 is made of four tandem repeats, each composed of 33 amino acids (marked by italics). These sequence data are available from EMBL/GenBank/DDBJ under accession number U04810.

— ...ine and tyrosine kinase /

→ and ...ine tyrosine /

otin and added to monolayers of HT-H and SNG-M cells. Binding of biotinylated proteins to the cell surface was detected under a fluorescence microscope using FITC–avidin. These fusion proteins also bound to the cell surface of COS-1 cells cotransfected with trophinin and tastin (Fig. 4C), whereas neither unfused GST nor GST fused to the amino-terminal domain (1–66) of trophinin showed such binding (not shown). These results indicate that soluble peptides of the cell surface domain of trophinin have the property of binding to the cell surface of trophinin-expressing cells. This supports the hypothesis that trophinin mediates homophilic cell adhesion.

F4

Characterization of tastin

Tastin cDNA covers 2578 nucleotides with an open reading frame encoding 732 amino acids (Fig. 3F). Searches through the data bank have revealed no significant homology between tastin and any other protein in the data base.[3]

778/

3/

In vitro translation of the tastin cDNA showed a prominent product of 80 kD (Fig. 3B), consistent with the predicted molecular mass of 78 kD. Hydropathy analysis (Kyte and Doolittle 1982) showed no obvious signal for secretory protein or transmembrane domains. Therefore, tastin is probably a cytoplasmic protein.

83/

Tastin is rich in prolines that account for 16.2% of the total amino acids of this protein. The region from amino acid residues 504 to 687 is rich in cysteines (Fig. 3F). Within this region, the peptide segment from 516 to 647 is made of four tandem repeats, each composed of 33 amino acids. Tastin contains many serines and threonines whose surrounding amino acid residues conform to motifs for phosphorylation sites by protein kinases (Fig. 3F). Two cAMP/cGMP-dependent phosphorylation sites are predicted at positions 235 and 350. Among the 13 protein kinase C phosphorylation sites predicted, the threonine at position 179 and serine at position 730 match the consensus sequence of R(K)-*X*-*X*-T(S)-*X*-R-(K) most closely (Kemp and Pearson 1990). There are a total of 11 serine and threonine residues predicted for casein kinase II phosphorylation sites. Threonines at positions 177 and 363 are within the consensus sequence for the mitogen-activated protein (MAP) kinase phosphorylation site P-*X*-S(T)-P (Gonzalez et al. 1991).

Tastin is necessary for trophinin to function as a cell adhesion molecule (Fig. 1B,C). When trophinin was expressed in COS-1 cells without tastin, trophinins distributed diffusely on the cell surface (Fig. 4A). However, when trophinin and tastin were coexpressed, trophinins showed a clustered distribution (Fig. 4B), indicating that tastin induces the clustering of trophinin. This implies that the role of tastin in cell adhesion is to create multivalent trophinin patches that serve as potent adhesion sites.

Subcellular localization of trophinin and tastin in HT-H and SNG-M cells

The localization of trophinin and tastin in HT-H and SNG-M cells was examined immunocytochemically. Anti-trophinin antibodies detected this protein both in HT-H cells and SNG-M cells (Fig. 5A,B). The trophinin molecules apparently cluster, showing a lacy pattern in these cells. Trophinin in HT-H and SNG-M cells (Fig. 4A,B) appears well organized compared with that in COS-1 cells, which are transfected with trophinin and tastin cDNAs (Fig. 5B).

F6

Anti-tastin antibodies detected this protein both in

[3]Computer searches using the nucleotide sequence of tastin revealed that the complementary sequence between nucleotide positions 2057 and 2340 matches the sequence of HFBCL29 cDNA (GenBank accession no. M85643) isolated from a human fetal brain cDNA library. It appears that the HFBCL29 sequence was recorded in the antisense direction.

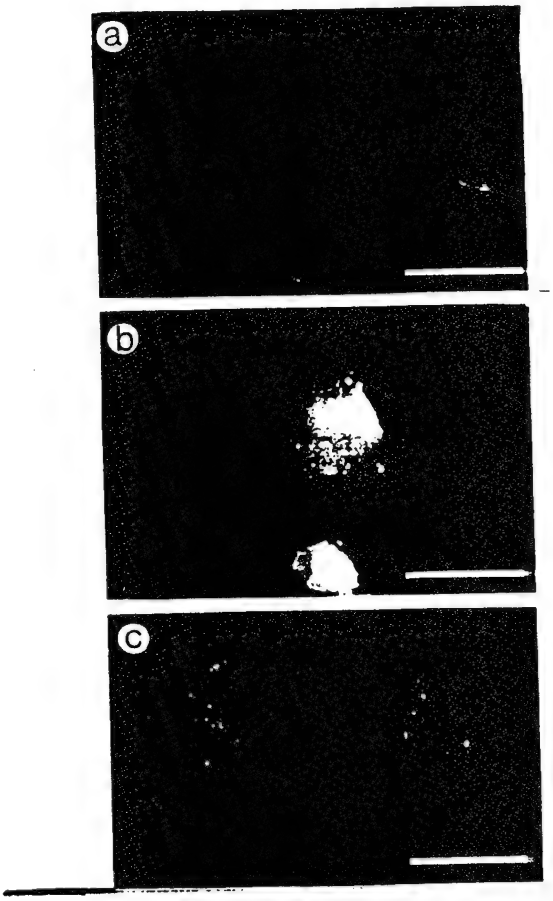

Figure 4. Fluorescence micrographs of transfected COS-1 cells. COS-1 cells were transfected with trophinin cDNA alone (*a*) or with a mixture of trophinin and tastin cDNAs (*b*). Cells were stained with anti-trophinin (GST553) antibodies followed by an FITC-conjugated $F(ab')_2$ fragment of goat antirabbit IgG (Cappel). (*c*) Binding of GST553 fusion protein (the predicted third outer cellular domain of trophinin) on the surface of COS-1 cells transfected with a mixture of trophinin and tastin cDNAs. Fusion protein GST553 was produced in bacteria, purified using glutathione–Sepharose beads, biotinylated with biotinamidocaproate-*N*-hydroxysuccinimide, and added to the monolayer of transfected COS-1 cells. Binding of GST553 fusion protein to COS-1 cells was visualized using FITC-conjugated avidin. Bar, 20 μm.

HT-H and SNG-M cells (Fig. 5C,D). Tastin is seen as a diffuse cytoplasmic protein as well as being found in fibers. The fibers spread from the perinuclear region toward the edge of the cells, suggesting that tastin associates with the cytoskeleton.

Expression of trophinin and tastin in various human tissues

Northern blot analysis using cDNA probe for trophinin showed a signal at 3.5, 7.5, and 10 kb in poly(A)$^+$ RNA isolated from both HT-H and SNG-M cells. The analysis using tastin cDNA as a probe showed a signal at 3.2 kb (major) and 3.5 kb (minor) in poly(A)$^+$ RNA isolated from both HT-H and SNG-M cells. A Northern blot of several human tissues detected weak signals for trophinin and tastin mRNAs in placenta, lung, and liver. However, immunohistochemistry of these tissues showed that only macrophages present in the tissues were positive. These results indicate that trophinin and tastin are normally not expressed in various types of human cells, with the exception of macrophages.

Expression of trophinin and tastin during implantation

In human endometrium, trophinin was not detected at the proliferation stage (days 6–13) or at the ovulation stage (day 14); however, trophinin was detected on the apical plasma membranes of the endometrial surface epithelium on day 16/17 (early secretory phase) (Fig. 5E,F). In middle and late secretory phases (days 20–28), trophinin was detected in mucus, apparently shed from epithelia (Fig. 5G). Similarly, tastin was detected in the trophinin-expressing endometrial epithelium cells on day 16/17 and in mucus in middle and late endometrium but was not detected at the proliferation and ovulation stages. These observations suggest that trophinin and tastin are expressed in surface epithelia at an early secretory phase and are quickly down-regulated from the cell surface by exocytosis.

In human placenta from early (5–10 weeks) pregnancy, trophinin and tastin were found in the lysosomes of syncytiotrophoblasts (not shown) but were not detected in placenta tissues later in pregnancy. These observations suggest that trophinin and tastin were expressed in the trophoblasts at the earliest stage in placenta but disappeared from the surface within the first few weeks of pregnancy.

Strong expression of trophinin was detected in the apical plasma membranes of the trophectoderm of monkey blastocysts (Fig. 5H). It is noteworthy that expression of the trophinin is more elevated at the embryonic pole than at the mural pole. Expression of tastin follows the same profile as that of trophinin in the blastocyst. Such a polarized distribution of trophinin and tastin may be consistent with the observations that in both primates and humans a blastocyst attaches to endometrial epithelium at its embryonic pole (Knoth and Larsen 1972; Enders et al. 1981; Lindenberg et al. 1986).

Figure 5I shows a section of monkey uterus that includes the implantation site. Trophinin was detected both in trophoblasts of the blastocyst and in endometrial epithelium cells (see inset), as well as in cytotrophoblasts, hypertrophic endometrial epithelium cells, and cells at anchoring villi.

Cell adhesion activity of trophinin- and tastin-expressing endometrial epithelium

To test whether naturally expressed trophinin and tastin could mediate cell adhesion, HT-H, SNG-M, and COS-1 cells were added to the endometrial tissue shown in Figure 5E. Both HT-H and SNG-M cells adhered to the site

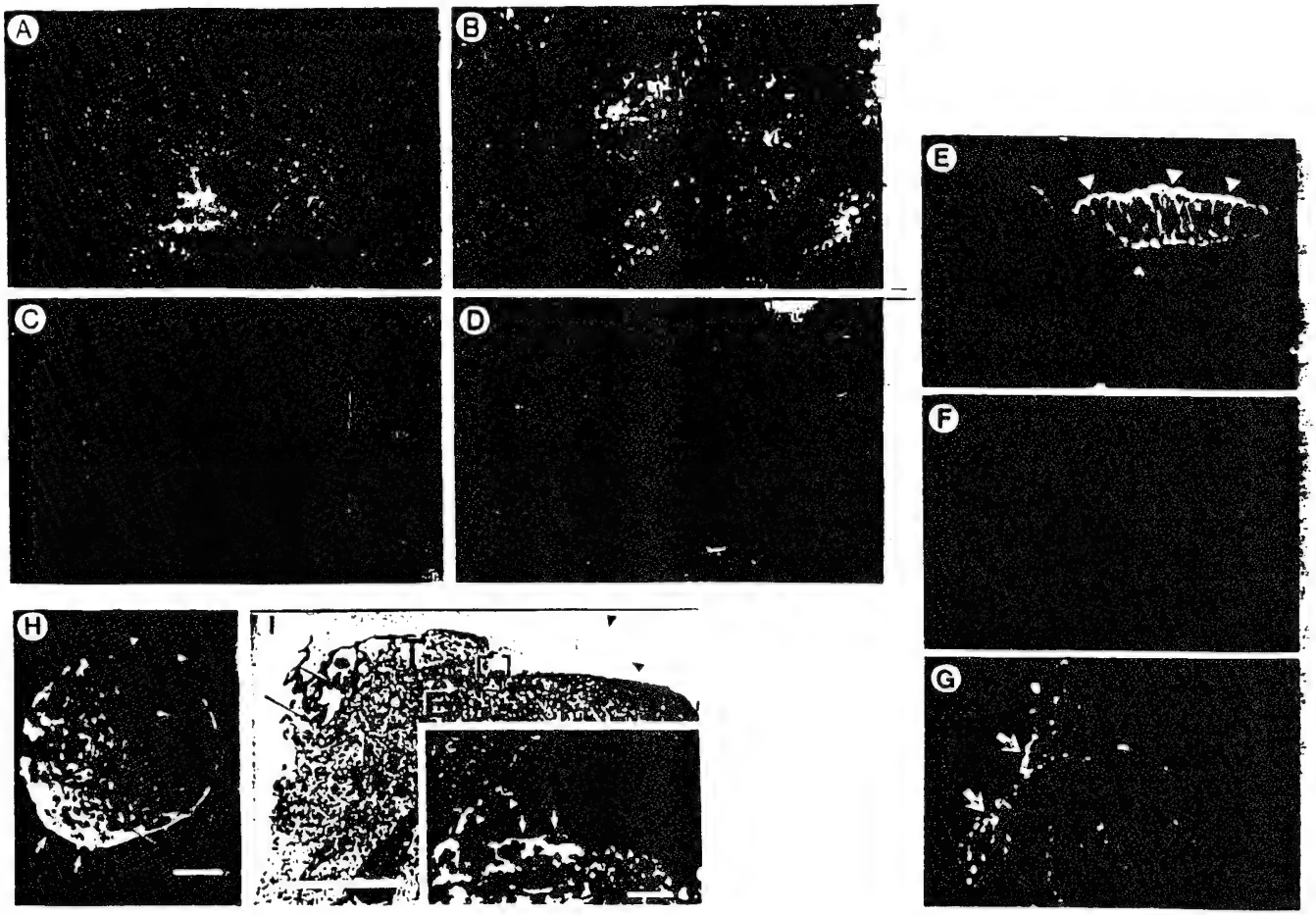

Figure 5. Fluorescence micrographs showing expression of trophinin and/or tastin in cultured cells and the cells involved in implantation. Shown are immunofluorescence micrographs of HT-H cells (*A*) and SNG-M cells (*B*) stained with anti-trophinin antibodies raised against the amino-terminal region of trophinin. Immunofluorescence micrographs of HT-H cells (*C*) and SNG-M cells (*D*) stained with anti-tastin antibodies are shown. (*E*) Immunofluorescence micrograph of a surface epithelium of day 16/17 (early secretory phase) endometrium. Trophinins are detected on the apical plasma membranes (arrowheads). (*F*) Immunofluorescence micrograph of the same series of sample shown in *E* stained with preimmune serum. (*G*) Presence of trophinin in mucus in endometrial epithelium at late secretory phase. (*A–G*) Bar, 10 μm. (*H*) Immunofluorescence micrograph of rhesus monkey blastocyst stained with anti-trophinin antibodies. Inner cell mass is shown by a long arrow. Note that cells at the embryonic pole (short arrows) were stained more intensely than those at the mural pole (arrowheads). Bar, 25 μm. (*I*) A light micrograph of macaque monkey uterus tissue with an implanted and ~11.5-day blastocyst. Arrowheads show cytotrophoblasts of blastocyst. Long arrows show anchoring villi (trophoblasts penetrating the endometrial epithelium). (T) Trophoblasts. (E) Hypertrophic endometrial epithelium. Bar, 200 μm. (*Inset*) An immunofluorescence micrograph of higher magnification of the area marked by a parenthesis. Both trophoblast (arrowheads) and endometrial epithelium cells (arrows) are stained by anti-trophinin antibodies. Bar, 10 μm. In *A*, *B*, *E*, *G*, *H*, and *I*, the antibodies raised against a synthetic peptide of the amino-terminal region (residues 23–31) of trophinin were used.

of endometrial surface epithelium expressing trophinin, and such adhesion was lost by treatment of the tissue with anti-trophinin (anti-GST553) antibodies (not shown). COS-1 cells cotransfected with trophinin and tastin cDNAs adhered to the trophinin-expressing site of endometrium, whereas untransfected COS-1 cells did not show any sign of adhesion.

Discussion

Two novel molecules, trophinin and tastin, have been identified by expression cDNA cloning. Trophinin is an intrinsic membrane protein and is directly responsible for homophilic cell adhesion; tastin is a cytoplasmic protein and is necessary for trophinins to function as adhesion molecules.

Although the simultaneous cloning of two genes is a low probability event, we believe that transfection of a cDNA library by electroporation was the key to the success of this experiment. Because electroporation opens pores in the plasma membrane of cells and allows plasmid DNA to enter through such pores, the amount of DNA entering the cells is dependent on the concentration of DNA in the solution. We also used a high con-

centration of plasmid DNA (100 μg/ml) in the electroporation, whereas the standard procedure uses 20 μg/ml of plasmid DNA. This high concentration of plasmid DNA during electroporation thus leads to cotransfection of many plasmid DNAs into a single cell. Another factor for coexpression cloning is the number of recipient cells. As described (see Materials and methods for details), we used enormous numbers of COS-1 cells for the first (1×10^8 cells) and second (1×10^7 cells) screenings.

Present studies also show that cytoplasmic protein tastin is necessary for the cell adhesion molecule trophinin to function. Many studies indicate that the functions of cell adhesion molecules are determined by their association with cytoplasmic proteins and cytoskeletal structures (Hynes 1992; Garrod 1993; Gumbiner 1993; Stappert and Kemler 1993). The association between the adhesion molecule and the cytoskeleton is also suggested in this study. Thus, the cytoplasmic domain of trophinin might associate with tastin, which apparently associates with the cytoskeleton. Such association would restrict the distribution of trophinins in the plasma membrane, creating highly concentrated trophinin patches in plasma membranes that may function as efficient adhesion sites (Fig. 4). We have made a mutant trophinin lacking the amino-terminal region, predicted cytoplasmic domain. When this mutant and tastin were coexpressed in COS-1 cells, mutant trophinin did not cluster and COS-1 cells did not exhibit adhesion activity (J. Zara and M.N. Fukuda, unpubl.). Therefore, the cytoplasmic domain of trophinin is necessary for cell adhesion.

Potential involvement of trophinin and tastin in embryo implantation is supported by the following evidence: (1) Human endometrium is under strict hormonal controls and is generally not permissive to implantation. Trophinin and tastin are not found in the proliferative phase and ovulation phase of human endometrium. These molecules are expressed in the endometrium only on the surface epithelium at the time expected for an implantation window (Yoshinaga 1988; Harper 1992). (2) Strong expression of trophinins and tastins were detected at the trophectoderm surface of the monkey blastocyst. Expression of these molecules was particularly strong at the embryonic pole where the blastocyst adheres to the endometrium (Enders et al. 1981; Lindenberg et al. 1986). (3) Trophinins were detected in both trophoblasts and endometrial epithelium cells at the monkey blastocyst implantation site.

Strictly regulated expression of trophinin and tastin in vivo and their unique cell adhesion activity displayed at apical surfaces of trophoblastic HT-H cells and endometrial epithelial SNG-M cells suggest the possibility that these molecules are involved in the initial adhesion of the blastocyst to the endometrium.

The study of embryo implantation at the molecular level is one of the most difficult subjects to study in developmental biology. Information provided in this paper and materials, such as cDNAs and antibodies, that became available from the present study will be useful for future studies of embryo implantation.

Materials and methods

Cell lines and cell culture

Trophoblastic HT-H cells were separated from undifferentiated HT-H cells as described (Izhar et al. 1986), subcloned, and used in the present study. Endometrial adenocarcinoma cell lines Hec1A, RL95-2, and AN3CA were obtained from American Tissue Culture Collection. All cell lines have been cultured in Dulbecco's modified Eagle medium (DMEM) containing 10% fetal bovine serum, 2 mM glutamine, 100 U/ml of penicillin, and 100 μg/ml of streptomycin.

Cell adhesion assay

HT-H cells were metabolically labeled with Tran^{35}S-label (New England Nuclear) in methionine- and cysteine-free RPMI medium for 20 min and chased with complete medium for 2 hr. The ^{35}S-labeled HT-H cells were detached from the bottom of the tissue culture dish using cell dissociation solution (Specialty Media, Lavalette, NJ) supplemented with 1 mM EDTA. The cells were pelleted by centrifugation and resuspended in HEPES-buffered saline (HBS). Cell suspensions (0.2 ml, 5×10^4 cells) were added to a monolayer of the endometrium epithelial cells that had been grown on the bottom of a 24-well tissue culture plate. The HT-H cells that did not adhere to the monolayer were washed three times with HBS with or without 1 mM EDTA. The cells remaining in each well were solubilized with 0.5 ml of 0.5 N NaOH and 1% SDS, and radioactivity was counted. Cell adhesion assays were also conducted using fixed cell monolayers. Cells grown on the bottom of a 24-well tissue culture plate were treated with 1% paraformaldehyde in PBS at room temperature for 15 min and were used for cell adhesion assays in the same manner described above.

Production of antibodies

Anti-trophinin (GST551, GST552, and GST553) antibodies were raised as follows: A cDNA encoding one of the hydrophilic domains (residues 278–364, 441–512, or 634–719) within the decapeptide repeats was amplified by polymerase chain reaction (Saiki et al. 1988) and was ligated into pGEX-4T-1 vector (Pharmacia, Piscataway, NJ). *Escherichia coli* HB101 was transformed with the plasmid vector, and a GST fusion protein was produced. The fusion protein was purified by glutathione–agarose beads and used for rabbit immunization.

The most antigenic sequence of trophinin and tastin was predicted by computer program (Hopp and Wood 1983). Peptides CFEIEARAQE (for trophinin, amino acid residues 23–31) and CDQENQDPRR (for tastin, amino acid residues 41–49) were synthesized. The first cysteine residue at the amino terminus of each peptide was added to link the peptide to keyhole limpet hemocyanin (KLH) by conjugation with meta-maleimidobenzoyl-*N*-hydroxysuccinamide ester (Kitagawa and Aikawa 1976). Rabbits were immunized with either of the peptide–KLH conjugates, and antisera were obtained. Anti-peptide antibodies were purified by protein A affinity column chromatography followed by peptide–Sepharose 4B affinity chromatography as described (Richardson et al. 1985).

Electron microscopy

SNG-M cells were cultured in a Falcon 3001 (25 × 10 mm) tissue culture dish to 50% confluence. The HT-H cells were detached from the tissue culture dish by trypsin/EDTA treatment and were added to a monolayer of SNG-M cells. The two cell types were cultured together for up to 4 days. For transmission elec-

tron microscopy, the cells were fixed at room temperature in freshly prepared fixative (10 mmoles/liter of $NaIO_4$, 75 mmoles/liter of lysine, 37.5 mmoles/liter of sodium phosphate buffer, 2% paraformaldehyde at pH 6.2) for 15 min. After washing with phosphate buffer, the cells were treated with glutaraldehyde and processed for electron microscopy as described previously (Klier et al. 1977). A Hitachi K-600 electron microscope was used.

Expression cDNA cloning of adhesion molecules

Coexpression cloning of trophinin and tastin was carried out as follows. Poly(A)$^+$ RNA was prepared from freshly harvested HT-H cells. A unidirectional cDNA expression library was constructed in pcDNAI vector. A custom-ordered cDNA library construction was provided by Invitrogen (La Jolla, CA), which consists of 2×10^6 independent clones with an insert size ranging from 0.5 to 3.0 kb. COS-1 cells (1×10^8 cells total, 1×10^7 to $\sim0.5\times10^7$cells/ml) were suspended in PBS containing plasmid DNA (100 μg/ml). Transfection was performed by electroporation using a Gene Pulser (Bio-Rad, Hercules, CA) at 0.4 kV with a capacitance of 125 μF. The transfected COS-1 cells were cultured for 48 hr in complete DMEM and subjected to adhesion assays. The single-cell suspensions of COS-1 cells were overlaid to a fixed monolayer of SNG-M cells in the presence of 1 mM EDTA. After 20 min, nonadherent COS-1 cells were removed by washing the monolayer with buffer containing EDTA. About 1×10^4 COS-1 cells appeared to be attached. The COS-1 cells remaining on the SNG-M cells were detached by flushing the buffer and were then added to a new fixed monolayer of SNG-M cells. About 1×10^3 COS-1 cells appeared to be attached. Plasmid DNAs were recovered from the twice-adhered COS-1 cells, were amplified in *E. coli* MC1061/P3 cells, and were used for the second round of screening.

A second screening was carried out in the same manner as the first except that the number of the cells transfected was scaled down as follows: COS-1 cells (1×10^7 cells) were transfected with plasmid DNA recovered from the adherent COS-1 cells in the first screen. Twice-adhered COS-1 cells were selected in the same manner as described above. About 2×10^3 COS-1 cells adhered to the first SNG-M monolayer and about 1×10^3 COS-1 cells adhered to the second SNG-M monolayer. *E. coli* MC1061/P3 cells were transformed by plasmid DNA obtained after the second round of screening.

Two hundred clones were chosen and divided into 10 groups. COS-1 cells transfected with one of the groups or a mixture of the 20 clones adhered to a monolayer of the SNG-M cells. However, COS-1 cells transfected with each clone individually failed to adhere to the SNG-M cells. The 20 clones were tested again as a mixture, eliminating each clone one by one. Finally, the adhesion assay showed that a mixture of two cDNAs was necessary for COS-1 cells to adhere to SNG-M cells.

Nucleotide sequence analysis

Nucleotide sequences were analyzed by the dideoxy nucleotide chain-termination method of Sanger et al. (1977) using a modified T7 DNA polynuclease (Sequenase, U.S. Biochemical, Cleveland, OH). The nucleotide sequence of trophinin cDNA was determined from restriction fragments subcloned into Bluescript from nested deletion mutants generated by exonuclease III (Boehringer Mannheim, Indianapolis, IN). The nucleotide sequence of tastin cDNA was determined using oligonucleotide primers. Editing and analysis of the sequence was done using DNASIS (Hitachi, Tokyo, Japan) and PCGENE (Intelligenetics, Mountain View, CA) software programs. Sequence comparisons with the data bases were performed using the BLAST network program (National Center for Biotechnology Information, NIH, Bethesda, MD).

Northern blot

Total RNA was isolated from HT-H cells, SNG-M cells, and COS-1 cells by the acid–guanidine/phenol/chloroform method (Chirgwin et al. 1979). Poly(A)$^+$ RNA was prepared using oligo(dT)–cellulose affinity chromatography. Five micrograms of poly(A)$^+$ RNA was separated in a 1% agarose–formaldehyde gel. The RNA was transferred to a nitrocellulose filter and fixed by heating at 80°C for 2 hr. Prehybridization and hybridization were performed as described by Thomas (1980). A human multiple-tissue Northern blot filter (MTN-1 filter, Clontech, Palo Alto, CA) was also processed in the same manner described above.

In vitro translation

The plasmid cDNA clones were subjected to in vitro translation using a T7 oligonucleotide as a primer, in rabbit reticulocyte lysate (Promega, Madison, WI), and using RNA polymerase in the presence of [^{35}S]methionine. The products were separated on a SDS–polyacrylamide gel and visualized by autoradiography.

Cell surface biotin labeling and Western blot

HT-H and SNG-M cells were scraped from the tissue culture plate using a rubber policeman. After washing the cells with cold PBS, 20 μl of dimethylformamide containing 10 μg of biotin–maleimide (Sigma, St. Louis, MO) was added to the cell suspension (1×10^6 cells in 1 ml of PBS), and biotinylation proceeded for 1 hr on ice. After washing the cells with cold PBS, cells were lysed with PBS containing 1% NP-40. NP-40-insoluble material was dissolved further with 0.1% SDS as described (Oshima et al. 1983). Each cell lysate was mixed with avidin–agarose beads (Sigma) and separated into avidin-bound and -unbound fractions. Proteins in each fraction were resolved by SDS–polyacrylamide gel electrophoresis and analyzed by Western blot using anti-GST553 antibodies. The Western blot was performed as described (Towbin et al. 1979), except an ECL kit (Amersham, Buckinghamshire, UK) was used for the detection of the immunoreactive bands.

Immunofluorescence microscopy

Immunostaining was carried out in the same manner as described previously (Aoki et al. 1992). Briefly, HT-H cells, SNG-M cells, and transfected COS-1 cells were grown on glass coverslips placed in a Falcon 3005 tissue culture dish for 2–3 days. The cells were fixed at room temperature for 15 min with 1% paraformaldehyde in PBS and permeabilized with 0.1% saponin in PBS. An FITC-conjugated F(ab')$_2$ fragment of goat anti-rabbit IgG (Cappel, Durham, NC) was used for second antibodies. Controls without the first antibodies were taken in each experiment. The cells were examined under a Zeiss Axioplan fluorescence microscope or a Zeiss LSM410 confocal laser scanning microscope.

Paraffin-embedded tissue sections of human endometrium and monkey uterus were deparaffinized with xylene and ethanol. To recover antigenic activities, deparaffinized tissue sections were microwaved in 10 mM citrate buffer (pH 6.0) to recover antigenic activities (Shi et al. 1991). Immunoreaction then proceeded in the same manner as described above.

Acknowledgments

W thank Dr. Allen C. Enders at the University of California at Davis for providing us with monkey implantation site samples and for his helpful comments, Dr. Don P. Wolf at Oregon Health Science University for providing us with monkey blastocysts, Drs. Osamu Yamagami and Tsutomu Katsuyama at Shinshu University, Japan, for collecting endometrium biopsy samples. We also thank Dr. Russell Doolittle at the University of California at San Diego for helpful suggestions, Drs. Erkki Ruoslahti, Robert G. Oshima, and Yu Yamaguchi for their critical reading of the manuscript, and Ms. Leslie DePry for her assistance in typing the manuscript.

The publication costs of this article were defrayed in part by payment of page charges. This article must therefore be hereby marked "advertisement" in accordance with 18 USC section 1734 solely to indicate this fact.

References

Andrews, P.W., P.N. Goodfellow, and I. Damjanov. 1983. Human teratocarcinoma cells in culture. *Cancer Surv.* 2: 41–73.

Aoki, D., N. Lee, N. Yamaguchi, C. Dubois, and M.N. Fukuda. 1992. Golgi retention of a trans-golgi membrane protein, galactosyltransferase, requires cysteine and histidine residues within the membrane-anchoring domain. *Proc. Natl. Acad. Sci.* 89: 4319–4323.

Aplin, J.D. 1991. Implantation, trophoblast differentiation and haemochorial placentation: Mechanistic evidence in vivo and in vitro. *J. Cell Sci.* 99: 681–692.

Armant, D.R., H.A. Kaplan, and W.I. Lennarz. 1986. Fibronectin and laminin promote in vitro attachment and outgrowth of mouse blastocysts. *Dev. Biol.* 116: 519–523.

Chirgwin, J.M., A.Z. Przybyla, R.J. MacDonald, and W.J. Rutter. 1979. Isolation of biologically active ribonucleic acid from sources enriched in ribonuclease. *Biochemistry* 18: 5294–5299.

Ducibella, M., D. Anderson, J. Aalberg, and W.C. DeWolf. 1982. Cell surface polarization, tight junctions and eccentric inner cells characterize human teratocarcinoma embryoid bodies. *Dev. Biol.* 94: 197–205.

Enders, A.C., D.J. Chavez, and S. Schlafke. 1981. Comparison of implantation in utero and in vitro. In *Cellular and molecular aspects of implantation* (ed. S.R. Glasser and D.W. Bullock), pp. 365–382. Plenum Press, New York.

Farach, M.C., J.P. Tang, G.L. Decker, and D.D. Carson. 1987. Heparin/heparan sulfate is involved in attachment and spreading of mouse embryos in vitro. *Dev. Biol.* 123: 401–410.

Garrod, D.R. 1993. Desmosomes and hemidesmosomes. *Curr. Opin. Cell Biol.* 5: 30–40.

Gonzalez, F., D. Raden, and R. Davis. 1991. Identification of substrate recognition determinants for human ERK1 and ERK2 protein kinases. *J. Biol. Chem.* 266: 22159–22163.

Gumbiner, B.M. 1993. Proteins associated with the cytoplasmic surface of adhesion molecules. *Neuron* 11: 551–564.

Harper, M.J. 1992. The implantation window. *Baillieres Clin. Obstet. Gynaecol.* 6: 351–371.

Hopp, T.P. and K.R. Wood. 1983. A computer program for predicting protein antigenic determinants. *Mol. Immunol.* 20: 483–489.

Hynes, R.O. 1992. Integrins—versatility, modulation and signalling in cell adhesion. *Cell* 69: 11–25.

Ishiwata, I., S. Nozawa, T. Inoue, and H. Okumura. 1977. Development and characterization of established cell lines from primary and metastatic regions of human endometrial carcinomas. *Cancer Res.* 37: 1777–1785.

Izhar, M., P. Siebert, R.G. Oshima, W.C. DeWolf, and M.N. Fukuda. 1986. Trophoblastic differentiation of human teratocarcinoma cell line HT-H. *Dev. Biol.* 116: 510–518.

John, N.J., M. Linke, and H.-W. Denker. 1993. Quantitation of human choriocarcinoma spheroid attachment to uterine epithelial cells monolayers. *In Vitro Cell. Dev. Biol.* 29A: 461–468.

Kaufman, M.H. 1985. The origin, properties and fate of trophoblast in the mouse. In *Biology of trophoblast* (ed. Y.W. Loke and A. Whyte), pp. 23–68. Elsevier Scientific, Amsterdam, The Netherlands.

Kemp, B.E. and R.B. Pearson. 1990. Protein kinase recognition sequence motif. *Trends Biochem. Sci.* 15: 342–346.

Kimber, S.J., S. Lindenberg, and A. Lundblad. 1988. Distribution of some Galβ1-3(4)GlcNAc related carbohydrate antigens on the mouse uterine epithelium in relation to the peri-implantation period. *J. Reprod. Immunol.* 12: 297–313.

Kitagawa, T. and T. Aikawa. 1976. Enzyme coupled immunoassay of insulin using a novel coupling reagent. *J. Biochem.* 79: 233–236.

Klier, G., D. Shubert, and S. Heinemann. 1977. The ultrastructural differentiation of the clonal myogenic cell line L6 in normal and high K+ medium. *Dev. Biol.* 57: 440–449.

Kliman, H.J., C. Coutifaris, R.F. Feinberg, J.F. Straus III, and J.E. Haimowitz. 1989. Implantation: In vitro models utilizing human tissues. In *Blastocyst implantation* (ed. K. Yoshinaga), pp. 83–91. Adams Publishing, Boston, MA.

Knoth, M. and J.F. Larsen. 1972. Ultrastructure of a human implantation site. *Acta Obstet. Gynecol. Scand.* 51: 385–393.

Kyte, J. and R.F. Doolittle. 1982. A simple method for displaying the hydropathic character of a protein. *J. Mol. Biol.* 157: 105–132.

Leivo, I., A. Vaheri, R. Timple, and J. Wartiovaara. 1980. Appearance and distribution of collagens and laminin in the early mouse embryo. *Dev. Biol.* 76: 100–114.

Lindenberg, S., P. Hyttel, S. Lenz, and P.V. Holmes. 1986. Ultrastructure of the early human implantation in vitro. *Hum. Reprod.* 1: 533–538.

Lindenberg, S., K. Sundberg, S.J. Kimber, and A. Lundblad. 1988. The milk oligosaccharide, lacto-N-fucopentaose I, inhibits attachment of mouse blastocysts on endometrial monolayers. *J. Reprod. Fertil.* 83: 149–158.

Martin, G.R. 1980. Teratocarcinomas and mammalian embryogenesis. *Science* 209: 768–776.

Oshima, R.G., W.E. Howe, G.F. Klier, E.D. Adamson, and L.H. Shevinskey. 1983. Intermediate filament protein synthesis in preimplantation murine embryos. *Dev. Biol.* 99: 447–455.

Richardson, C.D., A. Berkovich, S. Rozenblatt, and W.J. Bellini. 1985. Use of antibodies directed against synthetic peptides for identifying cDNA clones, establishing reading frames and deducing the gene order of measles virus. *J. Virol.* 54: 186–193.

Ringler, G.E. and J.F. Strauss III. 1990. Recent advances in understanding the process of implantation. *Curr. Opin. Cell Biol.* 2: 703–708.

Rohde, L.H. and D.D. Carson. 1993. Heparin-like glycosaminoglycans participate in binding of a human trophoblastic cell line (JAR) to a human uterine epithelial cell line (RL95). *J. Cell. Physiol.* 155: 185–196.

Romagnano, L. and B. Babiartz. 1990. The role of murine cell surface galactosyltransferase in trophoblast: Laminin interactions in vitro. *Dev. Biol.* 141: 254–261.

Saiki, R.K., D.H. Gelfand, S. Stoftel, S.J. Scharf, R.G. Higuchi,

G.T. Horn, K.B. Mullis, and H.A. Erlich. 1988. Primer-directed enzymatic amplification of DNA with a thermostable DNA polymerase. *Science* **239:** 487–491.

Sanger, F., S. Nicklen, and A.R. Coulson. 1977. DNA sequencing with chain terminating inhibitors. *Proc. Natl. Acad. Sci.* **7:** 5463–5467.

Sclafke, S. and A. C. Enders. 1975. Cellular basis of interaction between trophoblast and uterus at implantation. *Biol. Reprod.* **12:** 41–65..

Shi, S.R., M.E. Key, and K.L. Kalra. 1991. Antigen retrieval in formalin-fixed, paraffin-embedded tissues: An enhancement method for immunohistochemical staining band on microwave oven heating of tissue sections. *J. Histochem. Cytochem.* **39:** 741–748.

Stappert, J. and R. Kemler. 1993. Intracellular associations of adhesion molecules. *Curr. Opin. Neurobiol.* **3:** 60–66.

Sutherland, A.E., P.G. Calario, and C.H. Damsky. 1988. Expression and function of cell surface extracellular matrix receptors in mouse blastocyst attachment and outgrowth. *J. Cell Biol.* **106:** 1331–1348.

Thomas, P.S. 1980. Hybridization of denatured RNA and small DNA fragments transferred to nitrocellulose. *Proc. Natl. Acad. Sci.* **77:** 5201–5205.

Towbin, H., T. Staehelin, and J. Gordon. 1979. Electrophoretic transfer of proteins from polyacrylamide gels to nitrocellulose sheets: Procedure and some application. *Proc. Natl. Acad. Sci.* **76:** 4350–4354.

Yamagata, T. and K. Yamazaki. 1991. Implanting mouse embryo stain with a LNF-I bearing fluorescent probe at their mural trophectodermal sides. *Biochem. Biophys. Res. Commun.* **181:** 1004–1009.

Yoshinaga, K. 1988. Uterine receptivity for blastocyst implantation. *Ann. N.Y. Acad. Sci.* **541:** 424–431.